ADVANCED EVAPOTRANSPIRATION MEASUREMENT FOR CROP WATER MANAGEMENT IN THE RED RIVER VALLEY

A Dissertation
Submitted to the Graduate Faculty
of the
North Dakota State University
of Agriculture and Applied Science

By

Ali Rashid Niaghi

In Partial Fulfillment of the Requirements
for the Degree of
DOCTOR OF PHILOSOPHY

Major Department:
Agricultural and Biosystems Engineering

November 2019

Fargo, North Dakota

North Dakota State University
Graduate School

Title

ADVANCED EVAPOTRANSPIRATION MEASUREMENT FOR CROP WATER MANAGEMENT IN THE RED RIVER VALLEY

By

Ali Rashid Niaghi

The Supervisory Committee certifies that this ***disquisition*** complies with North Dakota State University's regulations and meets the accepted standards for the degree of

DOCTOR OF PHILOSOPHY

SUPERVISORY COMMITTEE:

Xinhua Jia
Chair

Dean D. Steele

Thomas F. Scherer

Peter G. Oduor

Approved:

11/26/2019 — Date

Kenneth J. Hellevang — Department Chair

ABSTRACT

As the main component of terrestrial energy and water balance, evapotranspiration (ET) moves a large amount of water and energy in the form of latent heat flux from bare soil and vegetated surfaces into the atmosphere. Despite the development of many methods and equations through past decades, accurate ET estimation is still a challenging task, especially for the Red River Valley of the North (RRV) that has limited updated information on ET either for landscape or agricultural water management.

The overall objective of first study was to evaluate the ASCE-EWRI reference ET (ET_o) method by developing an accurate crop coefficient (K_c) using an eddy covariance (EC) system over an unirrigated turfgrass site. The results showed that with mean ET_{grass}/ET_o ratio as 0.96 for the entire growing seasons of turfgrass, the ASCE-EWRI ET_o method is valid for guiding the turfgrass irrigation management in cold climate conditions.

In a Controlled drainage with subirrigation (CD+SI) field, an EC system was used to measure and quantify energy flux components along with soil water content (SWC) and water table depth (WTD) measurements during four corn growing. This study showed that the subsurface drainage along with the CD + SI system can be used for optimal water management with an improvement of 26.7% and 6.6% of corn yield during wet and dry year, respectively.

For the final task, ET was measured using EC, Bowen ratio system (BREB), and soil water balance (SWB) method during the corn growing season. The comparison of the EC and the BREB system illustrated the advantages of using the residual method to close the energy balance closure of EC. Among the different time approaches for SWB method, ET by the SWB method using the average soil water contents between 24:00 to 2:00 time period showed non-significant differences (alpha = 0.05) compared to the BREB system during the observation periods.

ACKNOWLEDGEMENTS

A PhD dissertation although authored by an individual, is the product of the generosity of many people, programs, and funding sources that contribute to making research happen. My committee has provided a tremendous amount of academic and emotional support along the way. I could not have asked for better guidance from such an amazingly intelligent and creative group of individuals.

My advisor, Xinhua Jia, has had more of an impact on my professional and scientific development than any other sole individual. Her patience, support, and expertise are appreciated beyond measure. Xinhua changed my life and I will be forever grateful. Dr. Dean Steele worked as a committee member and his critical eye and analytical expertise have contributed immensely to my development as a quantitative scientist. Dr. Thomas Scherer provided me with guidance beyond my dissertation, aiding in my development as an outbox thinker and expanded my knowledge on various scientific areas. I thank him for his kindness and genuine advice. Dr. Peter Oduor has provided insight and education regarding the finest scales of plant response to environmental change. He has provided an incredible sounding board for me at times when I was nearly broken.

Any good agricultural engineer must learn the mechanisms that drive plant productivity and behavior, and his attention to detail is exemplary. A big thank you to Drs. Aaron Daigh, Don Lin, Tom DeSutter, Debjit Roy and Ms. Debra Bauer for her time and assistance on reviewing my manuscripts. The later cohort of students helped me transition to a leadership role and I greatly appreciate their willingness to learn from me and help me with my development along the way. The field effort required to complete this study was enormous and overwhelming and it would have been impossible without a few key players and all undergraduate and graduate students who helped me along the way are greatly appreciated.

I am indebted to many people and organizations that provided funding to train me as a scientist. I received fellowships to fund my research and coursework from North Dakota Water Resource Research Institute (NDWRRI), USDA National Institute of Food and Agriculture project 2015-68007-23193, NASA ROSES Project NNX15AC47G, ND Water Resources Research Institute, ND Agricultural Experimental Station, and USDA Hatch project ND01475, NCR SARE project LNC11-332, and ND Soybean Council.

My friends and family have provided a critical personal support system throughout the duration of my PhD. My father, Esmaeil Rashid Niaghi, and mother, Rogayeh Khadipour, inspired me to keep going, gave me confidence that I could, and provided support in more ways than I can count.

Lastly, my dear wife, Sevda's unwavering support does not go unnoticed. I love her all very much. My wife is the most supportive, caring and patient woman. I have been in school for almost our entire relationship of 4 years. I would not exist as the person that I am without her. She was with me since I was waiting to get my Visa, she tolerated a long-distance relationship when I left her to come to the US alone, and she stand for all nights that left her alone to work on my projects. Well, here we are! We've got staying' power, you and I, through thick and thin. Thank you, Sevda, and I love you. And, above all, I am grateful to almighty God. Without the blessings, it would be impossible to complete my work successfully.

DEDICATION

To my beautiful wife, Sevda, and my parents that whom their unyielding love, support, and encouragement have enriched my soul and inspired me to pursue and complete this research.

TABLE OF CONTENTS

LIST OF TABLES

LIST OF FIGURES

LIST OF APPENDIX TABLES

LIST OF APPENDIX FIGURES

Figure Page

1. GENERAL INTRODUCTION

1.1. Evapotranspiration (ET)

Evapotranspiration (ET) is the sum of water loss from the soil surface (evaporation) and transpiration from the leaves of the growing plants. As the main component of terrestrial energy and water balance, ET moves a large amount of water and energy in the form of latent heat flux from bare soil and vegetated surfaces into the atmosphere (Anderson et al., 2012; Niaghi et al., 2019).

Factors that affect the rate of ET include the amount of solar radiation, atmospheric vapor pressure deficit, temperature, wind, and soil moisture. ET accounts for most of the water lost from the soil surface during crop growth and thus, is important for irrigation and water management.

Among all factors (i.e. soil properties, weather variability, and salinity), ET plays a dominant role in crop production and is a critical factor in the hydrological cycle. Accurately determining the actual crop ET (ET_a), which is the plants' actual use of water can reveal crop water status and provide water management information to enhance crop production (Kandel et al., 2013; Sharma & Minhas, 2005), and improve nitrogen use efficiency (Mejia et al., 2000). Therefore, quantifying the ET_a in field conditions could be a practical way to make appropriate decisions for water management and evaluate the different methods and approaches at various crop stages.

1.2. Reference evapotranspiration (ET_{ref}) and crop coefficient (K_c)

The evapotranspiration rate from a reference surface, not short of water, is called the reference crop evapotranspiration or reference evapotranspiration and is denoted as ET_{ref}. The reference surface is a hypothetical grass reference crop with specific characteristics.

The only factors affecting ET_{ref} are climatic parameters. Consequently, ET_{ref} is a climatic parameter and can be computed from weather data. ET_{ref} expresses the evaporating power of the atmosphere at a specific location and time of the year and does not consider the crop characteristics and soil factors. A large number of empirical or semi-empirical equations have been developed for assessing crop or ET_{ref} from meteorological data. Some of the methods are only valid under specific climatic and agronomic conditions and cannot be applied under conditions different from those under which they were originally developed. The FAO Penman-Monteith (Allen et al., 1998) method is recommended as the sole method for determining ET_{ref}. The method has been selected because it closely approximates grass ET_{ref} at the location evaluated, is physically based, and explicitly incorporates both physiological and aerodynamic parameters. Moreover, procedures have been developed for estimating missing climatic parameters.

Since Penman (1948) developed an equation for evaporation and evapotranspiration estimation, various improvement have been made to the original equation. The standardized ET_{ref} method by the American Society of Civil Engineers–Environmental and Water Resources Institute (ASCE-EWRI) (ASCE-EWRI, 2005) has been shown to provide an accurate estimation for grass as a reference crop (ET_o). The ASCE-EWRI method has been tested at different locations around the world (Anapalli et al., 2018; Chávez, et al., 2009; Majnooni-Heris, et al., 2013) but has not been tested in North Dakota.

The ratio between the ET_a and the ET_{ref}, which is known as a crop coefficient (K_c), may provide insights to guide the irrigation and drainage water management in northern cool climates and during drought periods when measured ET_a values are not available. Therefore, ET_a can be indirectly determined from the ET_{ref} calculated from weather data and the recommended K_c at various stages of the specified crop. The K_c represents regional climate characteristics, crop type, plant density, phenology, soil water status, and other parameters (Anderson et al., 2017), and should be developed for each study region. To develop the K_c values for each region, accurately measured ET_a at the field scale is necessary.

1.3. Crop evapotranspiration measurement (ET_a)

Over the last decades, development of instrumentation, data acquisition systems, and remote sensing have enhanced the ability of ET_a measurement and have significantly intensified the knowledge of ET_a (Fisher et al., 2017). Numerous methods and techniques are now being used either remotely (Reyes-González et al., 2017) or by in-situ experiment (e.g. eddy covariance, Bowen ratio, soil water balance, and lysimeter) for ET_a estimations (Fidantemiz et al., 2019; Verstraeten et al., 2008; Zhang et al., 2008). However, most of the ET_a methods, developed ET_a models, or proposed ET_a equations have large discrepancies, and exhibited systematic and random errors depending on the device's location and climate conditions (Dragoni et al., 2007). Despite the development of many methods and equations through past decades, accurate ET_a estimation is still a challenging task (Amatya et al., 2016), and more efforts need to be taken to increase our knowledge, the benefits, and the drawbacks of the available methods.

Several methods are available to measure daily ET_a directly. Some of the most used methods are ground-based, such as soil water balance and lysimeter (Djaman & Irmak, 2013; Niaghi et al., 2015; Rana & Katerji, 2000). Others are above ground methods, including eddy covariance (EC) (Niaghi & Jia, 2017; Niaghi et al., 2019; Shi et al., 2008; Tie et al., 2018), surface renewal (Brotzge & Crawford, 2003; Hu et al., 2018; Rosa & Tanny, 2015), Bowen ratio energy balance (Gong et al., 2016; S Irmak et al., 2014; Shi et al., 2008; Uddin, Hancock, Smith,

& Foley, 2013), and remote sensing technology (Nagler et al., 2005; Niaghi, 2014; Yang et al., 2017). Since ET_a is an important component of water balance and hydrologic studies, considerable research efforts have attempted to estimate the ET_a from weather data (Steele et al., 1996; Subedi et al., 2017).

Evaporation of water requires relatively large amounts of energy, either in the form of sensible heat or radiant energy. Therefore, the ET process is governed by energy exchange at the vegetation surface and is limited by the amount of energy available. Because of this limitation, it is possible to predict the ET rate by applying the principle of energy conservation. The energy arriving at the surface must equal the energy leaving the surface for the same time period.

All fluxes of energy should be considered when deriving an energy balance equation. The equation for an evaporating surface can be written as:

$$Rn - G = LE + H \quad (1.1)$$

where R_n is the net radiation, H the sensible heat, G the soil heat flux and LE the latent heat flux. The various terms can be either positive or negative. Positive R_n supplies energy to the surface and positive G, LE and H remove energy from the surface.

In Equation 1.1 only vertical fluxes are considered and the net rate at which energy is being transferred horizontally, by advection, is ignored. Therefore, the equation is to be applied to large, extensive surfaces of homogeneous vegetation only. The equation is restricted to the four components: R_n, LE, H and G. Other energy terms, such as heat stored or released in the plant, or the energy used in metabolic activities, are not considered. These terms account for only a small fraction of the daily net radiation and can be considered negligible when compared with the other four components.

The LE representing the ET fraction can be derived from the energy balance equation if all other components are known. R_n and G can be measured or estimated from climatic parameters. Measurements of H are however complex and cannot be easily obtained. H requires accurate measurement of temperature gradients above the surface.

1.3.1. Eddy covariance

The EC method is one of the most established techniques to determine the exchange of water, energy, and trace gases between the land surface and the atmosphere (Allen et al., 2011). The EC method has been applied to precisely measured carbon and water budget over various crops and ecosystems due to its appropriate measurement scale compared to the lysimeter, leaf cuvettes, and soil chambers (Baldocchi, 2003). Moreover, the EC method can provide direct approach to quantify net fluxes of energy balance components across the study area over different time series intervals. Currently, they are more than 400 flux tower sites operating worldwide, and many of them are included in the flux network such as FLUXNET, the National Ecological Observatory Network (NEON), and the Integrated Carbon Observation System (ICOS). The obtained data from the mentioned flux network provide many research opportunities for scientists, as well as inter-disciplinary projects. In this chapter, the entire EC measurement system procedure are described.

In the last 10 years, the EC method has been widely accepted as a standard method to estimate ET_a rates and was successfully used overseas (Li et al., 2008; Zhou et al., 2014) and in the United States (Castellví and Snyder, 2010; Jia et al., 2009; Sumner, 2001), including North Dakota (Niaghi et al., 2017; Rijal et al., 2012). The EC system is regarded as the most accurate method for *in situ* ET_a measurement at scales of 0.1–1 km (Rana & Katerji, 2000). The EC has been successfully used to measure ET_a over different crop fields and forest lands for decades (Baker & Griffis, 2005; Facchi et al., 2013).

With the development of flux measurements, the usage of EC is extended rapidly to more heterogenous stands (Gong et al., 2016; Wilson et al., 2002), and it has been compared with other ET_a methods (Consoli & Vanella, 2014). Gebler et al. (2015) showed a good ET_a correlation between lysimeter and EC for the summer time. However, measurement and comparison of ET_a between the EC and other methods is poorly documented for regions with a shallow water table and heavy clay soil. It is important to validate the ET_a by the EC method with other independent methods and to determine the most effective approach.

Rijal et al., (2012) used an EC system in a field with CD treatment to develop new K_c values for corn and soybean in the RRV based on data from one year. Due to climate, corn hybrids, and variable farming practices, one-year data will likely not fully represent the variability of ET_a and K_c; therefore, their range and fluctuation remain unclear. Exacerbating the problem, other studies that have provided the regional K_c values were conducted several decades ago (e.g., Steele et al., 1996; Stegman, 1986). Since then, corn hybrids have evolved from conventional to modified hybrids with different water use and water stress characteristics (Payero & Irmak, 2013).

1.3.1.1. Principle of measurement

The term "flux" can be defined as an amount of an entity that passes through a closed surface per unit of time (Burba & Anderson, 2007). Based on a conservation equation, scalar quantity can be computed as follows:

$$\frac{\partial c}{\partial t} + U_j \frac{\partial c}{\partial x_j} = S + R + D \qquad (1.2)$$

where C is the concentration of a scalar (e.g. H_2O) in atmosphere, t is time, U_j is the wind velocity vector that has three components (u, v, w), and X_j represents directions of x, y, and z. S is the source or sink term, R is chemical reaction, and D is molecular diffusion.

Reynolds' rules of averaging are used to provide a statistical representation of turbulent wind, its non-Gaussian attributes and turbulent fluxes. The motion of a turbulent fluid, like air, can be defined at any instant in time as being equal to the sum of its mean state ($\bar{x}$) and is fluctuation from the mean (x'). The overbar represents time averaging and the prime represent a fluctuation from the mean. The Reynold's rule are as follows:

The mean product of two fluctuating variables is a function of the products of the individual means plus a covariance: $\bar{x} + \bar{y} = \overline{xy} + \overline{x'y'}$

The average of any fluctuating component is zero, $\overline{x'} = 0$, and

The average of the sum of two components is additive: $\overline{x + y} = \bar{x} + \bar{y}$

By applying Reynold decomposition and knowing that the instantaneous C and U_j are the sums of the means over a certain averaging period and the fluctuating portions, equation 1.2 can be expanded into mean and turbulent parts as follows:

$$\frac{\partial(\bar{C}+c\prime)}{\partial t} + (\overline{U_j} + u_j')\frac{\partial(\bar{C}+c\prime)}{\partial x_j} = S + R + D \qquad (1.3)$$

By applying the Reynolds averaging rules, and simplifying the final equation, the equation 1.3 is left as:

$$\frac{\partial \bar{C}}{\partial t} + \frac{\overline{U_j}\partial \bar{C}}{\partial x_j} + \frac{\overline{u_j'\partial c\prime}}{\partial x_j} = \bar{S} + \bar{R} + \bar{D} \qquad (1.4)$$

The three components left on the right side are the storage term, the advection by the mean wind, and turbulent diffusion term, respectively. In order to further simplify the equation and then apply it to EC flux computation, the major assumptions are made as follow:

- No chemical reactions occur (R=0)
- Molecular diffusion is negligible compared to the turbulent flux (D=0)
- The mean wind direction is along the x direction ($\bar{\bar{v}} = \bar{w} = 0$)
- The system is under steady state over the averaging period ($\frac{\partial \bar{C}}{\partial t} = 0$)
- The site is homogenous and uniform in all directions ($\frac{\overline{U_J} \partial \bar{C}}{\partial x} = \frac{\overline{U_J} \partial \bar{C}}{\partial y} = 0$)

Therefore, the equation 1.4 reduced to:

$$\frac{\partial \overline{w'c'}}{\partial z} = \bar{S} \tag{1.5}$$

Integrating equation 1.5 over the measurement height (z_r) gives the final simplified flux computation equation for the EC system as follows:

$$\int_0^{z_r} \bar{s} dz = \int_0^{z_r} \frac{\partial \overline{w'c'}}{\partial z} dz = \overline{\rho_a w'c'} | z = z_r - \overline{\rho_a w'c'} | z = 0 \tag{1.6}$$

Flux of a certain trace gas across the boundary between the atmosphere and the surface is a covariance of vertical wind speed and gas concentration such as H_2O and C_2O. by replacing the gas concentration with temperature, sensible heat flux (H) can be calculated as follows:

$$\text{LE}= \lambda \overline{w'c'} \tag{1.7}$$

$$\text{H}= c_p \rho_a \overline{T'c'} \tag{1.8}$$

where λ is latent heat of vaporization, c_p is specific heat of air and ρ_a is air density.

More detail and information on EC method and equations can be found at EC covariance method for scientific, industrial, agricultural and regulatory applications field book by LI-COR (Burba & Anderson, 2007).

1.3.1.2. Energy balance closure

The lack of energy balance conservation among measured terms at EC field site known as the energy balance closure problem, is unsolved and common problem in field measurements

(Reed et al., 2018; Shi et al., 2008). In recent years, several researchers have worked to address this issue, with lack of energy closure through to be from, in part, landscape heterogeneity (Foken, 2008), error in flux observation (Wilson et al., 2002), averaging period and coordinate system (Fratini & Mauder, 2014), horizontal advection (Oncley et al., 2007), instrument bias (Frank et al., 2016), incorrect assumption from Taylor's frozen turbulence hypothesis (Cheng et al., 2017), time dependency of site energy balance (Reed et al., 2018), or combination of several issues (Leuning et al., 2012). However, there is no clear conclusion on how to improve energy closure.

To overcome the closure error and proceed with the flux processing, Twine et al. (2000) suggested one way to close the energy balance was to assume that the H was measured correctly with a sonic anemometer and then solve for LE as the residual in the energy balance equation ($LE = R_n - G - H$). This procedure was also used by Chávez et al. (2009) ;Niaghi, et al..(2019a,b), and Payero & Irmak, (2013) for the LE calculation. In general, the error in EC closure ranges between 10 and 30% in agricultural fields (Foken, 2008). However, findings from the literature show that there is no universal method to close the energy balance (Imukova et al., 2016).

1.3.2. Bowen ratio energy balance system

The BREB method considers the vertical movement of small parcels of air (eddies) above a large homogeneous surface. The eddies transport material (water vapor) and energy (heat, momentum) from and towards the evaporating surface. By assuming steady state conditions and that the eddy transfer coefficients for water vapor are proportional to those for heat and momentum, the ET_a rate can be computed from the vertical gradients of air temperature and water vapor via the Bowen ratio. These methods and other methods such as eddy covariance, require accurate measurement of vapor pressure, and air temperature at different levels above the surface. Therefore, their application is restricted to primarily research situations.

The Bowen ratio (β) was estimated from the vertical gradient of temperature (T_1, T_2) and vapor pressure (e_1, e_2) at two heights above the crop canopy. The β can be calculated as follows (Perez et al., 1999):

$$\beta = \frac{P.C_p}{\varepsilon.L_v}\frac{K_h}{K_w}\frac{(T_1 - T_2)}{(e_1 - e_2)} = \frac{H}{LE} \qquad (1.9)$$

where P is atmospheric pressure (kPa), C_p is specific heat of dry air (KJ/kg.°C), T_1 and T_2 are measured temperature at two height above the crop canopy (°C), ε is the ratio between the molecular weights of water vapor and air (0.622), L_v is the latent heat of vaporization (KJ/kg), e_1 and e_2 are vapor pressure measured at two height above the crop canopy (kPa), and K_h and K_w are the eddy diffusivity for heat and water vapor, respectively, and assumed to be equal. H is estimated as the residual of the energy balance and LE is estimated as follows:

$$LE = \frac{R_n - G}{1 + \beta} \qquad (1.10)$$

1.3.3. Soil water balance

The ET_a can be determined by measuring the various components of the soil water balance (SWB). Irrigation (I) and rainfall (P) add water to the root zone. Part of I and P might be lost by surface runoff (RO) and by deep percolation (DP) that will eventually recharge the water table. Water might also be transported upward by capillary rise (CR) from a shallow water table towards the root zone or even transferred horizontally by subsurface flow in (SF_{in}) or out of (SF_{out}) the root zone. In many situations, however, except under conditions with large slopes, SF_{in} and SF_{ou} are minor and can be ignored. Soil evaporation and crop transpiration deplete water from the root zone. If all fluxes other than ET_a can be assessed, the ET_a can be deduced from the change in soil water content (SW) over the time period:

$$ET = I + P - RO - DP + CR \pm SF \pm SW \quad (1.11)$$

Some fluxes such as subsurface flow and deep percolation are difficult to assess, and short time periods cannot be considered. The soil water balance method can usually only give ET_a estimates over long time periods of the order of week-long or ten-day periods. On the other hand, it is important to quantify and validate the accuracy of the SWB method by considering the capillary rise for heavy clay soil and compare the obtained values with more precise methods, such as EC and BREB methods via energy balance approaches.

1.4. Red River Valley (RRV)

When the last glacier in North Dakota melted about 12,000 years ago, glaciers still existed to the north in Canada. These glaciers formed a huge dam and blocked the rivers trying to flow north. The water was backed up and formed a gigantic lake, called Lake Agassiz (ag-a-see) (reference?). This lake existed for about 4,000 years. After the lake drained away, the once-hilly land that had been under this huge lake was almost as flat as a floor. This happened because the sediment left by the lake had filled in the low places and made the whole area level. The lakebed of the ancient Lake Agassiz is now called the RRV (Figure 1.1). It covers the eastern strip of North Dakota next to the Red River of the North and extends many miles into Minnesota and north into Manitoba. The RRV in North Dakota is about 10 miles wide near the South Dakota border, but it is about 40 miles wide near the Canadian border. With the lowest and highest elevation at 228 and 244 m above the sea level (17 cm/km slope), the RRV is the lowest land in North Dakota and drains about 104,118 km^2 (40,200 $miles^2$).

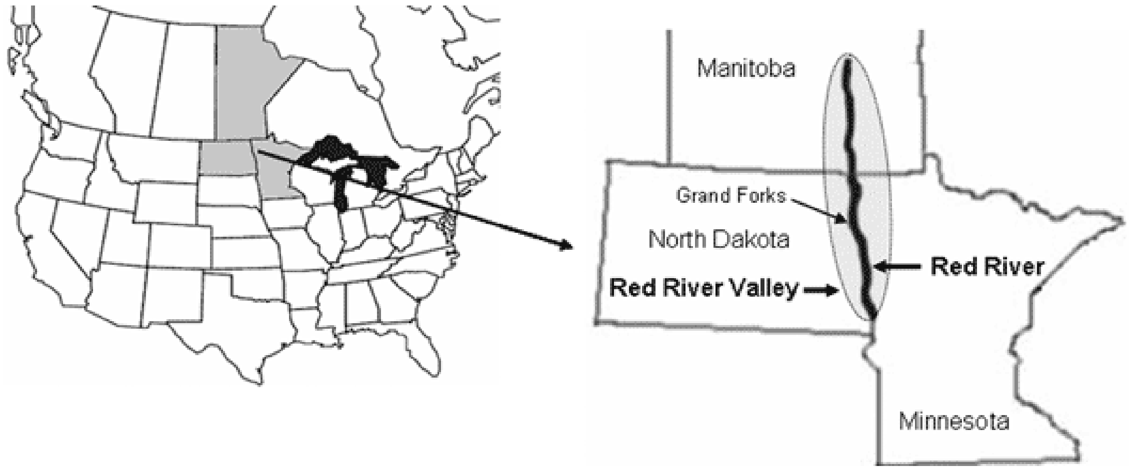

Figure 1.1. Red River Valley (RRV)[1]

1.4.1. Climate[2]

The annual average temperature ranges from about 3°C in northeastern North Dakota to 7°C along most of the southern border. However, annual averages are misleading because they hide the large seasonal temperature variations commonly throughout the State. January is the coldest month with average temperatures ranging from near -18°C in the northeast to -10°C in the southeast. The warmest month is July when average temperatures range from 18°C in the northeast to 22°C in the south. The average temperature range illustrates the pronounced continental climate of the region (NOAA, 2019). Average annual precipitation is about 559 mm for the RRV. On an average, about 75 percent of the annual precipitation falls during the crop-growing season in April to September (NOAA, 2019).

The average growing season is about 110 days in the northern RRV and increases to 120 days through the middle portion of the RRV and reaches 130 days in the farthest southern portion. The average date of the last freeze in spring ranges from May 15 in the south to late May in the north. In the fall, the first 0°C occurs between September 10 and 25 (NOAA, 2019).

[1] www.reshapingthetornadobelt.com/background/red-river-valley
[2] https://www.ncdc.noaa.gov/climatenormals/clim60/states/Clim_ND_01.pdf

1.4.2. Landforms and soil

Flat surfaces with poor drainage are the terrain left by glacial Lake Agassiz. Tall grasses, together with deciduous trees along the streams, can be found in the better drained portions. Poorly drained portions have sparse and scattered areas of a mosaic of boreal forest interspersed with peat bogs. Soils in the bed of Lake Agassiz vary considerably, depending upon locations. Fine silts and lacustrine clay cover most of the old lakebed up to the depth of 45 m. Sand deposits accumulated at the lake's margins. Deltas of silt and sand were formed where rivers emptied into the lake. Most of the soils are Aquolls. They are deep, somewhat poorly drained or poorly drained, and sandy to clayey and have a frigid temperature regime. Calciaquolls (Bearden, Hegne, Glyndon, and Ulen series), Haplaquolls (Fargo series), and Haploborolls (Gardena and Embden series) are on the glaciolacustrine plains.

1.4.3. Residential and landscape

Due to the flat topography and the sub-humid and harsh weather conditions in eastern North Dakota, mixed turfgrass cultivars are grown to keep the landscape green during the growing season. The majority of the turfgrass in residential areas and golf courses is grown without irrigation under natural rainfed conditions. For those irrigated turfgrasses, because there are no ET data available to guide turfgrass water management in this region, irrigation is frequently based on time from the last rain event or the condition of the turfgrass. Therefore, quantification of the turfgrass ET for landscape and residential turfgrass irrigation management became the first goal of the current study.

1.4.4. Agricultural practices

The RRV has some of the richest soil and best farmland in the world. There are two reasons for this: (1) fertile (rich) soil was brought down from Canada by the glaciers; and (2) a great deal of organic matter was left from Lake Agassiz. Organic matter makes the soil very rich, which means it is good for growing crops. Nearly all this area is cultivated, and about 80 percent is cropland that is in dryland farming. Important cash crops are spring wheat, soybeans, potatoes, sugar beets, and corn. Some oil-producing crops and edible beans are also grown. On some farms, grains for feed and forage for dairy cattle are the principal crops. Nearly 10 percent of the area in the northeast is wooded.

The planted area for grain corn in North Dakota has increased from about 334,000 ha in 1997 to over 1.3 million ha in 2017 (USDA NASS, 2017). Figure 2 shows the increase of harvested corn for grain from 2007 through 2012. The increased demand for corn has prompted many farmers to grow more corn in North Dakota and particularly in the RRV. Therefore, understanding corn water use in the RRV would be helpful for agricultural water resource management, which is the focus of my second manuscript.

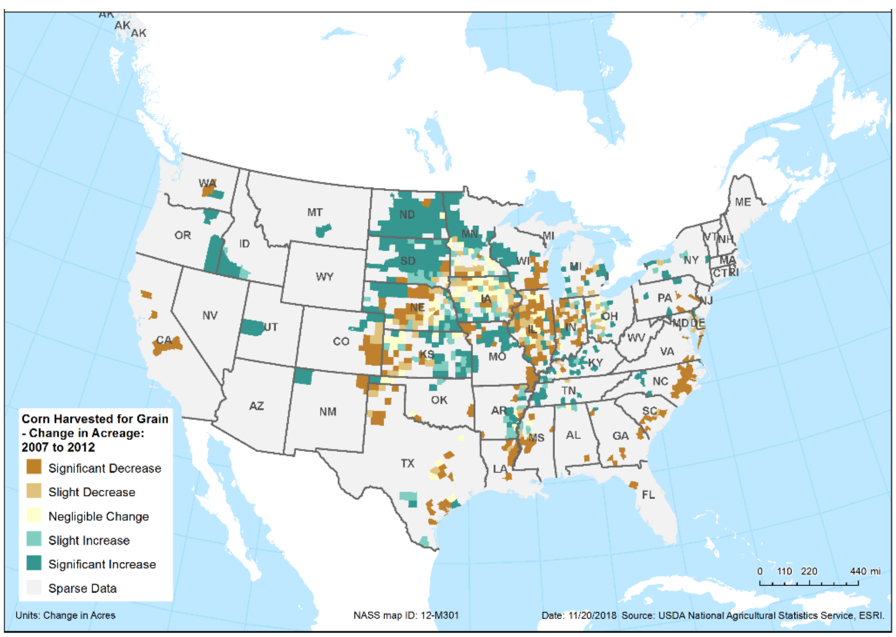

Figure 1.2. Increase of harvested corn for grain from 2007 through 2012 (USDA-NASS).

1.4.5. Subsurface drainage

Despite the RRV's rich soil condition, heavy clayey soils and increased salinity can hinder agricultural production, especially corn, due to a shallow water table and seasonal waterlogging conditions in spring and fall. Subsurface drainage (SD) is one of the most effective practices to remove the excess water from the soil and aid in earlier planting and a later harvest. The SD system employs buried perforated pipes to drain excess water and lower the water table in the soil profile. The major advantage of a SD system is the potential to be designed or retrofitted for controlled drainage (CD) and subirrigation (SI). Having a land slope of less than 0.5% allows landowners to not only drain during wet periods, but also retain or add water during the moderate to dry period (July-September) of the growing season. Figure 1.3 shows the percentage of land that has SD (SSURGO, 2018) and the increasing trend of approved permits to install SD systems within the RRV region (Finocchiaro, 2016).

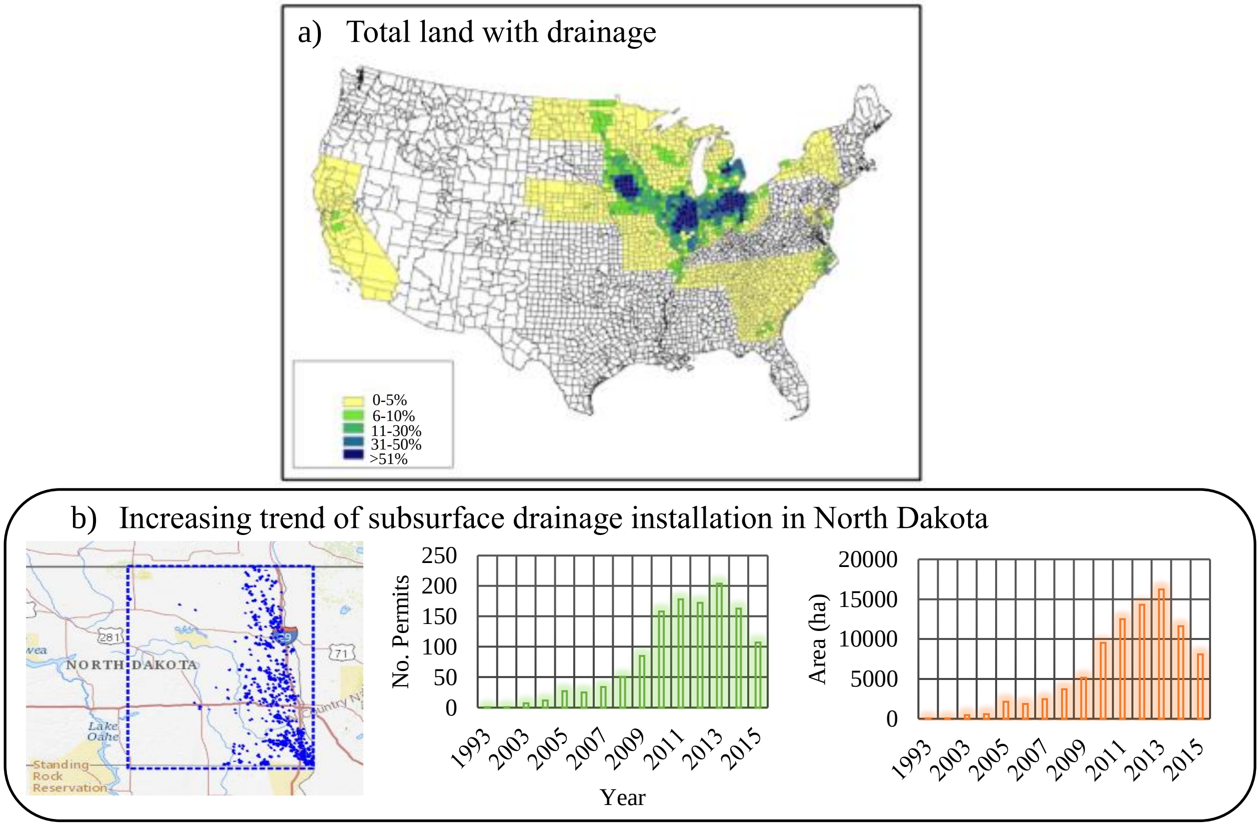

Figure 1.3. a) Total land with drainage in US, and b) increasing trend of subsurface drainage installation in North Dakota.

1.4.6. Controlled drainage

Water table management in agricultural fields can be improved by adding structures for CD to the SD system which may also include a subirrigation (SI) aspect. Using a weir or stop log in an outlet structure, CD controls the time and amount of drainage outflow and keeps water table depths at a desired level. The SI system is defined as the "application of irrigation water below the ground surface by raising the water table within or near the root zone" (ASABE Standards, 2015). In recent years, SI has become a supplementary component for drainage water management strategies by adding water through the SD system and control devices (Jia et al., 2017; Niaghi et al., 2019). Hence, the combination of CD and SI (CD + SI) can provide an optimal soil water condition to enhance crop production. While various studies reported yield increases for different crops using CD + SI (i.e. tomatoes, soybeans, and corn), questions remain regarding the effect of drainage water management via a CD + SI system on corn performance, such as the relationship between soil water content, water table depth, and ET during the crop growing season. Therefore, studying the effect of CD+SI practices on the corn production and quantification of in situ ET values became the second goal of the current research.

1.5. Influential parameters on ET

Evaporation and transpiration occur simultaneously and there is no easy way of distinguishing between the two processes. Apart from the water availability in the topsoil, the evaporation from a cropped soil is mainly determined by the fraction of the solar radiation reaching the soil surface. This fraction decreases over the growing period as the crop develops and the crop canopy shades more and more of the ground area. When the crop is small, water is predominately lost by soil evaporation, but once the crop is well developed and completely covers the soil, transpiration becomes the main process.

1.5.1. Climate

The principal weather parameters affecting ET are radiation, air temperature, humidity and wind speed. Several procedures have been developed to assess the ET rate from these parameters. The ET_{ref} , which represents the evapotranspiration from a standardized vegetated surface that can be either grass (ET_o) or alfalfa (ET_r), requires accurately measured climate parameters to quantify the potential of atmosphere for evaporation and transpiration act. Any of the climate parameters can be a limiting factor for the ET_{ref}.

1.5.2. Crop

The crop type, variety and development stage should be considered when assessing the ET from crops grown in large, well-managed fields. Differences in resistance to transpiration, crop height, crop roughness, reflection, ground cover and crop rooting characteristics result in different ET rates in different types of crops under identical environmental conditions. ET_a under standard conditions refers to the transpiration demand from crops that are grown in large fields under optimum soil water, excellent management and environmental conditions, and achieve full production under the given climatic conditions.

1.5.3. Management and environmental condition

The crop development and ET rate may be limited by some factors such as soil salinity, poor land fertility, limited application of fertilizers, the presence of hard or impenetrable soil horizons, the absence of control of diseases and pests and poor soil management. Other factors, such as climate condition, agricultural practices, and soil moisture may also affect the ET. The effect of soil water content on ET is conditioned primarily by the magnitude of the water deficit and the type of soil. On the other hand, too much water will result in waterlogging which might damage the root and limit root water uptake by inhibiting respiration.

1.5.4. Soil moisture

Soil moisture is an important variable in the climate system. Field soil moisture has a variable value ranging from permanent wilting point to saturation point over the time. It depends on rainfall, irrigation, and groundwater in the soil and the water consumption from the soil by evaporation, transpiration, and runoff. Balance in soil moisture is determined by climate, soil condition in the landscape, the type of vegetation, human activities, and the seasons. In addition, soil moisture depends on the properties of the soil, water holding capacity, water permeability, and hydraulic conductivity.

Soil moisture content is a soil status condition, directly connected with the process of ET since soil moisture content is usually related to moisture contained in the upper 1-2 m of a soil profile. Evidently, soil moisture is one of the prime environmental variables related to land surface climatology, hydrology and ecology (Vinnikov et al., 1999). Variations in soil moisture content entail a strong impact on land surface energy dynamics, regional runoff dynamics and vegetation productivity (actual crop yield) (Moran, et al., 2004).

Soil moisture content at the root zone is a limiting factor to the ET. If the soil moisture does not meet the water requirement of the crop, crop may face with a stressed situation and the reduced crop transpiration cause yield reduction (Allen et al., 1998). A strong linear relationship was reported between cumulative corn ET and irrigation application to prevent crop from facing any stressed condition (Payero & Irmak, 2008).

1.5.5. Water table depth

The shallow ground water table and clayey soil in the RRV have a great contribution to the crop ET for an average 35 to 41% for corn and 37% 51% for soybean during the growing season from May through October (Kolars et al., 2019). In the presence of a shallow water table, significant quantities of water can move into the root zone or be directly extracted by the root from the water table through root water uptake and capillary rise. A number of studies have shown that ET can be affected between 20 to 40% by capillary rise at water table depths of 0.7-1.5 m (Ragab & Amer, 1986; Wallender et al., 1979). Prathapar et al. (1993) reported 16-29% contribution of capillary rise to the ET measurement in a clay loam soil. Ragab and Amer (1986) found that a shallow water table and subirrigation application can contribute about 40% of ET over a 75-day period of a corn growing season.

1.6. Rationale and objectives

1.6.1. Evaluation of the ASCE-EWRI ET_{ref} method for the cold and sub-humid region

Hypothesis*: ASCE-EWRI method accurately estimates reference crop evapotranspiration rate for a cold and sub-humid climate of the Red River Valley.*

Many studies suggested that the ET_{ref} method underestimated measured ET_{ref} (either ET_o, which is the reference grass, or ET_r, which is the reference alfalfa) in windy areas with high evaporation demand. Some authors have claimed that the assumption of constant surface resistance is the main reason for the underestimation while others have expressed that the exclusion of the surface temperature in the Penman Montieth equation and the assumption of linearity of the saturation vapor pressure versus temperature is the responsible for the underestimation (Subedi et al., 2017).

Objectives: The overall objective of first study was to develop an accurate K_c using the unirrigation grass by selecting days with soil moisture greater than 50% of the available water in the soil profile. Specific objectives were (i) to quantify daily actual ET rates and other energy fluxes measured by eddy covariance system, (ii) to estimate the monthly ratio of measured ET_a to ET_{ref} (crop coefficient: K_c) obtained from the standardized reference ASCE-EWRI method, (iii) to evaluate the turfgrass ET_o under various weather conditions (dry, normal, and wet years), and (iv) to evaluate the performance of ASCE-EWRI standardized reference grass ET_o method for the Northern climate during the growing season (May–October) in the years 2011, 2012, and 2013.

1.6.2. Measurement of corn ET_a under controlled drainage with subirrigation practices

Hypothesis*: Control drainage and subirrigation (CD + SI) practices effect on crop ET_a through affecting the upward flux and crop root development and gain higher yield in controlled drainage field compared to free drainage or undrained field.*

Objectives*:* The specific objectives were to (1) analyze the effect of CD + SI on soil water content and water table depth; (2) analyze daily, diurnal, and cumulative energy fluxes during various corn growing stages; (3) evaluate the crop yield along with the estimated ET_a; and (4) develop new crop coefficients at various growing stages.

1.6.3. Comparison of different in situ ET_a measurement by including the capillary rise effect

***Hypothesis**: Considering the contribution of the shallow water table on ET_a can improve the accuracy of the soil water balance method compared to the in-situ eddy covariance and Bowen ratio measurement methods.*

***Objectives**:* Our objective was to evaluate the validity of measured Bowen ratio during corn growing season. The Bowen ratio method is often accepted as accurate enough to calibrate and test alternative methods as well as soil water balance method (Irmak et al., 2014). Thus, to close the energy balance of the eddy covariance system, the residual method is evaluated using the Bowen ratio obtained values. The measured ET_a values with eddy covariance and Bowen ratio were compared with obtained values from different soil water balance approaches.

1.7. Organization of the dissertation

This manuscript-based dissertation divided into five chapters, and two appendixes to provide and meet the required information on the aforementioned objectives. Chapter one offers a comprehensive introduction, background, and the general scope of this research. Chapter 2 presents a paper published in *Vadose Zone Journal 18 (1), 11*. This chapter includes comprehensive field study for turfgrass using eddy covariance measurements to guide for precision irrigation scheduling and management for the landscaping and agricultural purposes of the sub-humid and cold northern climate.

At chapter three, the impact of drainage water management along with subirrigation and controlled drainage practices during the corn growing seasons are monitored using the eddy covariance instrumentation, pair of soil moisture sensors, observation wells, and weather station. The energy flux components and actual crop evapotranspiration are measured during corn growing seasons for four years and crop coefficient for corn is developed based for better water resource management at the northern region. Content of this chapter is published as peer review article at *Agricultural and Water Management Journal 225:105760*.

Due to the variety in actual evapotranspiration measurement, chapter four dedicated for comparison of three in situ crop evapotranspiration methodologies, including eddy covariance, Bowen ratio, and soil water balance. In this chapter, one year of corn growing season is studied and specific observation periods are selected to compare the daily obtained crop evapotranspiration using different mentioned methodologies. The result of this task is published as a peer review article at *Water Journal 11(12) 2478*. At the end, in chapter five, the conclusion and summary of the work is provided.

1.8. References

Allen, R. G., Luis, S. P., RAES, D., & Smith, M. (1998). FAO Irrigation and Drainage Paper No. 56. Crop Evapotranspiration (guidelines for computing crop water requirements). *Irrigation and Drainage*. https://doi.org/10.1016/j.eja.2010.12.001

Anderson, M. C., Allen, R. G., Morse, A., & Kustas, W. P. (2012). Use of Landsat thermal imagery in monitoring evapotranspiration and managing water resources. *Remote Sensing of Environment*. https://doi.org/10.1016/j.rse.2011.08.025

Finocchiaro, R. G. (2016). *Agricultural Subsurface Drainage Tile Locations by Permits in North Dakota*. https://doi.org/dx.doi.org/10.5066/F7QF8QZW.

Irmak, S., Skaggs, K. E., & Chatterjee, S. (2014). A Review of the Bowen Ratio Surface Energy Balance Method for Quantifying Evapotranspiration and other Energy Fluxes. *Transactions of the ASABE*, *57*(6), 1657–1674. https://doi.org/10.13031/trans.57.10686

Jia, X., Scherer, T. F., Steele, D. D., & DeSutter, T. M. (2017). Subirrigation System Performance and Evaluation in the Red River Valley of the North. *Applied Engineering in Agriculture*, *33*(6), 811–818. https://doi.org/10.13031/aea.12286

Kandel, H. J., Brodshaug, J. A., Steele, D. D., Ransom, J. K., DeSutter, T. M., & Sands, G. R. (2013). Subsurface drainage effects on soil penetration resistance and water table depth on a clay soil in the Red River of the North Valley, USA. *Agricultural Engineering International: CIGR Journal*, *15*(1), 1–10.

Kolars, K., Jia, X., Steele, D. D., & Scherer, T. F. (2019). A soil water balance model for subsurface water management. *Applied Engineering in Agriculture*.

Mejia, M. N., Madramootoo, C. A., & Broughton, R. S. (2000). Influence of water table management on corn and soybean yields. *Agricultural Water Management*. https://doi.org/10.1016/S0378-3774(99)00109-2

Moran, M. S., Peters-Lidard, C. D., Watts, J. M., & Mc Elroy, S. (2004). Estimating soil moisture at the watershed scale with satellite-based radar and land surface models. *Canadian Journal of Remote Sensing*. https://doi.org/10.5589/m04-043

Niaghi, A. R., Jia, X., Steele, D. D., & Scherer, T. F. (2019). Drainage water management effects on energy flux partitioning, evapotranspiration, and crop coefficients of corn. *Agricultural Water Management*, *225*, 105760. https://doi.org/10.1016/j.agwat.2019.105760

Payero, J. O., & Irmak, S. (2008). Construction, installation, and performance of two repacked weighing lysimeters. *Irrigation Science*. https://doi.org/10.1007/s00271-007-0085-9

Prathapar, S. A., & Meyer, W. S. (1993). Measurement and estimation of capillary upflow from watertables under maize on irrigated soils. *Australian Journal of Soil Research*. https://doi.org/10.1071/SR9930119

Prathapar, S. A., Robbins, C. W., Meyer, W. S., & Jayawardane, N. S. (1992). Models for estimating capillary rise in a heavy clay soil with a saline shallow water table. *Irrigation Science*, *13*(1), 1–7. https://doi.org/10.1007/BF00190238

Ragab, R. A., & Amer, F. (1986). Estimating water table contribution to the water supply of maize. *Agricultural Water Management*, *11*(3–4), 221–230. https://doi.org/10.1016/0378-3774(86)90040-5

Sharma, B. R., & Minhas, P. S. (2005). Strategies for managing saline/alkali waters for sustainable agricultural production in South Asia. *Agricultural Water Management*, *78*(1–2), 136–151. https://doi.org/10.1016/j.agwat.2005.04.019

Soil Survey Geographic (SSURGO) Database. (2018). Available online at https://sdmdataaccess.sc.egov.usda.gov. Accessed [11/01/2019]

Subedi, A., Chávez, J. L., & Andales, A. A. (2017). ASCE-EWRI standardized Penman-Monteith evapotranspiration (ET) equation performance in southeastern Colorado. *Agricultural Water Management*. https://doi.org/10.1016/j.agwat.2016.07.002

USDA NASS. (2018). United States Department of Agriculture, National Agricultural Statistics Service.

Vinnikov, K. Y., Robock, A., Qiu, S., Entin, J. K., Owe, M., Choudhury, B. J., … Njoku, E. G. (1999). Satellite remote sensing of soil moisture in Illinois, United States. *Journal of Geophysical Research Atmospheres*. https://doi.org/10.1029/1998JD200054

Wallender, W. W., Grimes, D. W., Henderson, D. W., & Stromberg, L. K. (1979). Estimating the Contribution of a Perched Water Table to the Seasonal Evapotranspiration of Cotton. *Agronomy Journal*, *71*, 1056–1060. https://doi.org/10.2134/agronj1979.00021962007100060038x

2. MEASUREMENT OF UNIRRIGATED TURFGRASS EVAPOTRANSPIRATION RATE IN THE RED RIVER VALLEY[3]

2.1. Abstract

Turfgrass actual evapotranspiration (ET_a) measurements are critical for water management and irrigation scheduling. With no historical ET_a measurements in eastern North Dakota, turfgrass ET_a rates were measured with the residual method using eddy covariance instrumentation and two arrays of soil moisture sensors on unirrigated turfgrass under natural conditions in the 2011, 2012, and 2013 growing seasons. An on-site weather station provided weather data to calculate the standardized grass-based reference evapotranspiration (ET_o) (Allen et al., 2005). The daily ET_a/ET_o ratios were screened using the criteria of soil moisture 50% of available water for the top 30 cm of the root zone, rain amounts 10 mm, and a recovering period after drought. The screened monthly average ET_a/ET_o ratios for the unirrigated turfgrass were 1.03, 0.98, 0.94, 0.90, 0.82, and 1.18 from May to October. The mean ET_a/ET_o ratio for the entire growing seasons was 0.96, implying that the American Society of Civil Engineering–Environmental and Water Resource Institute ET_o method was valid for guiding the turfgrass ET_a calculation even in unirrigated and cold climate conditions. Because this is the first reported study on ET_a measurement of a turfgrass site, the limited data can provide a baseline on water management for turfgrass under various weather conditions in this region. The results indicated that a monthly refinement of ET_a/ET_o values might be required to maintain the landscape turfgrass quality more precisely in terms of water management.

---

[3] The material in this chapter was co-authored by Ali Rashid Niaghi, Xinhua Jia, Thomas F. Scherer, and Dean D. Steele was published in the Vadose Zone Journal as peer review article. Ali Rashid Niaghi had primary responsibility for analyzing the collected data, interpreting the results, developing the conclusion that are advanced here. Co-authors served as technical and editorial consultants in the development of the manuscript represented by this chapter.

Niaghi, A.R., X. Jia, T. Scherer, and D. Steele. 2019. Measurement of unirrigated turfgrass evapotranspiration rate in the Red River Valley. Vadose Zone J. 18:180202. doi:10.2136/vzj2018.11.0202.

2.2. Introduction

As the main component of terrestrial energy and water balance, evapotranspiration (ET) moves a large amount of water and energy in the form of latent heat flux from bare soil (evaporation) and vegetated surfaces (transpiration) into the atmosphere (Anderson et al., 2012; Bastiaanssen, 2000; Jensen et al., 2017). Accurate ET estimates are essential for the management and allocation of water resources, while inaccurate or rough estimates of ET rates can lead to an incorrect distribution of water resources.

Due to the flat topography, sub-humid and harsh weather conditions of eastern North Dakota, mixed turfgrass cultivars are grown to keep the landscape green during the growing season. The majority of the turfgrass in residential areas and golf courses are grown under non-irrigated and natural rainfed conditions. For irrigated turfgrass, since there is no ET data available to guide turfgrass water management in this region, frequently, irrigation is based on days since the last rain event or the condition of the turfgrass.

The actual evapotranspiration (ET_a) can be estimated through direct ET_a measurement, e.g. eddy covariance (EC) (Niaghi et al., 2017; Tanner and Greene, 1989), lysimeters (Allen and Fisher, 1990; Howell et al., 1995; Niaghi et al., 2015) and Bowen ratio (Irmak et al., 2014; Payero et al., 2003). Among these methods, the EC system has become widely used in ET_a measurement due to its more precise and accurate sensors and its ability to quantify energy balance components separately. Also, in the last 10 years, the EC method has been widely accepted as a standard method to estimate ET_a rates and was successfully used overseas (Li et al., 2008; Zhou et al., 2014), and in the United States (Castellvi and Snyder, 2010; Jia et al., 2009; Sumner, 2001), and even in North Dakota (Niaghi et al., 2017; Rijal et al., 2012).

The concept of EC is to measure the statistical covariance (correlation) between the vertical vapor or sensible heat fluxes within upward or downward legs of turbulent eddies. This can be done by measuring the temperature, wind speed and vapor pressure with high speed and quick response sensors at frequency of 10 Hz (Allen et al., 2011). Since Tanner et al. (1993) described the initial use of an EC system, there have been many instrumentation improvements (Allen et al., 2011; Baldocchi, 2003). Aside from all efforts to maintain and process the EC data, the EC method provides more spatial constancy, less site disturbance and allows a better temporal resolution compared to the lysimeter method (Sumner, 2001). Lack of closure of the surface energy balance is a common feature of EC measurements (Shi et al. 2008). In general, EC closure ranges between 70 and 90% as observed over agricultural fields (Foken, 2008). However, findings from literature shows that there is no universal method to close the energy balance closure (Imukova et al. 2016). The standardized reference evapotranspiration (ET_o) method by the American Society of Civil Engineers, Environmental and Water Resources Institute (Allen et al., 2005) has been shown to be an accurate estimation for grass as a reference crop. It has been widely accepted worldwide (Anapalli, 2018; Jia et al., 2013; Majnooni-Heris et al., 2013; Niaghi et al., 2017), but has not been tested in North Dakota. The ratio between the ET_a and the ET_o may provide some insights to guide the water management of irrigated turfgrass in northern cool climates and during drought periods when measured ET_a values are not available.

The overall objective of this study was to improve our knowledge of non-irrigated turfgrass in natural condition. Specific objectives were to: 1) quantify daily actual evapotranspiration rates and other energy fluxes measured by eddy covariance; 2) estimate the monthly ratio of measured ET_a to ET_o obtained from the standardized reference ASCE-EWRI method; 3) evaluate the turfgrass ET_o under various weather conditions (dry, normal and wet years); and 4) evaluate the performance of ASCE-EWRI standardized reference grass ET_o method for the Northern climate during 2011-2013 growing season (May-October).

2.3. Materials and methods

2.3.1. Study area and climate

The experiment was conducted at the North Dakota Agricultural Weather Network (NDAWN) site in Cass county (46° 53' 49.2" N and 96° 48' 43.2" W) with an elevation of 275 m, located near North Dakota State University in Fargo (Fig. 2.1). Field data were collected from 2011 to 2013 on a non-irrigated turfgrass site, while only the data during the growing seasons in May-October were used in this paper. The site is located in a sub-humid continental climate zone with a mean temperature of 17.3 ^oC for May- October. The cumulative rainfall amounts, and distribution of rain events were different in each growing season (May-October), with 411, 215, and 598 mm in 2011, 2012, and 2013, respectively, with an average annual precipitation of 500 mm (NDAWN, 2018).

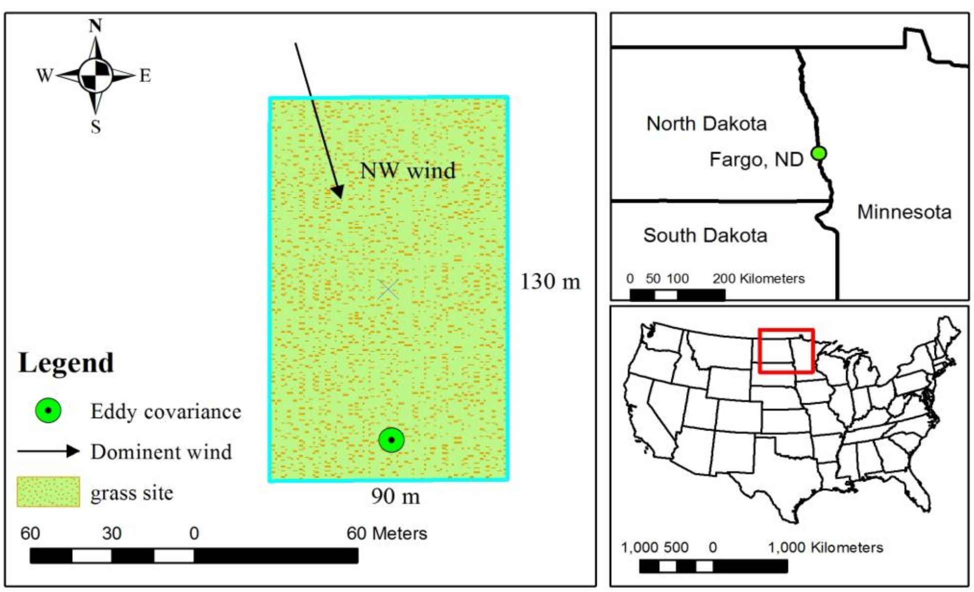

Figure 2.1. Study site and the eddy covariance system at the research site in Fargo, North Dakota.

The average water table was relatively shallow. From April to mid-May, it was near the soil surface. No irrigation was applied to the turfgrass site. The dominant soil in the study area is a Fargo silty clay loam (fine, montmorillonitic, frigid Vertic Haplaquolls) (NRCS, 2018) with a measured bulk density of 1.09 g/cm^3 and an available water holding capacity of 0.234 cm/cm for the top 30 cm layer. Saturated water content was calculated from the soil bulk density assuming a particle density of 2.65 g/cm^3 for mineral soil. Soil water content (SWC) at field capacity (FC) was obtained from Goos et al. (1988), and SWC at permanent wilting point (PWP) was measured using the WP4 Dewpoint Potentiometer (Roy et al., 2018), respectively. The average water content over the two depths (15 and 30 cm) for saturation point, FC and PWP were 0.59, 0.454 and 0.22 cm^3/cm^3, respectively. The soil properties are shown in Table 2.1.

Table 2.1. Soil properties at the research site in Fargo, North Dakota.

Soil Series	Fargo Silty Clay
Plant rooting depth	30 cm
Available water holding capacity (top 30 cm)	0.234 cm/cm
Water content at saturation	0.59 cm^3/cm^3
Water content at field capacity (FC)	0.454 cm^3/cm^3
Water content at permanent wilting point (PWP)	0.22 cm^3/cm^3
Bulk density	1.09 g/cm^3

Mixed turfgrass was established on the NDAWN site in 1990, has been grown continuously since then, and is mowed frequently during the study period in order to maintain the grass at about 12 cm in height. The planted turfgrass is categorized as Kentucky Bluegrass, Park cultivar. Kentucky Bluegrass is the most adaptable cold hardy, cool-season grass species for home lawns and has great restoration and competitive capacity which repairs itself in a week after severe conditions (Smith and Herman, 2009). Kentucky Bluegrass (*Poa pratensis L.*) has many cultivars based that on drought and water scarcity tolerance. The Park cultivar which does not need much water to survive is very drought tolerant and used as low maintenance. Although hundreds of new cultivars are available today, Park is still considered as a benchmark for drought tolerance (Deying Li, personal communication, 2018). Also, there is a significant amount of quackgrass (*Agropyron repens L.*) in the stand, making the mixture even more drought tolerant.

2.3.2. Field measurements

The EC system (Campbell Scientific, Inc., Logan, Utah) was mounted on a tripod at the research site and was in operation from October 2010 until April 2014. The fetch distance for the measurements was estimated for the height of the instrument above the grass canopy. The EC system was installed 1.5 m above the turfgrass surface, facing the northwest prevailing wind direction (Campbell and Norman, 1998) (Fig. 2.1).

Instrumentation used in this study and the variables measured are listed in Table 2.2. The energy balance components and primary meteorological variables were measured using the EC system during the study period. A CR3000 data logger (Campbell Scientific, Inc., Logan, UT) recorded and stored the data from the sensors. The wind speed, temperature, and relative humidity data sampling frequency was 10 Hz. All data were stored as 30-minute averages.

A CSAT3 sonic anemometer was used to estimate sensible heat flux (H) through the use of 3D sonic anemometer measurements along with virtual air temperature. The H values were calculated from the covariance between the vertical wind speeds and air temperature. Also, the KH20 hygrometer measured the vapor density fluctuation to quantify latent heat flux (LE).

Table 2.2. Instrumentation for the eddy covariance station at the research site in Fargo, North Dakota.

Instrument	Measurements
CSI CSAT3 3D Sonic Anemometer [a]	Turbulent fluctuations of horizontal and vertical wind
CSI KH20 Krypton Hygrometer	Rapid fluctuations in atmospheric water vapor
Texas Elec. TE525WS Tipping Bucket [b]	Precipitation
Kipp & Zonen CNR1 [c]	Net radiation
Vaisala HMP45C Temp/RH Sensor	Air temperature and relative humidity
HFP HFP01SC Soil Heat Flux Plates (2) [d]	Heat flux
CSI TCAV Averaging Soil Thermocouple Probes (2)	Soil temperature
CSI CS616 Water Content Reflectometer (2)	Volumetric water content

[a] CSI= Campbell Scientific, Inc.

[b] Texas Elec.= Texas Electronics, Inc.

[c] CNR1= Campbell Scientific, Inc.

[d] HFP= Hukseflux Thermal Sensors B.V.2.3 Energy Flux Calculation

The SWC values were measured at the EC system location using calibrated Hydra Probe II sensors (Stevens Water Monitoring Systems Inc., Portland, OR) at six depths (15, 30, 45, 60, 75, and 90 cm), with an accuracy of ±3% for heavy clay soils (Burns et al., 2014; Ojo et al., 2015). The Hydra Probe II records were used to monitor the soil profile moisture content and screening the days with sufficient moisture for turfgrass ET_a consideration. Rain events and amounts were measured using an automated tipping bucket rain gauge along with a manual rain gage, both with an accuracy of 0.25 mm. The SWC near surface soil at 15 and 30 cm were chosen to determine the soil moisture status for the turfgrass in the root zone.

2.3.3. Energy flux calculation

The net radiation (R_n) at the canopy surface should be the sum of H, LE, and soil heat flux (G). When using the EC for LE measurement, however, the energy was not balanced. Twin et al. (2000) found the 10-30% closure error for EC system over grassland. In order to make the energy balance, or close the energy budget, they stated that one way was to use the residual method and the other way was to utilize Bowen ratio method. Payero and Irmak (2013) used the residual method to estimate LE values, and Rijal et al. (2012) used Bowen ratio method to close the energy balance. Chaveaz et al. (2009) found that both the residual and Bowen ratio methods have similar results. Due to a malfunction of the KH20 hygrometer, the LE was estimated by the residual method. Therefore, the LE values were estimated via the following relationship:

$$LE = R_n - G - H \tag{2.1}$$

where LE is the latent heat flux in W/m^2, R_n is net radiation in W/m^2, H is sensible heat flux in W/m^2, and G is soil heat flux in W/m^2. Power units are typically integrated over daily, hourly or 30-minute time frames to obtain energy values.

2.3.3.1. Calculation of H

The H was calculated as follows (Jia et al., 2009; Rijal et al., 2012):

$$H = \rho C_p \overline{w'T'} \tag{2.2}$$

where ρ is the density of air (ranged from 1.09 to 1.39 g/m^3), C_p is the specific heat of air (1,004.67 J/(g °C)), T' is the fluctuation of air temperature in °C, and w' is the fluctuation of vertical wind speed in m/s.

The measured wind speed and sound velocity in three orthogonal directions by the sonic anemometer provided more refined direction of the collected data with the natural coordinate systems (Sumner, 2001). These measured components in three directions depends on air density, atmospheric pressure, vapor pressure and absolute air temperature. In practice, the sonic anemometer computes the sonic temperature, and for H estimation, the sonic temperature was corrected for the difference between sonic and actual air temperature. The wind vectors (u, v, w) formed in the three coordinate directions (x, y, z) with direction z initially oriented with respect to gravity and the other two directions were arbitrary. The measured wind speed in term of orientation should be mathematically rotated to the natural coordinate system (Summer, 2001). These rotations force $\bar{v}$ and $\bar{w}$ to equal zero, and thus, $\bar{u}$ is pointed directly into the airstream as previously described (Sumner, 2001).

2.3.3.2. Calculation of G

The G at the soil surface was measured with soil heat flux plates at a fixed depth of 8 cm (Jensen and Allen, 2017) to ensure that the sensors were located below the zone of soil water vaporization. Due to strong thermal gradients near the soil surface during the late morning and early evening, two soil temperature sensors were placed above each soil heat flux plate at depths of 2 and 6 cm. The soil heat flux at the soil surface was the sum of the measured G at 8 cm depth and the stored energy above the soil heat plate. The measured G was calculated from the average values of two soil heat flux plates to decrease the impact of spatial variation. The storage energy was then corrected using the change in soil temperature over time, and the soil thermal properties. The G calculation was as follows:

$$G = G_{plate} + C_s\ (\Delta T/t)\ Z_{plate} \qquad (2.3)$$

where G_{plate} (W/m^2) is the measured G by the soil heat flux plate at depth Z_{plate} (0.08 m) beneath the soil surface, ΔT is the change in soil temperature in °C at 2 and 6 cm over the time, and t (time interval between the measurement in seconds, 1,800 s) at depth Z_{plate}. C_s is the heat capacity of moist soil in J/(m^3 °C), which is calculated using the soil water content and other soil properties as follow:

$$C_s = \rho_b * c_d + \theta_v * \rho_w * c_w \qquad (2.4)$$

where ρ_b is bulk density, 1.09 g/cm^3 from Table 2.1, c_d is heat capacity calculated for the study area soil (786.4 J/(kg °C)) (Prunty and Bell, 2005), θ_v is soil volumetric moisture content in

cm^3/cm^3, ρ_w is the density of water (assumed constant at 1000 kg/m^3), and c_w is heat capacity of water (4,190 J/(kg °C)).

In 2012, from May 12 through July 12 (62 days), the soil heat flux plate and soil temperature sensors stopped working and no record was available for measured soil heat flux. Therefore, as recommended by Allen and Jensen (2017) for clipped grass, 10 percent of the daily R_n was used to estimate the missing G values.

The 30-minute LE values (W/m^2) were used to calculate the 30-minute ET_a (mm/30-min) during the daytime when the R_n became positive, mainly between 8 a.m. and 8 p.m. (Campbell and Norman, 1998) as follows:

$$ET_a = \left(\frac{1800*LE}{\lambda_{LE}*\rho_w}\right) \tag{2.5}$$

where 1800 is a time conversion from second to half-hour, and λ_{LE} is the latent heat of vaporization which varies with the air temperature (T_a) as Lee et al. (2004):

$$\lambda_{LE} = (3147.5 - 2.37T_a) * 10^3 \tag{2.6}$$

2.3.4. Reference evapotranspiration

The daily ET_o values were calculated from the ASCE-EWRI standardized equation (Allen et al., 2005) using data from the Fargo NDAWN weather station, located 100 m from the EC system:

$$ET_o = \frac{0.408\Delta(R_n - G) + \gamma\left[\frac{900}{T_{mean}+273}\right]u_2(e_s - e_a)}{\Delta + \gamma(1 + 0.34u_2)} \tag{2.7}$$

where R_n and G are net radiation and soil heat flux in MJ/m^2, Δ is the slope of the saturation vapor pressure curve (kPa/ °C), γ is the psychrometric constant (kPa/ °C) calculated as a function of atmospheric pressure (P) ,T_{mean} is the mean of air temperature (°C), e_s and e_a are the saturation and actual vapor pressure (kPa) calculated for daily time steps using measured relative humidity, maximum and minimum air temperature, and u_2 (m/s) is the wind velocity at 2-m height. The calculation for the parameters in Eq. (10) followed the detailed procedures in the ASCE-EWRI method (Allen et al., 2005).

2.4. Results and discussion

2.4.1. Climate

The average monthly air and soil temperatures, wind speed, incoming solar radiation and precipitation amounts from daily data obtained from the Fargo NDAWN station are listed for each year in Table 2.3.

Table 2.3. Average monthly weather data during the growing season (2011-2013) at the North Dakota Agricultural Weather Network (NDAWN) Fargo site.

Year	Month	T_{avg} (°C)[a]	T_{soil} (°C)[b]	U_2 (m/s)[c]	R_s (MJ/m^2)[d]	Precipitation (mm)
2011	May	12.9	11.5	4.4	16.4	110
Normal	Jun.	19.2	18.5	3.9	19.9	101
	Jul.	23.7	23.5	3.1	21.6	104
	Aug.	21.7	22.1	3.3	19.6	73
	Sep.	15.4	16.4	3.4	15.3	4
	Oct.	11.3	10.7	3.9	10.2	21
	Average/Total	**17.4**	**17.1**	**3.7**	**17.2**	**411**
2012	May	16.0	16.0	4.2	18.2	43
Dry	Jun.	21.0	21.5	3.7	21.2	57
	Jul.	24.9	26.7	3.1	21.9	30
	Aug.	20.5	23.7	2.9	20.3	21
	Sep.	15.3	17.0	3.4	15.2	1
	Oct.	6.6	8.0	4.4	7.7	62
	Average/Total	**17.4**	**18.8**	**3.6**	**17.4**	**215**
2013	May	14.0	13.0	4.2	17.9	141
Wet	Jun.	19.7	19.1	3.6	20.1	199
	Jul.	22.0	23.4	3.1	20.9	26
	Aug.	21.7	23.2	2.9	18.6	12
	Sep.	18.0	18.5	3.4	12.3	106
	Oct.	7.1	8.1	3.5	6.8	112
	Average/Total	**17.1**	**17.3**	**3.4**	**16.1**	**598**

[a] T_{avg}: average air temperature, [b] T_{soil}: average soil temperature, [c] U_{avg}: wind speed, [d] R_s: monthly average incoming solar radiation

The highest monthly rainfall typically occurs in May and June. In 2013, the highest rainfall amounts of 141 and 200 mm occurred in May and June, respectively. In 2011 and 2013, several large rain events happened, with the highest rainfall amounts recorded on June 21, 2011

(47 mm), and June 25, 2013 (77 mm). The cumulative rainfall amounts, and distribution of rain events were different in each growing season (May-October), with 411, 215, and 598 mm in 2011, 2012, and 2013, respectively. The 30-year normal rainfall amount based on NDAWN records is about 450 mm. Thus, according to the weather of the study years, 2011 was categorized as a normal year while 2012 with less than half of the average rainfall amount was categorized as a dry year, and 2013, with about 50% more rainfall than average was a relatively wet year.

The amount and distribution of daily rainfall amounts, and the average SWC at the 15, 30, 45, 60, 75 and 90 cm depths during the three study years are shown in figure 2.2.

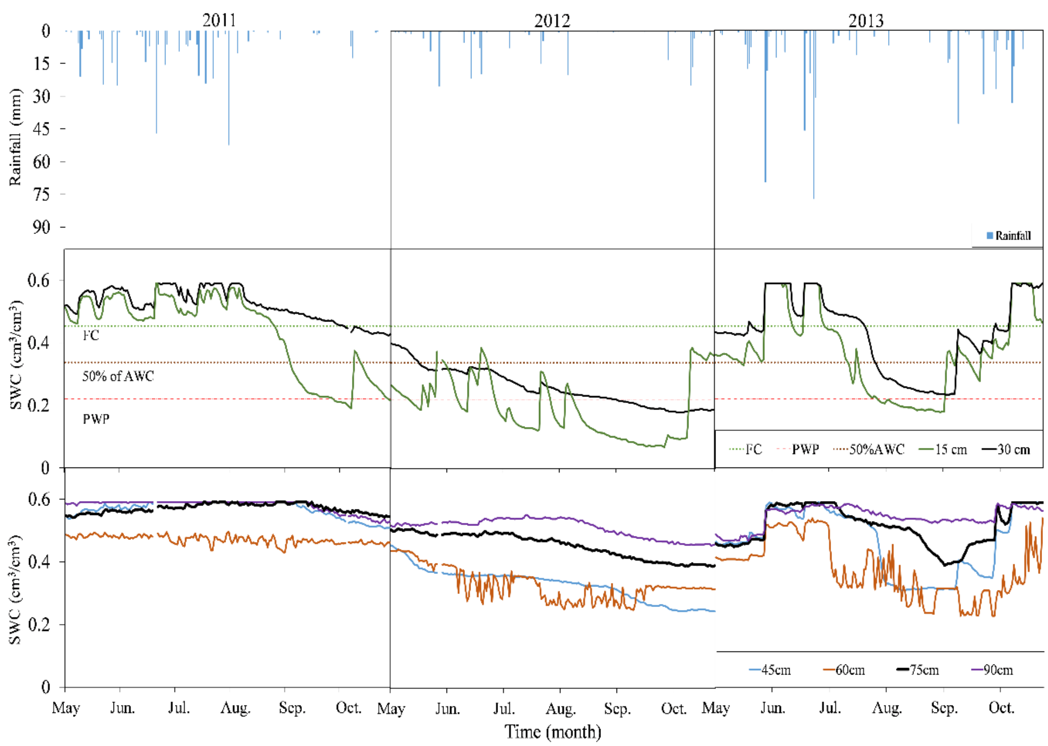

Figure 2.2. Rain amounts (top figure), soil water content (SWC) at field capacity (FC), permanent wilting point (PWP), 50% of available water content (50% AWC), and 15 and 30 cm depth (middle figure), and SWC at 45, 60, 75 and 90 cm depth (bottom figure) during the growing season at the research site in Fargo, North Dakota. Labels indicate the start of each month.

For the 2011 growing season, rain events occurred more frequently with a higher magnitude from May to August during the high-water demand period of turfgrass. In 2012, the largest daily rainfall amount of 25 mm occurred in late May. In 2012, the turfgrass experienced severe stress in term of sufficient water availability.

During the grass growth period between July and September of 2012 and 2013, a small amount of rain was observed, and the SWC in the root zone approached the PWP. However, after a couple of rain events in late August 2013, the SWC increased to an acceptable range and the grass turned green again.

In comparison with the 2012 and 2013 study years, 2011 had better average SWC (0.53 m^3/m^3) up to mid-growing season (Fig. 2.2). Because of frequent rain events, the saturated zone (59% SWC) fluctuated between the 75 and 90 cm depth. The available soil water content for the turfgrass was above the FC line until the mid-growing season when no water-related stress was observed. The average of SWC for 60, 75 and 90 cm soil layers 0.47, 0.57 and 0.57 m^3/m^3, respectively. In 2012, the soil moisture down to 60 cm was less than 50% AWC for most of the growing season, indicating that there was insufficient water in the assumed root zone (30 cm) for plant uptake. As described before, the study area has a Fargo silty clay loam with a very high rate of shrinkage during dry periods. Due to the shrinking of the soil at low SWC, surface cracks formed which potentially generated air pockets with a very low dielectric constant that caused the underestimation of SWC by the soil water sensors which is in agreement with Ojo et al. (2015) observations. Despite low accessible water for turfgrass at shallow depths, water from the deeper soil layers could have supported grass growth due to capillary action (Carrow, 1995). Since the study area was planted around 1990, the grass has experienced several drying and wetting cycles. Harivandi et al. (2009) reported that the approximate root depth under normal conditions were up to 1 and 2 meters for cool and warm season turfgrass, respectively. Self-evidently, the depth in drought and deficit water conditions can be deeper than that under normal growing conditions and turfgrass can survive by obtaining available moisture from deeper zones. The root depth was likely deeper than the assumed 30 cm, thus, it had the capability to obtain the deeper moisture in the soil. Therefore, due to the soil shrinkage and cracking in drought conditions and a deeper root zone than assumed, the soil moisture sensors at 60, 75 and 90 cm were considered to explain the SWC at a deeper soil layer. The average of the SWC for 60, 75 and 90 cm of soil layers was 0.34, 0.45 and 0.51 m^3/m^3 respectively which could overcome the water deficiency.

During the 2013 growing season, the magnitude of the rain events were larger but less frequent than that in 2011. During the high-water demand period from July to August 2013, the average SWC was low (0.28 m^3/m^3) because of insufficient rainfall events and amounts. Even though the soil was dry in the top 30 cm, the capillary rise from the deeper soils and the development of the root zone may have provided additional water to the grass and prevented it from going into the dormant stage. During drought condition of soil surface layer, the average of the SWC at 60, 75 and 90 cm depths was 0.33, 0.51 and 0.54 m^3/m^3, respectively.

According to Younger et al. (1981), the SWC at the beginning of the growing season affects the turfgrass growth. During the study period, the SWC was greater than the FC (0.45 cm^3/cm^3) at the deeper soil layer (75 and 90 cm) in 2011 and 2013 (Fig. 2.2), which contributed to turfgrass growth during drought periods, such as August and September 2013. The mixed turfgrass exhibited high drought tolerance by developing a deep, extensive, and viable root system (Carrow, 1995). The turfgrass survived by going dormant during drought period, but its crown remained alive and regrew when adequate water became available, similar to what Hanson and Juska (1969) had indicated.

2.4.2. Energy fluxes and evapotranspiration

The daily average daytime R_n, LE, H, and G values for the study period are shown in figure 2.3. All energy fluxes showed high day-to-day variability, mainly due to changes in weather conditions and SWC. The daily R_n values above the canopy varied from 18 to 537 W/m^2, with an average of 254 W/m^2; the H was between -25 and 269 W/m^2, and the smallest energy component G ranged from -22 to 67 W/m^2. The LE values were correlated to the R_n trend, representing the relationship between the ET to net received energy. This relationship was also presented in Jia et al. (2009), who observed the highest values of LE and the R_n during the spring and summer and lower values in winter for a turfgrass site in Florida. The LE values were lower at the beginning of the growing season except for 2013, in which illustrated high evaporation rate due to the water availability. Most of the available energy was partitioned to H rather than LE on late part of 2011 and all over of 2012 growing season due to the soil water deficit.

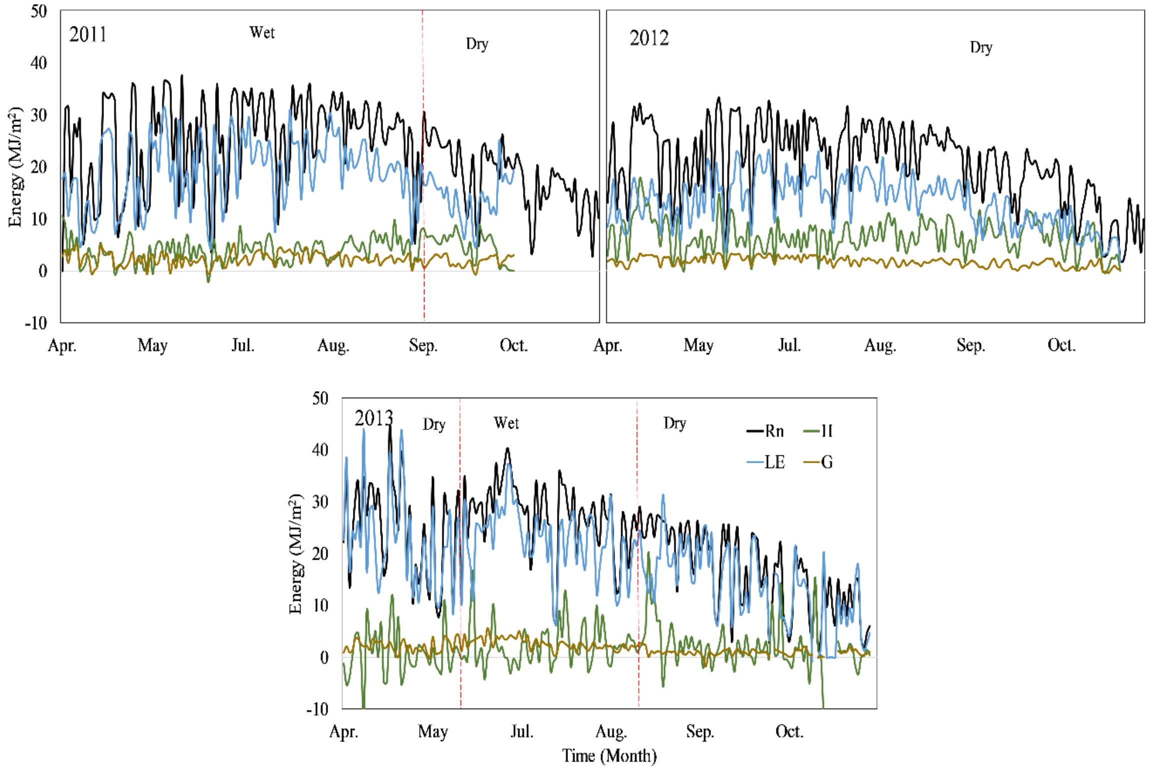

Figure 2.3. Daily average energy balance components (Rn: net radiation, LE: latent heat flux, H: sensible heat flux, and G: soil heat flux) for turfgrass during the growing season at the research site in Fargo, North Dakota.

Due to the drought condition in 2012, 31% of R_n was partitioned to H, while in 2011 and 2013, 19% and 6% of the R_n were partitioned into H, respectively. The highest measured H/R_n was 28% in September 2011, 39% in September 2012, and 12% in August 2013, respectively. The minimum H/R_n ratio was measured during the peak growth period with 13% in June 2011, 25% in June and July 2012, and 6% in June 2013. The higher H/R_n ratio indicated a greater heat energy transfer and larger temperature difference between the surface and the atmosphere. Due to frequent rain events in 2011 and 2013, the SWC in soil was high, therefore, large amount of R_n was partitioned to LE, yielding 73% and 83% of LE/R_n in 2011 and 2013, respectively. In 2012, the amount of R_n partitioned to LE did not exceed 67%, while the average partitioned LE was 62% of total R_n which was about 16% less than that in the other two years.

As shown in figure 2.3, in all of the study years, during the time when the H was negative, the LE was close to exceeding R_n. This represents the presence of advection from the surrounding areas due to horizontal movement of wind, similar to what has been reported by Payero and Irmak (2013) in Nebraska. High transpiration and evaporation rates were the main reason for the LE excess during the days with or after heavy rain. The LE values came close or even exceeded the R_n values sometimes in 2013 after several heavy rain events. Overall, the results are in agreement with the conclusion by Li et al. (2008), where the period which had the highest crop ET_a, also had the highest total available energy to increase ET_a.

Average monthly daytime energy fluxes and the average daily ET_a values are summarized in Table 2.4. The maximum and the minimum R_n values were found in July and October, respectively. Similarly, the LE values were at the maximum level in July due to the high SWC and the minimum level in October due to low air temperature. For the three years, the highest cumulative ET_a was found in 2013, a wet year due to the high rain amounts and relative humidity, and the lowest ET_a was observed in 2012, a dry year. The cumulative ET_a for 2011, a normal year, was more than that in 2012, but less than that in 2013. The ET_a rates showed similar seasonal patterns as the rainfall, higher from May to August in 2011 due to sufficient water supply for grass growth. In the winter of 2010 and spring 2011, a record high snowfall and sequential spring flood caused by snowmelt runoff water provided sufficient moisture in the root zone that also helped the grass growth. Regarding the 2011 climate variables, more energy in terms of R_n was received and the average air temperature was about 2 °C higher than that in other study years. Therefore, the high availability of the energy and water in the soil along with higher average wind speed rate enhanced measured ET_a values.

Table 2.4. Monthly averages of daily fluxes (Rn: net radiation, G: soil heat flux, H: sensible heat flux, and LE: latent heat flux) and actual evapotranspiration (ETa) and cumulative monthly rain amount during the 2011-2013 growing season at the research site in Fargo, North Dakota.

Month	R_n[a] (MJ/m^2)	G[b] (MJ/m^2)	H[c] (MJ/m^2)	LE[d] (MJ/m^2)	ET_a[e] (mm/day)	Rain (mm/month)
2011						
May	19.1	1.7	3.0	14.4	3.3	110
Jun	24.3	1.5	3.1	19.7	4.5	101
Jul	27.5	2.8	3.9	20.8	4.7	104
Aug	27.1	2.1	4.6	20.4	4.1	73
Sep	20.7	1.8	5.7	13.2	2.4	4
Oct	7.7	0.3	-	-	-	21
Average	**21.0**	**1.7**	**4.1**	**17.7**	**3.8**	**-**
2012						
May	21.9	1.9	7.7	12.2	2.6	43
Jun	24.4	2.4	6.1	15.9	3.5	57
Jul	24.8	2.2	6.1	16.5	3.7	30
Aug	24.2	1.6	7.2	15.5	3.3	21
Sep	18.9	1.2	7.3	10.3	1.8	1
Oct	10.6	0.6	3.2	6.7	1.0	62
Average	**20.7**	**1.7**	**6.2**	**12.8**	**2.7**	**-**
2013						
May	26.7	3.1	-0.7	24.2	4.6	141
Jun	28.0	4.5	0.9	22.6	4.6	199
Jul	27.3	3.3	2.6	21.3	4.4	27
Aug	24.2	2.6	2.9	18.6	3.7	12
Sep	18.1	1.8	1.0	15.3	2.7	106
Oct	11.5	1.1	0.7	9.6	1.5	112
Average	**22.6**	**2.7**	**1.3**	**18.6**	**3.6**	**-**

[a] R_n: net radiation (average of instantaneous positive Rn), [b] LE: latent heat flux, [c] H: sensible heat flux, [d] G: soil heat flux, [e] ET_a: crop evapotranspiration.

2.4.3. Ratio of ET_a/ET_o

Daily rainfall amounts, calculated ET_o, measured ET_a, and the ratio of ET_a/ET_o from May to October for the three study years are shown in figure 2.4. To represent the well-water turfgrass growth condition during the study period, days with sufficient soil moisture (> 50% AWC) in the root zone were selected for the ET_a/ET_o analysis. During raining days, water might affect the EC instrument performance, therefore, the days with rainfall > 10 mm amount were also excluded.

After the turfgrass experienced a prolonged drought stress period, a post-stress recovery period of 6 days (t> 6) was considered in the ET_a/ET_o calculation even the SWC was greater than 50% AWC in the root zone due to rainfall events. In figure 2.4, the screened days with SWC> 50% AWC, rainfall less than 10 mm and 6 days recovery period were selected to obtain the ET_a/ET_o ratio, which were shown as shaded area.

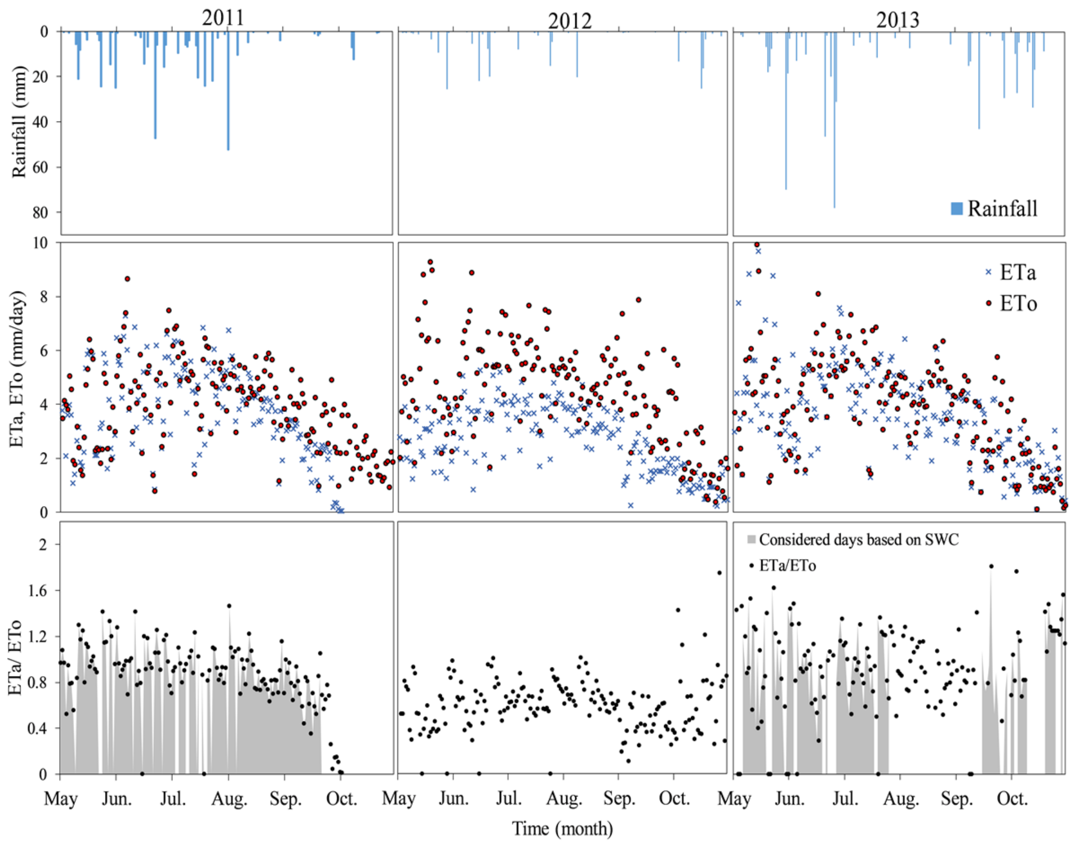

Figure 2.4. Daily rainfall, actual and reference evapotranspiration rates (ET_a and ET_o) and the ratio of ET_a/ET_o after screening (SWC>50% AWC, rainfall<10 mm, and 6 days of recovery period: shaded area) for 2011, 2012 and 2013 growing seasons.

The seasonal ET_o and ET_a for the three study years showed similar trends with the difference in daily values. In 2011, most parts of the growing season had sufficient water in the root zone to enhance the ET_a rate and the number of screened days were more than in other study years. The ratio of ET_a/ET_o was impossible to obtain in 2012 because the available water was less than 50% for the entire growing season, and there were no days to satisfy the defined screening criteria (SWC>50% AWC, rain<10 mm, and recovery period of 6 days). The 2013 growing season had slightly higher average air temperature than that in 2011, a lower rate of received solar radiation but higher amounts of rain amount which gained higher measured LE and ET_a values than 2011 and 2012 study years. Due to frequent rain events in June, sufficient water was available to enhance ET_a. The ratio of ET_a/ET_o was reduced from August to September due to a reduction in soil moisture. From the middle of September to the end of the growing season several rain events occurred enabling a grass recovery period for ET_a/ET_o calculation.

Table 2.5 shows the monthly and average of daily measured ET_a and calculated ET_o values for each month of study years where the total number of days used to calculate the ET_a/ET_o ratio were based on the criteria of SWC>50%AWC, rainfall<10 mm, and considering 6 days for recovery after heavy rain events. Only the days that satisfied the mentioned criteria were used to calculate the optimum ET_a/ET_o ratio for each day and the results are reported as a monthly average for each month of the study years.

Table 2.5. Summarized monthly and daily measured turfgrass evapotranspiration by eddy covariance (ET_a), reference evapotranspiration (ET_o), and averages monthly ET_a/ET_o ratio for turfgrass during the growing season in 2011, 2012, and 2013.

Year	Month	Rainfall	ET_a	ET_o	Avg. daily ET_a/ET_o	No. of days considered	Screened ET_a/ET_o**
		mm	mm/month, (mm/day)	mm/month, (mm/day)		days*	
2011	May	110	108 (3.5)	109 (3.4)	1.01	26	1.01
Normal	Jun.	101	134 (4.5)	140 (4.7)	1.00	26	1.00
	Jul.	104	147 (4.7)	156 (5.0)	0.94	19	0.94
	Aug.	73	126 (4.1)	141 (4.6)	0.90	29	0.90
	Sep.	4	71 (2.4)	103 (3.5)	0.67	21	0.71
	Oct.	21	-	63 (2.0)	-	-	-
2012	May	43	82 (2.6)	155 (5.0)	0.60	0	-
Dry	Jun.	57	109 (3.6)	165 (5.5)	0.65	0	-
	Jul.	30	118 (3.8)	173 (5.6)	0.68	0	-
	Aug.	21	102 (3.3)	149 (4.8)	0.70	0	-
	Sep.	1	56 (1.9)	128 (4.2)	0.44	0	-
	Oct.	62	32 (1.0)	56 (1.9)	0.66	0	-
2013	May	141	142 (4.6)	122 (4.2)	1.06	23	1.05
Wet	Jun.	199	137 (4.6)	144 (4.8)	0.99	25	0.96
	Jul.	27	136 (4.4)	152 (4.9)	0.94	25	0.95
	Aug.	12	115 (3.7)	136 (4.4)	0.88	0	-
	Sep.	106	82 (2.7)	96 (3.2)	0.88	12	0.93
	Oct.	112	46 (1.5)	42 (1.5)	1.12	19	1.18
	Average				**0.83**		**0.96**

*Only days with sufficient soil moisture (>50% AWC), rainfall<10 mm, and without the preceding 6 days of water stress condition were considered for ET_a/ET_o calculation.
** ET_a/ET_o ratio from screened days

The bimonthly ET_a/ET_o ratios for the three years with and without the screening are shown in figure 2.5. A strong relationship between the ET_a/ET_o ratio and the available SWC can be easily found. The bimonthly ET_a/ET_o ratio was low when the soil water status, rainfall, and recovery period were not considered. However, after applying the SWC, rainfall, and recovery period criteria, the daily ET_a/ET_o ratio used for the bimonthly ET_a/ET_o ratio calculation stayed the same, but the number of days used for ET_a/ET_o ratio calculation was reduced and the screened ET_a/ET_o ratios were increased.

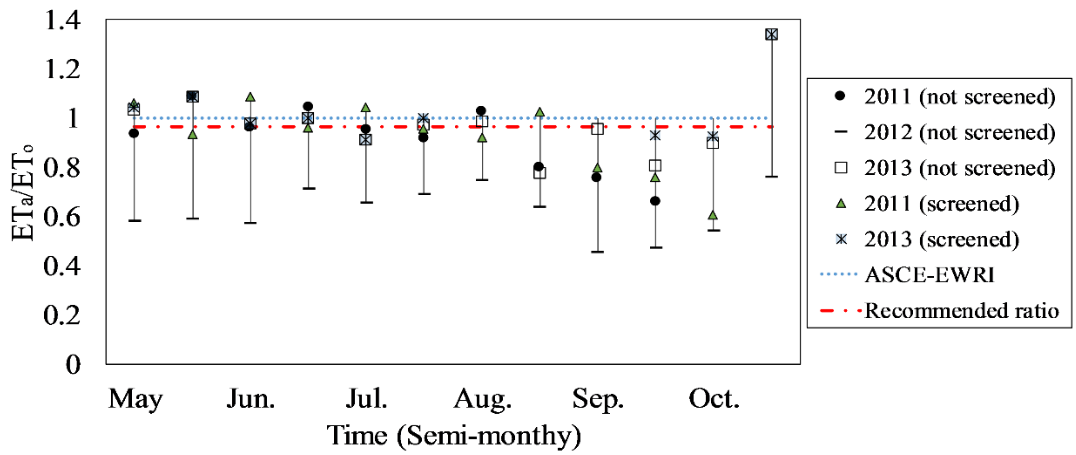

Figure 2.5. Average bimonthly ratio of measured and reference evapotranspiration (ET_a/ET_o) of turfgrass (with and without considering the screening criteria) obtained from eddy covariance measurement for the research site in Fargo, North Dakota.

The impact of plant stress and SWC during the growing season of 2012 decreased the calculated ET_a/ET_o values because the available soil water was not able to meet the plant water consumption. Due to insufficient SWC for grass growth (Fig. 2.2), the ratio of daily ET_a to ET_o in 2012 was lower than that for the other two years. Harivandi et al. (2009) reported the minimal rate for cool and warm season grass to survive as 0.2 and 0.4, respectively, which confirmed that the turfgrass in the current study would not die because of the drought stress condition. The minimal ET_a/ET_o ratio of 0.23 in 2012 showed that the grass survived by utilizing the upward flux water from deeper soil zones.

Water table depth affected the groundwater table contribution to ET. For example, Zhu et al. (2017) found that upward flux contributed 58, 47, and 69 percent of the total ET for dry, normal and wet seasons, respectively. Kolars (2016) showed that the upward flux ranged from 0 to 7.5 mm/day during the growing season due to shallow groundwater for a similar soil. Therefore, turfgrass may use water in deeper soil layer to satisfy water requirements during a drought situation. The ET_a/ET_o ratio for 2013 follows the trend in 2011 with a lower ratio by the end of August. A large rain event in September 2013 supported the grass water requirement, thus the measured ET_a increased and showed a higher ET_a/ET_o ratio than those during any other month of the growing season. Overall, for the chosen days based on 50% AWC, 2011 and 2013 had the similar ET_a/ET_o ratios, which suggests that the turfgrass experienced similar conditions for both a normal and wet year during the growing season and had sufficient water for evapotranspiration.

The average ET_a/ET_o ratios for 2011, 2012 and 2013 with all measured data were 0.91, 0.62 and 0.98, respectively. After excluding the 50%AWC, rainy days, and recovery period after drought, the ET_a/ET_o ratios were 0.91 and 1.01 for 2011 and 2013, respectively, and there was no days left in 2012 for the calculation. The average screened ET_a/ET_o ratios on a monthly basis using the acceptable data were 1.03, 0.98, 0.94, 0.90, 0.82 and 1.18 from May to October, respectively.

Since the ASCE-EWRI ET_o method was developed with one of the primary reference crops as clipped grass on well-watered and ideal conditions, it was expected that the ET_o was higher than the actual field measured ET_a unless the field was comparable with favorable reference crop growing conditions. Based on the result obtained from EC method and considering the SWC, the average ET_a/ET_o ratio 0.96 can be recommended as a general value to estimate ET_a in eastern North Dakota under non-stressed condition.

In Nebraska, Kopec et al. (1988) observed a measured ET_a/ET_o value of 0.80 for moderate moisture stressed turfgrass. In California, Meyer and Gilbeault (1987) reported 0.85 as the mean value for cool season turfgrass. A review of grass ET_a and ET_o by Romero and Dukes (2016) stated that the ET_a/ET_o value for stressed turfgrasses ranged from 0.79 to 0.82. In a similar study, Harivandi et al. (2009) reported that the ET_a/ET_o ratio for an optimally performing cool-season turfgrass was 0.8 for irrigation purposes. The average ET_a/ET_o value obtained in this study by including turfgrass ET_a measurements during normal, dry and wet years under non-irrigated conditions was 0.96 (Table 2.5) with the screening criteria. Therefore, this value can be recommended to represent trufgrass water requirement under a well-watered ideal condition for the region. For water conservation purposes, drought-tolerant turfgrass cultivars would be highly recommended, and over the growing season, adjustment of the ET_a/ET_o ratio for continual green turfgrass should be considered for maintenance purposes.

2.5. Conclusion

During the 2011, 2012 and 2013 growing seasons, an eddy covariance system and two sets of soil moisture sensors were used to measure the actual evapotranspiration rates on a mixed turfgrass field in eastern North Dakota. Meteorological data from the Fargo NDAWN site was used to calculate the grass-based reference ET rates using the standardized ASCE-EWRI method. Due to high variability in the precipitation amounts (411, 215 and 598 mm in 2011, 2012, and 2013, respectively), the turfgrass ET measurements were also different. The latent heat flux that is equivalent to turfgrass ET comprised 73%, 62%, and 83% of net radiation in 2011, 2012, and 2013, respectively. The mean ratio of actual turfgrass ET to reference ET (ET_a/ET_o) was estimated to be 0.96 using screened daily data from all three years when the soil had greater than 50% of the available water (50% AWC) in the root zone, with rainfall less than or equal to 10 mm, and a 6 day recovery period after drought. For non-irrigated and natural condition, the soil moisture sensors can be useful for turfgrass stress detection, and a useful tool to select well-watered and ideal turfgrass growing conditions for reference evapotranspiration measurements.

The ASCE-EWRI grass-based reference ET can be used to estimate turfgrass ET even in cold and sub-humid climate conditions and can be used for water management of turfgrass in northern climates. Since this is the first reported study on turfgrass ET_a measurement in this area, the results can provide a baseline on turfgrass water management under various weather conditions. The results indicated that a monthly refinement of ET_a/ET_o values may be required to maintain the landscape turfgrasses more precisely in terms of water consumption. This research also verified that the standardized ET_o equation can be applied in eastern North Dakota to guide crop water management.

2.6. References

Allen, R. G., & Fisher, D. K. (1990). Low-cost electronic weighing lysimeters. Transactions of the American Society of Agricultural Engineers. https://doi.org/10.13031/2013.31546

Allen, R. G., Pereira, L. S., Howell, T. A., & Jensen, M. E. (2011). Evapotranspiration information reporting: I. Factors governing measurement accuracy. Agricultural Water Management. https://doi.org/10.1016/j.agwat.2010.12.015

Allen, R. G., Walter, I. A., Elliot, R., Itenfisu, D., Jensen, M. E. (2005). ASCE Standardized Reference Evapotranspiration Equation. ASCE-EWRI Task Committee. Final Rep. Jan.

Anapalli, S. S., Green, T. R., Reddy, K. N., Gowda, P. H., Sui, R., Fisher, D. K., … Marek, G. (2018). Application of an energy balance method for estimating evapotranspiration in cropping systems. Agricultural Water Management. https://doi.org/10.1016/j.agwat.2018.04.005

Anderson, M. C., Allen, R. G., Morse, A., & Kustas, W. P. (2012). Use of Landsat thermal imagery in monitoring evapotranspiration and managing water resources. Remote Sensing of Environment. https://doi.org/10.1016/j.rse.2011.08.025

Baldocchi, D. D. (2003). Assessing the eddy covariance technique for evaluating carbon dioxide exchange rates of ecosystems: Past, present and future. Global Change Biology. https://doi.org/10.1046/j.1365-2486.2003.00629.x

Bastiaanssen, W. G. M. (2000). SEBAL-based sensible and latent heat fluxes in the irrigated Gediz Basin, Turkey. Journal of Hydrology. https://doi.org/10.1016/S0022-1694(99)00202-4

Burns, T. T., Adams, J. R., & Berg, A. A. (2014). Laboratory calibration procedures of the hydra probe soil moisture sensor: Infiltration wet-up vs. dry-down. Vadose Zone Journal. https://doi.org/10.2136/vzj2014.07.0081

Campbell, G. S., & Norman J. M. (1998). An introduction to environmental biophysics, 2nd ed. Springer, New York.

Carrow, R. N. (1996). Drought avoidance characteristics of diverse tall fescue cultivars. Crop Science. https://doi.org/10.2135/cropsci1996.0011183X003600020026x

Castellví, F., & Snyder, R. L. (2010). A comparison between latent heat fluxes over grass using a weighing lysimeter and surface renewal analysis. Journal of Hydrology. https://doi.org/10.1016/j.jhydrol.2009.11.043

Chávez, J. L., Howell, T. A., & Copeland, K. S. (2009). Evaluating eddy covariance cotton ET measurements in an advective environment with large weighing lysimeters. Irrigation Science. https://doi.org/10.1007/s00271-009-0179-7

Foken, T. (2008), The Energy Balance Closure Problem: An Overview. Ecological Applications, 18:1351-1367. doi:10.1890/06-0922.1

Goos, R. J., & Fairlie, T. E. (1988). Effect of ammonium thiosulfate and liquid fertilizer droplet size on urea hydrolysis. Soil Science Society of America Journal. https://doi.org/10.2136/sssaj1988.03615995005200020040x

Hillel, D. (1998). Environmental Soil Physics: Fundamentals, Applications, and Environmental Considerations. In Environmental Soil Physics.

Howell, T. A., Schneider, A. D., Dusek, D. A., Marek, T. H., & Steiner, J. L. (1995). Calibration and scale performance of Bushland weighing lysimeters. Transactions - American Society of Agricultural Engineers. https://doi.org/10.13031/2013.27918

Hanson A. A., & Juska F. V. (1969). Turfgrass Science. American Society of Agriculture. Madison, WI.

Harivandi, A. M., Baird, J., Hartin, J., Henry, M., & Shaw, D. (2009). Managing turfgrasses during drought. Division of Agriculture and Natural Resources, Publication 8395.

Howell, T. A., Schneider, A. D., Dusek, D. A., Marek, T. H., & Steiner, J. L. (1995). Calibration and scale performance of Bushland weighing lysimeters. Transactions - American Society of Agricultural Engineers. https://doi.org/10.13031/2013.27918

Imukova, K., Ingwersen, J., Hevart, M., & Streck, T. (2016). Energy balance closure on a winter wheat stand: Comparing the eddy covariance technique with the soil water balance method. Biogeosciences, 13(1), 63–75. https://doi.org/10.5194/bg-13-63-2016

Irmak, S., Skaggs, K. E., & Chatterjee, S. (2014). A Review of the Bowen Ratio Surface Energy Balance Method for Quantifying Evapotranspiration and other Energy Fluxes. Transactions of the ASABE, 57(6), 1657–1674. https://doi.org/10.13031/trans.57.10686

Jensen, M. E., & Allen, R. G. (2016). Evaporation, evapotranspiration, and irrigation water requirements. In Evaporation, Evapotranspiration, and Irrigation Water Requirements. https://doi.org/10.1061/9780784414057

Jia, X., Dukes, M. D., & Jacobs, J. M. (2009). Bahiagrass crop coefficients from eddy correlation measurements in central Florida. Irrigation Science. https://doi.org/10.1007/s00271-009-0176-x

Jia, X. Scherer, T. F., D. Lin, Zhang, Z., & Rijal, I. (2013). Comparison of Reference Evapotranspiration Calculations for Southeastern North Dakota. Irrigation & Drainage Systems Engineering. https://doi.org/10.4172/2168-9768.1000112

Kolars, K. (2016). INCORPORATION OF SUBSURFACE DRAINAGE AND SUBIRRIGATION INTO THE CHECKBOOK METHOD. M.S. Thesis, Department of Agricultural and Biosystems Engineering, North Dakota State University, Fargo, ND.

Kopec, D. M., Shearman, R. C., Riordan T. P. (1988). Evapotranspiration of tall fecuse turf. Horticultural Science, 23:300-301.

Li, S., Kang, S., Li, F., & Zhang, L. (2008). Evapotranspiration and crop coefficient of spring maize with plastic mulch using eddy covariance in northwest China. Agricultural Water Management. https://doi.org/10.1016/j.agwat.2008.04.014

Majnooni-Heris, A., Rashid Niaghi, A., Asadi, E., & Haghi, D. Z. (2013). Calibrating Net Solar Radiation of FAO56 Penman-Monteith Method to Estimate Reference Evapotranspiration. J. Appl. Environ. Biol. Sci.

Meyer, J. L., and Gilbeault, V. A. (1987). Turfgrass performance when underirrigated. Applied Agricultural Research. 2(2):17-119.

NDAWN. (2018). North Dakota Agricultural Weather Network. Fargo, ND. North Dakota State Uni. https://ndawn.ndsu.nodak.edu/ (accessed 22 Oct. 2018).

NRCS. (2018). Natural Resources Conservation Services, Web Soil Survey, https://websoilsurvey.sc.egov.usda.gov/App/HomePage.htm (access 22 Oct. 2018).

Niaghi, A. R., Vand, R. H., Asadi, E., & Majnooni-Heris, A. (2015). Evaluation of Single and Dual Crop Coefficient Methods for Estimation of Wheat and Maize Evapotranspiration. Advances in Environmental Biology, 9(3), 963–971.

Niaghi, A. R., & Jia, X. (2017). Determination of grass evapotranspiration rates and crop coefficients using eddy covariance method in Eastern North Dakota. World Environmental and Water Resources Congress 2017: Watershed Management, Irrigation and Drainage, and Water Resources Planning and Management - Selected Papers from the World Environmental and Water Resources Congress 2017. https://doi.org/10.1061/9780784480601.040

Ojo, E. R., Bullock, P. R., & Fitzmaurice, J. (2015). Field performance of five soil moisture instruments in heavy clay soils. Soil Science Society of America Journal. https://doi.org/10.213b/sssaj2014.0b.0250

Payero, J. O., Neale, C. M. U., Wright, J. L., & Allen, R. G. (2003). Guidelines for Validating Bowen Ratio Data. Transactions of the American Society of Agricultural Engineers. https://doi.org/10.13031/2013.13967

Payero, J. O., & Irmak, S. (2013). Daily energy fluxes, evapotranspiration and crop coefficient of soybean. Agricultural Water Management. https://doi.org/10.1016/j.agwat.2013.06.018

Prunty, L., & Bell, J. (2005). Soil temperature change over time during infiltration. Soil Science Society of America Journal. https://doi.org/10.2136/sssaj2004.0219

Rijal, I., Jia, X., Zhang, X., Steele, D. D., Scherer, T. F., & Akyuz, A. (2012). Effects of subsurface drainage on evapotranspiration for corn and soybean crops in southeastern North Dakota. Journal of Irrigation and Drainage Engineering. https://doi.org/10.1061/(ASCE)IR.1943-4774.0000508

Romero, C. C., & Dukes, M. D. (2015). Review of turfgrass evapotranspiration and crop coefficients. Joint ASABE/IA Irrigation Symposium 2015: Emerging Technologies for Sustainable Irrigation. https://doi.org/10.13031/trans.59.11180

Roy Xinhua Jia, D., & Steele Dongqing Lin, D. D. (2018). Development and comparison of soil water release curves for three soils in the red river valley. Soil Science Society of America Journal. https://doi.org/10.2136/sssaj2017.09.0324

Shi, T. T., Guan, D. X., Wu, J. B., Wang, A. Z., Jin, C. J., & Han, S. J. (2008). Comparison of methods for estimating evapotranspiration rate of dry forest canopy: Eddy covariance, Bowen ratio energy balance, and Penman-Monteith equation. Journal of Geophysical Research Atmospheres. https://doi.org/10.1029/2008JD010174

Steele, D. D., Sajid, A. H., & Prunty, L. D. (1996). New corn evapotranspiration crop curves for southeastern North Dakota. Transactions of the American Society of Agricultural Engineers. https://doi.org/10.13031/2013.27578

Sumner, D. M. (2001). Evapotranspiration from a cypress and pine forest subjected to natural fires, Volusia County Florida, 1998-99. Water Res. Inves. Rep. No. 01-4245, U.S. Geo. Survey, Tallahassee, FL.

Tanner, B. D., & Greene, J. P. (1989). Measurement of sensible heat and water vapor fluxes using eddy correlation methods. Final Report to U.S. Army, Dugway Proving Ground Duway UT. Contract No DAAD09-87D-0038.

Tanner, B. D., Swiatek, E., & Greene, J. P. (1993). Density fluctuations and use of the krypton hygrometer in surface flux measurements. Management of Irrigation and Drainage Systems: Integrated Perspectives.

Twine, T. E., Kustas, W. P., Norman, J. M., Cook, D. R., Houser, P. R., Meyers, T. P., … Wesely, M. L. (2000). Correcting eddy-covariance flux underestimates over a grassland. Agricultural and Forest Meteorology. https://doi.org/10.1016/S0168-1923(00)00123-4

Zhou, X., Bi, S., Yang, Y., Tian, F., & Ren, D. (2014). Comparison of ET estimations by the three-temperature model, SEBAL model and eddy covariance observations. Journal of Hydrology. https://doi.org/10.1016/j.jhydrol.2014.08.004

3. DRAINAGE WATER MANAGEMENT EFFECTS ON ENERGY FLUX PARTITIONING, EVAPOTRANSPIRATION, AND CROP COEFFICIENTS OF CORN [4]

3.1. Abstract

Over the past 20 years, marketplace demand for corn has prompted many farmers in the Red River Valley (RRV) of the north to include more corn in their crop rotations. With a very flat topography and heavy clayey soils, the RRV can have shallow water tables in the spring and fall but can be dry in the summer. Due to these field conditions, some farmers have installed subsurface drainage (SD) systems with structures for controlled drainage (CD, manage the water table in a field) and subirrigation (SI, add water to the field via the SD system) to improve corn production. In a CD + SI field, an eddy covariance system was used to measure and quantify energy flux components along with soil moisture content (SWC) and water table depth (WTD) measurements during four corn growing seasons in 2012, 2013, 2016 and 2017. The results show that the average SWC in 2012 was significantly different from the other three years. The SWC and WTD in 2016 were more stable compared to the other years. The CD practice had a positive effect during a wet year in 2013, which resulted in 26.7% higher yield than the county average. During the dry growing season of 2017, the use of subirrigation resulted in 6.6% higher yield than the county average. The corn evapotranspiration totals (ETa) were 468, 476, 551, and 537 mm for 2012, 2013, 2016, and 2017 growing seasons, respectively. The average crop coefficients were 0.49, 0.73, 0.88, 0.86, and 0.69 for the initial, development, tasseling, reproductive, and maturity stages, respectively. They were calculated from the daily ETa, values

[4] The material in this chapter was co-authored by Ali Rashid Niaghi, Xinhua Jia, Thomas F. Scherer, and Dean D. Steele was published in the Vadose Zone Journal as peer review article. Ali Rashid Niaghi had primary responsibility for analyzing the collected data, interpreting the results, developing the conclusion that are advanced here. Co-authors served as technical and editorial consultants in the development of the manuscript represented by this chapter. Niaghi, A.R., X. Jia, D. Steele, and T. Scherer. 2019. Drainage water management effects on energy flux partitioning, evapotranspiration, and crop coefficients of corn. Agricultural Water Management. doi.org/10.1016/j.agwat.2019.105760.

only from days with more than 45% of total available water in the root zone, and the ASCE-EWRI standardized grass-based reference evapotranspiration. This study showed that the SD along with the CD + SI system can be used for optimal water management of field corn during both wet and dry years.

3.2. Introduction

Corn is an important cereal crop in the United States with over 385 million metric tons of production in 2016/2017 (US Grains Council, 2019), which accounts for about one third of global corn production. The planted area for grain corn in North Dakota has increased from about 334,000 ha in 1997 to over 1.3 million ha in 2017 (USDA NASS, 2017). The increased demand for corn has prompted many farmers to grow more corn in North Dakota and particularly in the Red River Valley (RRV) of the north. Higher yields have been achieved due to improvements in farming technology and higher yield hybrids.

The RRV area has some of the most productive soils in the US, but the near flat topography, heavy clay soils, and increased salinity can hinder corn production due to shallow water table and seasonal waterlogging conditions in spring and fall. One of the most effective practices to aid in earlier planting and later harvest is to utilize subsurface drainage (SD) system. The SD system employs buried perforated pipes to drain excess water and lower the water table in the soil profile (Wang et al., 2004).

The SD system can be improved with controlled drainage (CD), with or without SI, to manage the water table elevation in agricultural fields. Using a weir or stop log, CD controls the time and amount of drainage outflow and keeps water table depths at a desired level. The SI system is defined as the “application of irrigation water below the ground surface by raising the water table within or near the root zone” (ASABE Standards, 2015). In recent years, SI has become a supplementary part for drainage water management strategies by adding water through the SD system and control devices (Jia et al., 2017). Hence, the combination of CD and SI (CD+SI) can provide an optimal soil water condition to enhance crop production. While various studies reported yield increase for different crops using CD+SI (i.e. tomatoes, soybeans, and corn), questions remain regarding the effect of drainage water management via a CD+SI system on corn performance, such as the relationship between soil water content, water table depth, and evapotranspiration (ET) during the crop growing season.

Among all factors (i.e. soil properties, weather variability, and salinity), ET plays a dominant role in crop production and is a critical factor in the hydrological cycle. Accurately determining the actual crop ET (ET_a), which is the plants' actual use of water in a CD+SI field can reveal crop water status and provide water management information to enhance crop production (Kandel et al., 2013; Sharma and Minhas, 2005), and improve nitrogen use efficiency (Mejia et al., 2000). Therefore, quantifying the ET_a in field conditions could be a practical way to make appropriate decisions under CD+SI water management and evaluate the use of CD+SI on various crop stages.

Several methods are available to measure daily ET_a directly. Some of the most used methods are ground-based, such as soil water balance and lysimeter (Djaman and Irmak, 2013; Niaghi et al., 2015). Others are above ground methods, including eddy covariance (Niaghi and Jia, 2017;Niaghi et al., 2019; Shi et al., 2008), surface renewal (Rosa and Tanny, 2015), Bowen ratio energy balance (Shi et al., 2008; Uddin et al., 2013), and remote sensing technology (Nagler et al., 2005; Niaghi, 2014). Since ET_a is an important component of water balance and hydrologic studies, considerable research efforts have attempted to estimate the ET_a from weather data (Allen et al., 1998). Therefore, ET_a can be indirectly determined from the reference evapotranspiration (ET_{ref}) calculated from weather data and the recommended crop coefficient (K_c) at various stages of the specified crop. The K_c represents regional climate characteristics, crop type, plant density, phenology, soil water status, and other parameters (Anderson et al., 2017), and should be developed for each study region.

Numerous studies, both in the past and ongoing, are or have been conducted to evaluate different approaches for estimating ET_a at the field scale (Anapalli et al., 2018; O'Brien et al., 2018; Majnooni-Heris et al., 2013). However, studies conducted under the CD+SI condition are limited. To develop the K_c values for each region, accurately measured ET_a in a field scale is necessary. The eddy covariance (EC) system is regarded as the most accurate method for *in situ* ET_a measurement at scales of 0.1 –1 km (Rana and Katerji, 2000). The EC has been successfully used to measure ET_a over different crop fields and forest lands (Facchi et al., 2013; Baker and Griffis, 2005) for decades. When using the EC method for energy balance research, the sum of sensible heat (H) and latent heat (LE) fluxes is about 10 –30% less than the available energy, R_n - G, where R_n is net radiation and G is soil heat flux (Russell et al., 2015). Twine et al. (2000) suggested to close the energy balance by assuming that the H was measured correctly with a sonic anemometer and then solve for LE as the residual in the energy balance equation ($LE=R_n-G-H$). This procedure was also used by Chávez et al.(2009), Niaghi et al. (2019), and Payero and Irmak (2013) for the LE calculation.

The EC system used by Rijal et al. (2012) in a field with CD treatment was used to develop new K_c values for corn in the RRV based on a one year's data. Due to climate, corn hybrids, and variable farming practices, one-year data will likely not fully represent the deviation of ET_a and K_c; therefore, their range and fluctuation remain unclear. Exacerbating the problem, other studies that have provided the regional K_c values were conducted several decades ago (e.g., Steele et al., 1996; Stegman, 1986). Since then, corn hybrids have evolved from conventional to modified hybrids with different water use and water stress characteristics (Payero and Irmak, 2013).The overall objective of this study was to estimate corn ET_a in a field for four years under CD+SI management, but with various climate conditions and different corn hybrids. The specific objectives were to (1) analyze the effect of CD+SI on soil water content and water table depth; (2) analyze daily, diurnal, and cumulative energy fluxes during various corn growing stages; (3) evaluate the crop yield along with the estimated ET_a; and (4) develop new crop coefficients at various growing stages.

3.3. Materials and methods

3.3.1. Field description

The experiment was conducted in the RRV on an agricultural field located in the Buffalo River watershed in Clay County, west central Minnesota (46 59’ 20’’ N, 96 41’ 06’’ W), with an altitude of 271 m above sea level (Fig 3.1). The area of the study field was 16.6 ha, characterized as poorly drainable containing a Bearden silt loam (50% of the total area), an Overly silty clay loam (27% of the area), and a Colvin silty clay loam (23% of the area) with an impermeable layer at about 3 m depth (Jia et al., 2017).

The SD system was installed in August, 2010 with 12.2 m spacing, 0.91 m of average tile depth on a 0.1% grade with a drainage coefficient of 9.5 mm/day (Jia et al., 2017). The diameter of the drainage main was 254 mm along the west side of the field. A second main line with 152 mm diameter corrugated non-perforated pipe was installed for SI water delivery purposes at the higher elevation (east) end of the field to account for slow flow caused by flat topography and small size of the laterals (76.2 mm). Thus, both irrigation and drainage followed the same flow path and direction with different application times during the season. Irrigation water for SI was provided by gravity flow from a storage tank located at the north side of the field. The water deliver pipe to the south side of the field had an uphill grade resulting in 0.6 m elevation difference (Jia et al., 2017) between the base of the storage tank and the end of the irrigation delivery pipe. A water pump was used to fill the tank from the legal ditch on the north side of the field and was monitored during the entire irrigation period using a current sensor. The volume and flow rate of the SI water was measured with an inline propeller meter (McCrometer, Hemet, California).

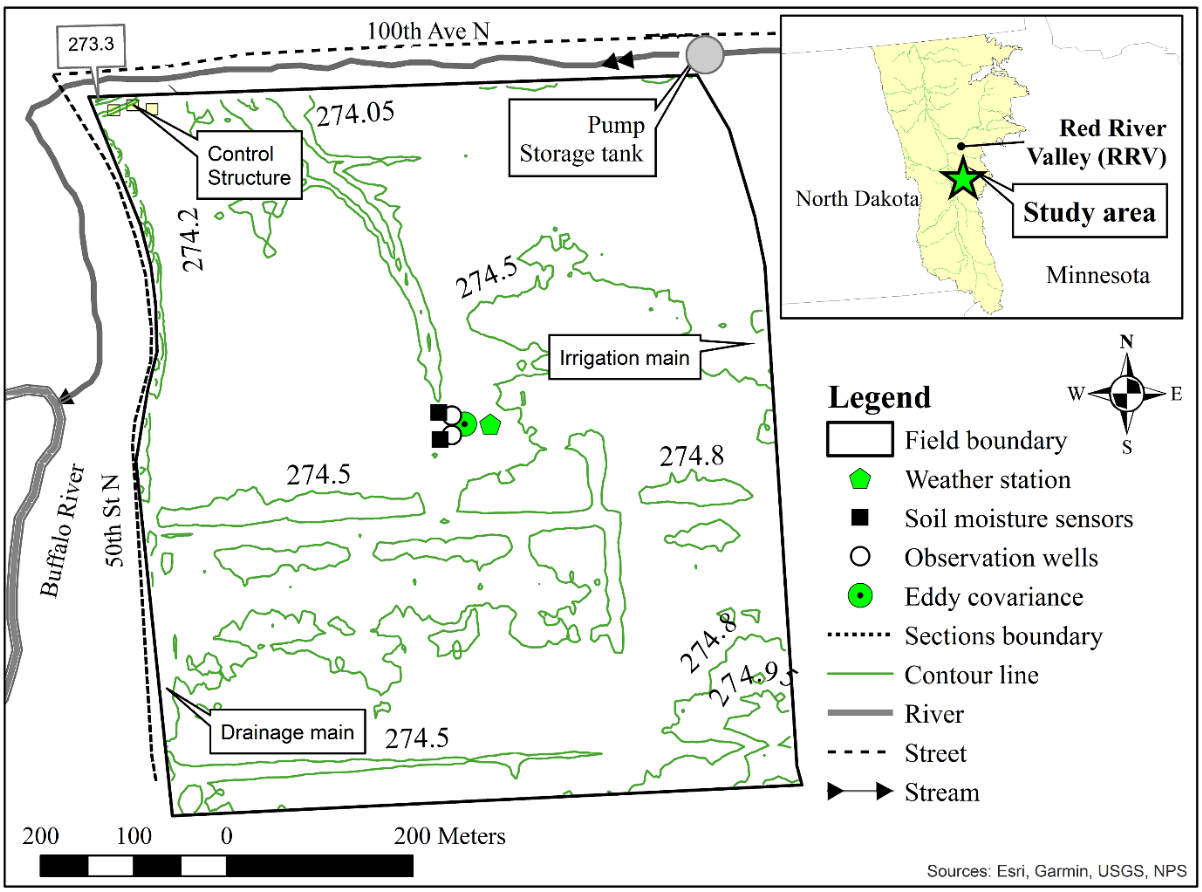

Figure 3.1. Study site in Clay County, MN.

Corn was grown in 2012, 2013, 2016, and 2017, while soybean was planted in 2014 and sugarbeets was in 2015. Corn row space was 76 cm with a plant spacing of about 10 cm. Emergence occurred within an average of 10 days after planting, and the emergence date was estimated from images taken by an automatic in-situ camera. The nitrogen fertilizer was applied as top dressing at the emergence stage according to the farmer. Corn height was measured weekly from the soil surface to the highest point of the arch of the uppermost leaf tip pointing downward. The grain was harvested with approximately 15% moisture, although the exact date changed each year. Hybrid nomenclature, planting, emergence, and harvesting dates, fertilizer rate, SI water application, and maximum crop heights during the four study years are shown in table 3.1.

Table 3.1. Field management information and weather conditions during the experimental time at Clay County, MN. CD is for controlled drainage and SI is for subirrigation.

Year/information	2012	2013	2016	2017
Corn hybrid	Dekalb 4310	Pioneer 38M58	Pioneer 9703	Golden Harvest 90YO11
Fertilizer* (N- P_2O_5) (kg ha^{-1})	235-78.5	224-90	224-73	168-78
Seeding date	1 May	May 14	Apr. 24	Apr. 28
Emergence date	May 15	May 22	May 7	May 8
Maximum Crop height (cm)	269	251	263	264
CD duration	May 23- Nov. 12	Apr. 15- Jul. 29; Aug. 15-Oct. 6	Apr. 6- Sept. 4; Sept. 7 - Nov. 16	May 1- Jul. 26; Oct. 20
CD weir depth from soil surface (cm)	-	51.7, 23.7, 0**	164.7	42.7
SI duration	-	Jul. 30- Aug. 14	Sept. 5-Sept. 6	Jul. 27-Aug. 10; Sept. 08; Oct. 9- Oct. 27; Nov. 1
SI amount (mm/season)	0	4.1	5.2	21
Harvesting date	Oct. 15	Nov. 7	Oct. 31	Oct. 20
Temperature (°C)	2.1-31.3	2.6-28.1	4.6-27.5	2.4-29.0
Rainfall (mm)	182	524	428	296

* Provided by the landowner.

** From June 20 to June 26 in 2013, 174 mm of rainfall was measured, which filled up the ditch and flooded the CD structures.

3.3.2. Monitoring climate variables, soil moisture, and water table depth

The climate at the study site was categorized as sub-humid with short and mild summer (long term average temperature of 19.8°C) and cold winter (average temperature of -8.5°C) with average annual rainfall between 533 and 635 mm according to North Dakota Agricultural Weather Network (NDAWN, 2019) data. A HOBO weather station (Onset Corporation, Pocasset, MA) was used near the EC system to collect daily rainfall, air temperature, and relative humidity data. A standard tipping bucket rain gauge with 0.25 mm accuracy was located on an independent support at 2.5 m above the ground and measured the rain events and amounts. During the crop growing season (May-October), the average temperature was approximately 17.4, 16.1, 18, and 18.1 °C, and the measured rainfall was 182, 524, 427, and 296 mm in 2012, 2013, 2016 and 2017, respectively. Growing season rainfall in the field was measured with a tipping bucket rain gauge. The off-season (October- May) precipitation was obtained from the Minnesota State Climatology Office for Morken Township (MN DNR, 2019).

Pairs of Hydra Probe II sensors (Stevens Water Monitoring Systems Inc., Portland, OR), located on tile (1 m near the drain tile) and between two tiles (5.2 m near the drain tile) at 5, 15, 30, 45, 60, 75, and 90 cm depths, measured the soil water by volume and temperature at 30-minute intervals. Average of soil water volume at two locations were used to compare the statistical difference of the SWC for each month of the study year. For statistical analysis, one-way ANOVA and Bonferroni-Holm test were used (Kraus, 2014). Based on HYPROP and WP4 experiment for each 30 cm of soil profile (Roy et al., 2018), the average volumetric soil water contents (SWC) at field capacity (FC, 1/3 bar), permanent wilting point (PWP, 15 bar), and saturation for the 0-90 cm soil layer were 41%, 17% and 53.4%, respectively. The management allowed depletion was set at 55% of the total available water recommended by FAO56 (Allen et al., 1998) and was used as an indicator for a well-watered crop. The TAW is the difference between the SWC in the root zone at the FC and the PWP (Allen et al., 1998). Thus, TAW was used to determine the number of days for crops without water stressed conditions when estimating the K_c values. Therefore, the days with a SWC<45% TAW were considered crops under stress condition and were eliminated from the K_c calculations.

The WTD was monitored using a pair of observation wells 2 m deep, installed near the EC system located on tile and between the tiles, similar to the paired soil moisture sensors. The WTD fluctuations were measured automatically by the water level transducers (Model U 20-001-01, Onset Computer, Pocasset, MA), with 1-hour intervals. The automatically measured WTDs were adjusted by manually measured WTDs on a monthly basis. Also, the measured WTDs were corrected for barometric pressure and air temperature compensation. The barometric pressure was measured for a period of time but was later eliminated due to limited space on the datalogger. The measured barometric pressure between the field and the NDAWN site were compared and did not show significant differences since the NDAWN station was located 13.7 km away from the study site. Therefore, the NDAWN measured values were used for barometric pressure compensation due to the short distance and flat topography (Kolars et al., 2019).

3.3.3. Measuring evapotranspiration and energy fluxes

To monitor the energy fluxes, an EC station (Campbell Scientific, Inc., Logan, Utah) was placed at the center of the CD+SI field with more than 400 m fetch distance in all directions (Fig. 1). The EC system consisted of a quick response three-dimensional sonic anemometer (model CSAT3, Campbell Scientific, Inc, Logan, UT, USA) faced into the predominant wind direction (northwestern) and coupled with a krypton hygrometer (KH20, Campbell Scientific, Inc, Logan, UT, USA) to measure the wind speed and vapor density fluctuations, respectively. The net radiometer (model Q7.1, REBS, Campbell Scientific, Inc) was oriented southerly and was kept 1.5 m above the crop canopy during the initial stages of the crop growing season. As the corn height increased, the sensor was raised to keep it 1 m above the crop canopy. The CSAT3 sonic anemometer and KH20 gas analyzer were installed on the tower with maximum height of 3 m. Due to the tower height limitation, the instruments were kept approximately 0.4 m above the canopy when corn reached its maximum height. As a rule of thumb for agricultural weather stations, the EC system should be kept at least 1 m above the crop canopy (ASABE Standard, 2004) to avoid any site aridity effects. However, for a humid region with high wind speed conditions during most of the time, the instrumentation height would have minimal effect to the flux measurement (Jia et al., 2007). Additional 10 Hz flux data analysis also revealed that the shapes of the spectral and co-spectral analysis were valid. The CR3000 datalogger recorded signals from these instruments at a frequency of 10 Hz were corrected for wind speed rotation (based on double rotation and detrending by block method), time lags (using maximum covariance approaches), spike effect (plausibility range of 5 standard deviations), and amplitude resolution (with range variation as 7 standard deviations), while the corrected data were averaged over 30-minute intervals. Two 12 V deep-cycle rechargeable marine batteries were connected in parallel and recharged by two solar panels (model SP70L, Campbell Scientific, Inc, Logan, UT, USA), which powered the EC system even in cloudy and cold climate conditions. The two batteries were placed inside a sealed box with small holes drilled only allowing wires to be extended outside the box. In this way, it prevented any animal damages and weather effects to the batteries. A pair of self-calibrating soil heat flux plates (HFP01SC-L, Campbell Scientific, Inc.) were used in 2012 and 2013. Due to frequent sensor malfunctions, they were replaced with a pair of HFT3-L soil heat flux plates (REBS Soil Heat Flux Plate, Campbell Scientific, Inc.) in

2016 and 2017 study years. These soil heat flux plates were installed in the ground at 8 cm with 0.5 m distance to reduce the spatial variability, and two soil thermocouples were placed 2 and 6 cm above each of the soil heat flux plates. For soil heat storage correction, a pair of soil water content reflectometers (model CS616, Campbell Sci., Inc, Logan, UT, USA) were installed at 5 and 15 cm depths on the outer sides and between the soil heat flux plates.

Using the EC system, the land surface exchange fluxes derived from all sensors were averaged to 30-min, including solar radiation (R_s), R_n, LE, H, and G (all in units of W m^{-2}). Due to various source of errors in flux measurement by the EC, which can be related to weather conditions, site properties, or system maintenance, the site was visited on a weekly basis to download the data for post processing. The measured R_n was corrected for wind effect. The G was calculated from the two soil heat flux plates and corrected based on a pair of soil temperature sensors and water content reflectometers to account for the stored heat above the soil heat flux plate. The 30-min collected H values by the CSAT3 was corrected for coordinate rotation and sonic temperature. Moreover, because of the widely recognized energy balance closure problem in EC measurements, the 30-min energy fluxes were plotted each day to visually detect inconsistent or outlier data. Only daytime (R_n> 0 W m^{-2}) data were used in the analysis. Days with rain events greater than 10 mm were not considered in the ET_a and K_c calculations (Niaghi et al., 2019). The daily ET_a values were calculated by summing up the 30-min calculated ET_a from the calculated residual LE values. Details associated with meteorological and calculation procedures of the flux were reported previously (Niaghi et al., 2019).

3.3.4. Calculation of the reference evapotranspiration and crop coefficient

The ASCE-EWRI (2005) standardized Penman-Monteith method, recommended by the American Society of Civil Engineering (ASCE), is the most widely used and accepted method to calculate ET_{ref} (Subedi et al., 2017) based on grass reference crop (ET_o) or alfalfa (ET_r). Daily K_c values based on grass (K_{co}) and alfalfa (K_{cr}) were derived as a ratio of daily estimated ET_a by EC and daily calculated ET_{ref} (ET_r and ET_o) (Allen et al., 1998). The derived K_{co} curves for days after planting (DAP) were adjusted using relative humidity and wind speed for the study region, as recommended in FAO56 (Allen et al., 1998). The K_{cr} values from the current research will be compared with Steele et al. (1996) developed polynomial curves using Penman (denoted as "S-P" and based on Allen, 1986) and Jensen-Haise equations (denoted as "S-JH" and based on Jensen and Haise, 1963).

3.4. Results and discussion

3.4.1. Water table and soil moisture relations

Figure 5 shows rain amounts and distribution, timing and volumetric SWC for the two soil layers (0–30 cm, and 45–90 cm) as a function of DAP. The FC, PWP, and 45% TAW lines indicate the SWC condition and water accessible to the crop. Furthermore, the WTDs on tile and between drainage tiles during the corn growing season in 2012, 2013, 2016, and 2017 are shown in Figure 3.2.

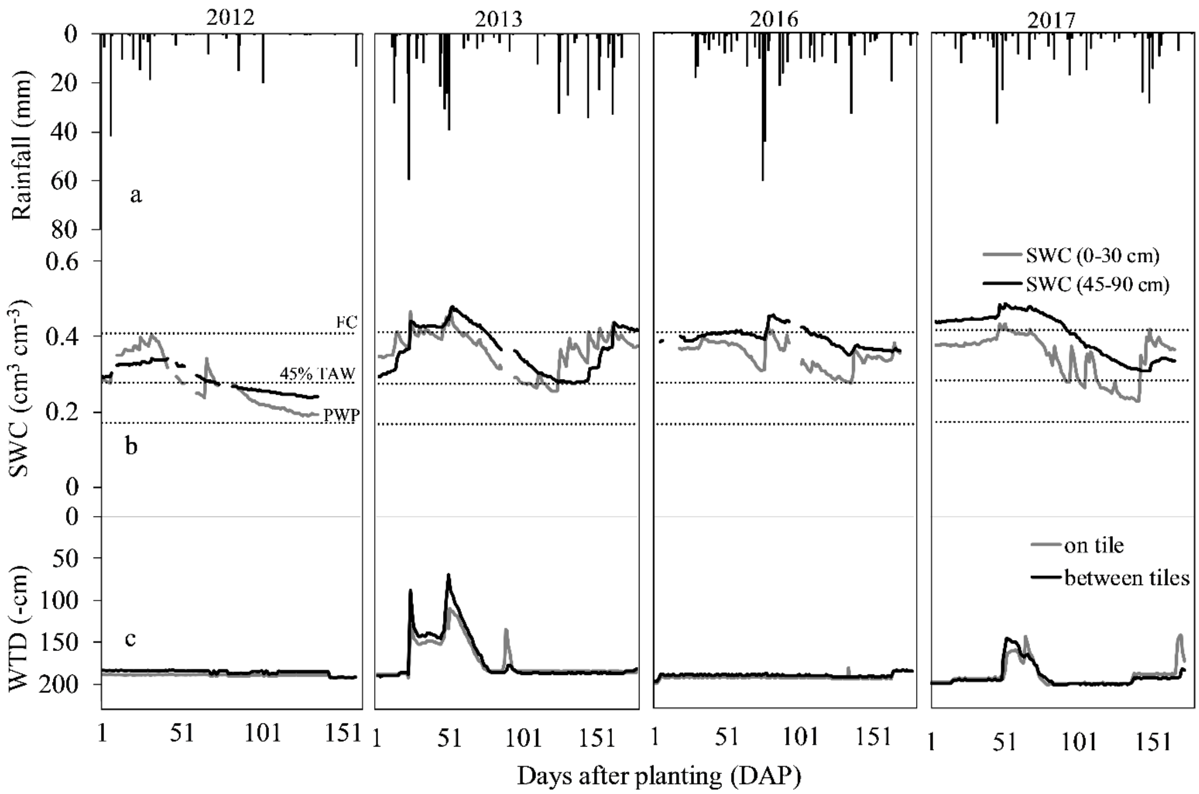

Figure 3.2. (a) Rainfall amount and distribution, (b) volumetric soil water content (SWC), field capacity (FC), 45% of the total available water (45% TAW), and permeant wilting point (PWP) lines, and (c) water table depth (WTD) on tile and between drainage tiles during corn growing season.

The lowest amount of in-season (May–October: 182 mm) and off-season (October 2011–April 2012: 198 mm) precipitation was recorded in 2012. The lowest SWC with an average of 0.28 m^3 m^{-3} was observed in both 0–30 cm and 45–90 cm soil layers in 2012. With increasing crop water requirements and root development, the SWC dropped to below 45% TAW for both 0–30 cm and 45–90 cm soil layers. However, the SWC in deeper layers was close to 45% TAW line for a longer time without receiving moisture from either rainfall or through the SI application. Despite drought conditions in 2012 and low amounts of rainfall, the mild slope of SWC reduction for 45–90 cm soil layer revealed that the capillary rise and possible contribution of the deeper WTD could contribute to crop water requirement (Beltrão et al., 1996; Fidantemiz et al. 2019; Niaghi et al., 2019) .

In 2013, the SWC went above the FC line due to heavy rain events at the initial and development corn stages. Figure 3.2 shows the sudden WTD reduction from about 60 cm to 140 cm below the surface due to the SD system after the first heavy rain event in 2013. The mild slope of the reduction in WTD from 51 DAP to about 80 DAP after a heavy rain event showed the CD ability that kept the SWC above 45% TAW to meet crop water requirement. Crop development and non-uniform distribution of rain in 2013 caused a shortage in water supply from 90 to 100 DAP. However, utilizing the SI system on August 3 (88 DAP) had kept the SWC above the 45% TAW and reduced the effect of limited SWC on the crop growth. The amount of off-season precipitation from 2012–2013 winter was about 332 mm (MN DNR, 2019) that recharged the WTD and helped with better crop growth in 2013.

In 2016, in addition to a uniform distribution of rainfall, 322 mm off-season precipitation from the 2015-2016 winter season was stored in the soil profile. A small depth of water (5.4 mm) was applied through the SI system between September 2 and 6 (129 and 133 DAP) to keep the SWC near the FC point, or to test the SI system performance. Despite a good amount of rainfall and WTD recharge, the WTD was not measured in the range of observation wells depth (2 m).

During the early growing season of 2017, due to sufficient stored water in the soil profile from the off-season precipitation (334 mm), the SWC was near the FC point at the shallower depth (0–30 cm) and above the FC line for the deeper layer (45–90 cm) of the soil profile early in the season. Therefore, application of CD was necessary to keep the infiltrated water in the soil profile for a longer time. With the first heavy rain event on 50 DAP, the SWC increased for the 0-30 cm and 45-90 cm soil layers, and the WTD was raised from 190 cm to 140 cm below the soil surface. At 59 DAP, water was applied to the field through the SI system to keep SWC near the FC point. Following the crop growth, the plant water uptake caused the WTD to drop from 140 cm to 190 cm and decreased the SWC to below the FC point. For the days when the SWC of the 0-30 cm layer was below the 45% TAW, the deeper layers had enough moisture to support the crop water requirement since they stayed above the 45% TAW until the end of the growing season.

Table 3.2 summarizes the monthly differences of the volumetric SWC for all study years obtained from one-way ANOVA and Bonferroni-Holm tests (Kraus, 2014). The table shows a diagonal matrix with upper triangle for the surface soil (0–30 cm) and lower triangle for the deeper layer (45–90 cm), respectively. Among the study years, almost all months during the 2012 growing season had significant differences ($P \leq 0.05$) in SWC with other study years and experienced a lower SWC (drier condition) than the other years due to the lowest amount of rainfall. Despite a 97 mm difference of in-season rainfall between 2013 and 2016, the statistical analysis showed non-significant SWC differences between the 2013 and 2016 study years. Furthermore, with 296 mm of in-season rainfall in 2017, it showed a non-significant SWC difference with 2016 for May, July and August. Therefore, this implied that the off-season precipitation had an important effect on soil moisture recharge, and thus, on crop growth during the growing season.

Table 3.2. Percentage differences of monthly average soil water content (SWC) (May–October) for the 0–30 cm (upper right triangle) and 45–90 cm (lower left triangle, shaded grey) soil layers.

Year	2012	2013	2016	2017
Year	SWC- differences (%)			
2012	-	**3*,8,9,6,16,8**	**2,4,9,10,12,3**	**2,6,9,8,8,5**
2013	**-4*,-11,-14,-7,-5,-16**		*-1*,**-4**,*0*,**4,-4,-5**	-1,**-2**,*0*,*2*,**-8,-3**
2016	**-7,-8,-15,-15,-13,-13**	*4*,**-4**,*1*,**8,8,-4**		**0,2,0,-2,-5,2**
2017	**-11,-13,-17,-12,-7,-9**	**-8,-1,-4,-5,-3,7**	**-4,-5,-3,3,5,3**	-

Note: For a given row, numbers illustrate the differences of average of SWC for May, June, July, August, September, and October, respectively between that year and the corresponding SWC for the year of the corresponding column.

* For example, SWC for May 2013 at top 30 cm depth was 3% higher than that for May 2012, and SWC for May 2012 at 45-90 cm depth was 4% (-4) lower than that for May 2013. Non-significant (italic) and significant variance (bold).

To study the WTD, SWC, and energy balance partitioning effect on crop performance, the growing season in each year was divided into five stages: initial, development, tasseling, reproductive and maturity. Figure 3.3 summarizes the cumulative amounts of in-season rainfall for each stage, while Figure 3.4 summarizes the analysis of SWC and WTD as boxplots for the five growing stages of the four study years. The range of SWC variation for the 0-30 cm soil layer was higher than that for the deeper soil profile in all four years. This range was 0.22, 0.22, 0.15, and 0.20 $m^3\ m^{-3}$ for the 0–30 cm soil layer and 0.11, 0.20, 0.10, and 0.18 m^3/m^3 for the 45–90 cm soil layer in 2012, 2013, 2016, and 2017, respectively. The WTD in 2012 had the lowest fluctuation of about 4.3 cm and 9.2 cm for on tile and between tiles locations, respectively. These ranges were 17.8 cm and 12.6 cm for on tile and between tiles in 2016. The largest range of variation was observed in 2013 due to the recharged soil profile with pronounced off-season precipitation, early snow melting, and several rain events during the growing season. The shallowest WTD in 2013 was observed as 117 cm for on tile and 81 cm for between tile locations, respectively. The WTD variation was high during tasseling stage in 2017 due to the application of SI, and the WTD fluctuation for both on tile and between tile locations were about 54 cm. Application of SI and rain events decreased the WTD from the soil surface during the development and tasseling stages in 2017. The SI application also recharged the soil profile and increased the potential for capillary rise.

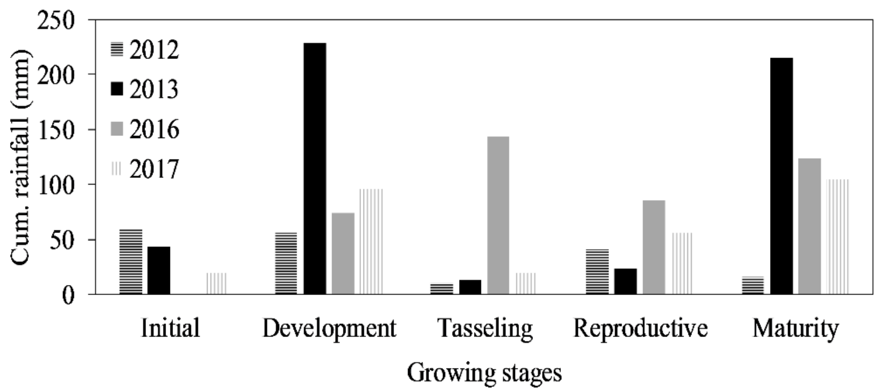

Figure 3.3. Cumulative rainfall at each stage of the study year.

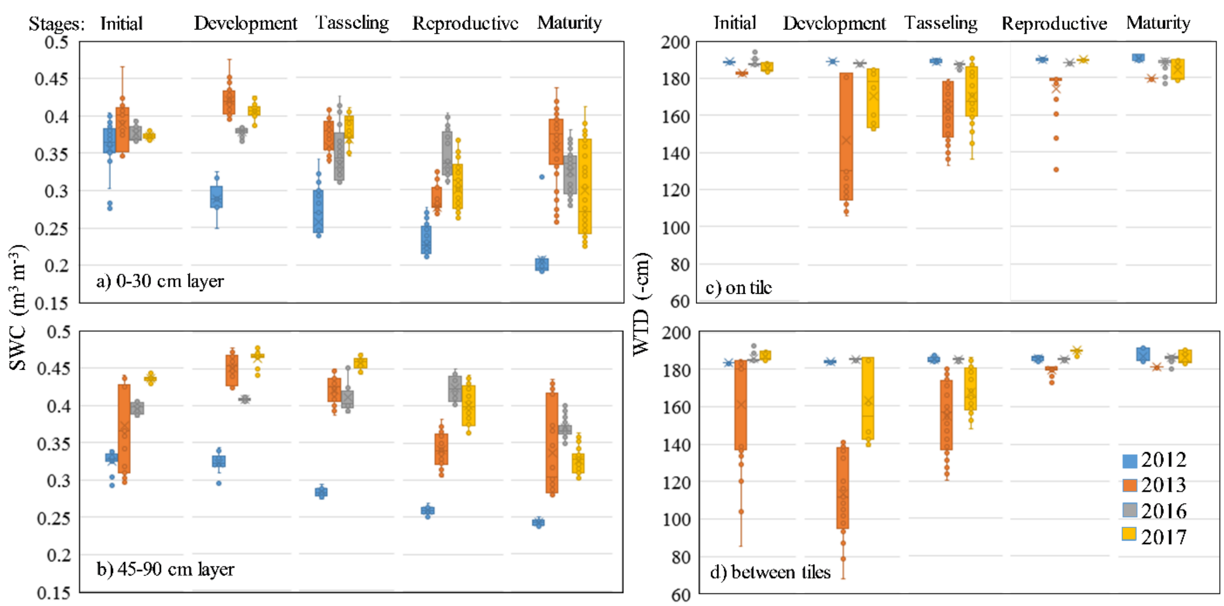

Figure 3.4. (a,b) Box-plot of daily soil water content (SWC) for the top 30 cm and 45-90 cm soil layers, and (c,d) histogram of water table depth (WTD) for on tile and between tiles locations during different corn growing stages, respectively.

The SWC and WTD analysis showed that the highest SWC was found in 2013 during the development stage, and the WTD was about 110 cm from the soil surface. In the tasseling stage, the SWC was similar in 2013, 2016, and 2017, but the WTD in 2013 and 2017 was closer to the soil surface than that in 2016. During the reproductive stage, the highest SWC was found in 2016. During the maturity stage, a higher SWC variability was found in 2013 for the 45-90 cm soil layer. Overall, 2016 experienced more stable SWC and WTD than all other study years, and 2013 had the highest range of SWC and WTD fluctuations. The SWCs in 2013 and 2016 were always above the 45% TAW for all growing stages, indicating that they had the optimal condition for crop growth.

A field study by Mejia et al. (2000) found that corn yield was greater in the CD plots than that in the free drainage plots. Ghane et al. (2012) reported an average 6% increase on corn yield due to the CD practice in northwest Ohio. In addition, Jia et al. (2014) found that a CD+SI field had 10% higher yield than the CD field. Ng et al. (2002) reported a 64% increase in corn yield by using a CD+SI system. Cooper et al. (1991) found a 58% yield advantage for a CD+SI system over a non-irrigated field. Overall, different studies have shown the advantages of the CD and SI application for crop production. However, depending on the climate, and regional and land characteristics, the effect could be different. For this current study, according to the SWC and WTD observations, the best crop yield was observed in 2013 (wet year) due to the CD practice and in 2017 (dry year) due to the SI application as expected.

3.4.2. Energy fluxes

All measured energy fluxes (R_n, G, and H) and the calculated LE using the residual approach showed high day to day fluctuations due to weather conditions, crop stages, canopy coverage, and soil water availability. Due to the drought condition in 2012, the gap between the estimated LE and R_n was the highest among all four years. Crop stress and lack of water in 2012 decreased the LE/(R_n-G) ratio. Therefore, the remaining available energy (R_n-G) enhanced the measured H and G values and increased the H/(R_n-G) ratio. The measured energy fluxes in 2013 were affected by rain events, SWC, and WTD. Daily energy flux pattern also showed high variation for the estimated LE and H among the four seasons. This variation was related to the SWC or the WTD fluctuation or the variation in the climate condition. By following the growing season with rain events and following the crop to reproductive and maturity stages in 2013, the estimated LE and H become similar in terms of ratio to the available energy. The daily trend of measured fluxes in 2016 illustrated an increase in the estimated LE and decrease in measured H from planting to the reproductive stages. Among the study years, the highest partitioned energy to LE was in 2016. At crop maturity, the estimated LE was reduced and the H was increased. Keeping the SWC near the FC point using the CD practice until 60 DAP resulted in a greater LE estimate in 2017, with the LE/(R_n-G) ratios 0.57 and 0.68 in May and June, respectively. After the SI application, the water was held in the soil profile with the CD practice, therefore, the CD+SI provided benefits over an extended period that might enhance the LE and the LE/(R_n-G) ratio. Table 3.3 summarizes the average measured energy components for each month.

Table 3.3. Monthly amount of rainfall (mm), daily average net radiation (R_n), soil heat flux (G), sensible heat flux (H), and latent heat flux (LE), (all in MJ m^{-2}), and daily average H/(Rn-G) and LE/(Rn-G) during the study years.

Year	Month	Rainfall	R_n	G	H	LE	H/(R_n-G)	LE/(R_n-G)
2012	5	48	27.1	3.4	11.8	12.0	0.50	0.50
	6	61	30.3	5.4	9.1	15.8	0.36	0.64
	7	14	30.8	3.5	7.9	19.4	0.29	0.71
	8	43	28.1	2.7	8.1	17.3	0.32	0.68
	9	1	20.0	3.3	9.0	7.8	0.54	0.46
	10	14	12.3	0.9	4.9	6.5	0.43	0.57
	Average		**24.8**	**3.2**	**8.4**	**13.1**	**0.41**	**0.59**
	Std*		**(6.4)**	**(1.7)**	**(3.6)**	**(3.7)**		
2013	5	120	23.2	2.6	10.0	10.5	0.49	0.51
	6	147	25.4	4.7	6.8	13.9	0.33	0.67
	7	22	25.6	2.2	4.9	18.5	0.21	0.79
	8	21	21.0	1.9	5.7	13.3	0.30	0.70
	9	109	18.1	1.4	7.2	9.5	0.43	0.57
	10	104	11.8	0.2	6.4	5.3	0.55	0.45
	Average		**20.8**	**2.2**	**6.8**	**11.8**	**0.38**	**0.62**
	Std		**(7.5)**	**(1.3)**	**(4.2)**	**(4.3)**		
2016	5	39	25.9	2.6	12.4	10.9	0.53	0.47
	6	50	27.7	2.7	8.6	16.4	0.35	0.65
	7	179	24.5	1.5	3.6	19.4	0.16	0.84
	8	59	23.9	0.9	4.6	18.3	0.20	0.80
	9	58	17.3	0.6	4.4	12.3	0.26	0.74
	10	47	11.1	0.1	4.2	6.8	0.38	0.62
	Average		**21.7**	**1.4**	**6.3**	**14.0**	**0.31**	**0.69**
	Std		**(6.8)**	**(1.0)**	**(3.6)**	**(4.1)**		
2017	5	29	22.5	2.9	9.5	11.2	0.49	0.57
	6	87	26.3	2.7	7.7	16.1	0.33	0.68
	7	34	29.3	2.2	5.9	21.0	0.22	0.77
	8	45	23.8	0.9	6.8	15.9	0.30	0.69
	9	79	18.0	0.9	7.0	10.2	0.41	0.59
	10	23	9.3	-0.3	7.2	5.0	0.75	0.52
	Average		**21.5**	**1.5**	**7.4**	**13.2**	**0.42**	**0.64**
	Std		**(7.3)**	**(1.9)**	**(4.4)**	**(4.3)**		

* Std: Standard deviation.

3.4.3. Diurnal and growth stage processes

Figure 3.5 shows the diurnal pattern of the energy flux components for each stage of the study years. The LE, H, and G showed a parabolic pattern during the various growing stages, corresponding to the diurnal R_n changes. The effect of different planting dates in each year resulted in different peaks and trends of the energy fluxes. Based on the diurnal comparison in the initial stage, a higher R_n value was measured in the early time of the day (12 pm) in 2016 and 2017 but delayed in 2012 and 2013 (2 pm) due to the late planting dates (Table 3.4). The higher estimated LE value was measured at the initial stage in 2016 due to the higher R_n value and longer day time, as well as a higher SWC. The other study years showed a similar trend for estimated LE and H values at the initial stage of the crop growth.

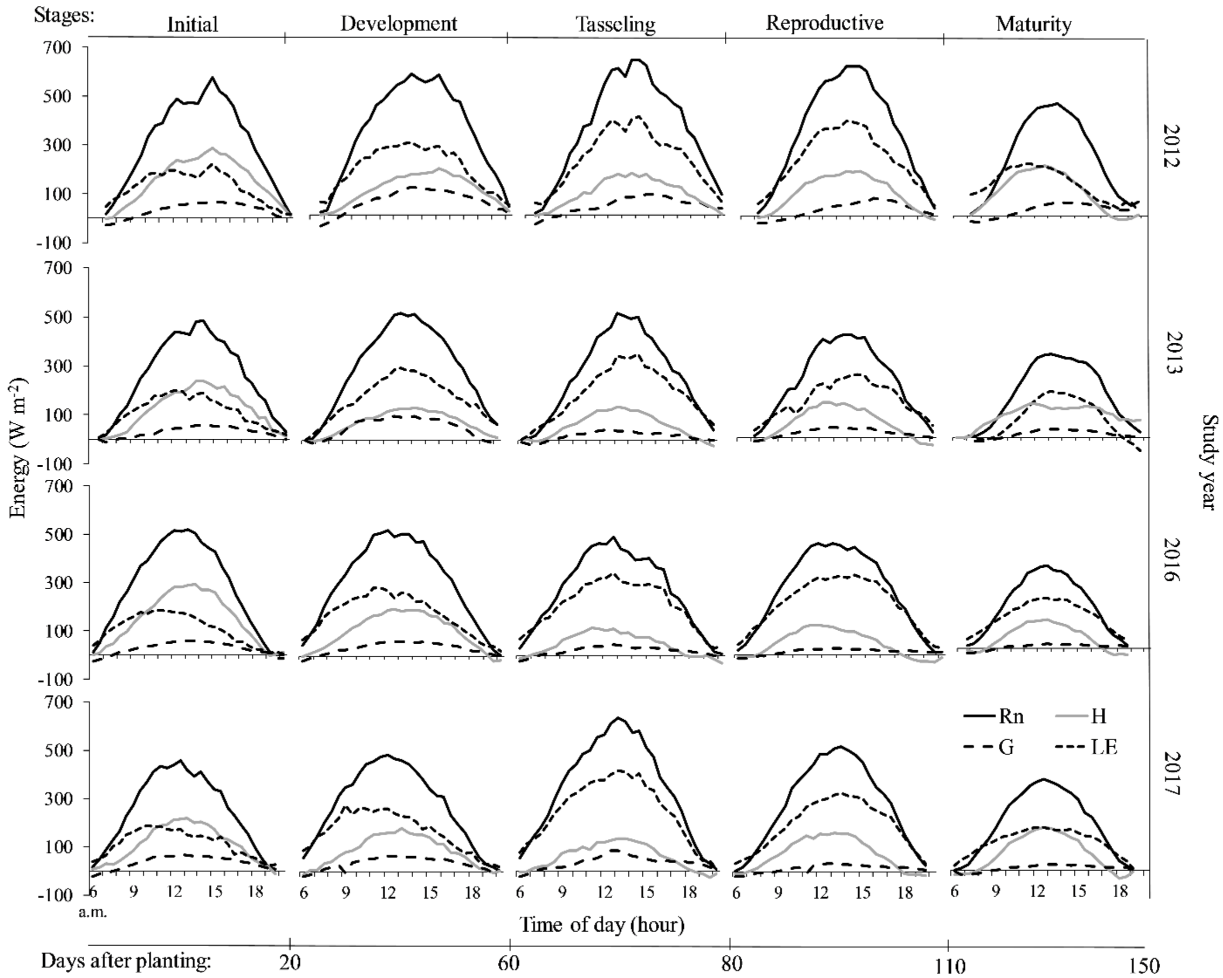

Figure 3.5. Average 30-min estimated energy fluxes (Rn: net radiation, H: sensible heat flux, G: soil heat flux, LE: latent heat flux) for different corn growing stages in Clay County, MN.

During the development stage, higher amounts of rainfall in 2013 led to a near saturation point of SWC, which increased the estimated LE compared to the other study years. The longer duration of R_n in the development stage was observed in 2012 and 2016, however, due to the limited SWC in 2012, the estimated LE was not as high as in 2016.

The tasseling stage is critical for corn yield since the yield components of ear and kernel number can no longer be increased by the plant growth and the potential size of the kernel is defined in this stage (Ransom and Endres, 2014). Thus, optimal soil water conditions should be provided to obtain better crop performance in the tasseling stage. The SWC was limited during the tasseling stage in 2012 (Fig. 3.2) compared to the other study years. Despite the sufficient SWC in 2013, the average daily estimated LE was less than that in 2016 and 2017. This indicated that both SWC and R_n had higher effects on the estimated LE.

During the reproductive stage, the highest and lowest LEs were measured in 2017 and 2013, respectively. The estimated LE was the lowest in 2013 due to the rainy days and cloudy conditions. As the crop approached the maturity stage, the estimated LE decreased, and most of the available energy was partitioned into H and G. However, due to the optimal SWC at maturity and reproductive stages in 2017 and higher R_n than the other study years, the estimated LE was higher, and therefore, the crop growth was also better.

3.4.4. Cumulative energy fluxes

Figure 3.6 shows the cumulative energy fluxes versus DAP for the study years. The difference between the cumulative LE and H illustrated how well the available energy had partitioned between the LE and the H. In 2012, the highest cumulative R_n (4377 MJ m^{-2}) and the lowest cumulative LE (2320 MJ m^{-2}) was observed. In 2013, the cumulative R_n (3698 MJ m^{-2}) was lower than the all other study years due to cloudy conditions and several rain events. Although it had the lowest cumulative R_n, the slope of cumulative LE (14.3 MJ m^{-2} d^{-1}) and H (6.5 MJ m^{-2} d^{-1}) in 2013 was higher than that in 2017 (LE: 13.5 MJ m^{-2} d^{-1}, H: 6.3 MJ m^{-2} d^{-1}). The highest cumulative LE was observed in 2016 (2507 MJ m^{-2}) that led to better crop growth and yield.

In comparison with the other study years, the highest slope of the estimated LE was observed in 2016 (16.6 MJ m^{-2} d^{-1}), which was related with the potential ET_a.

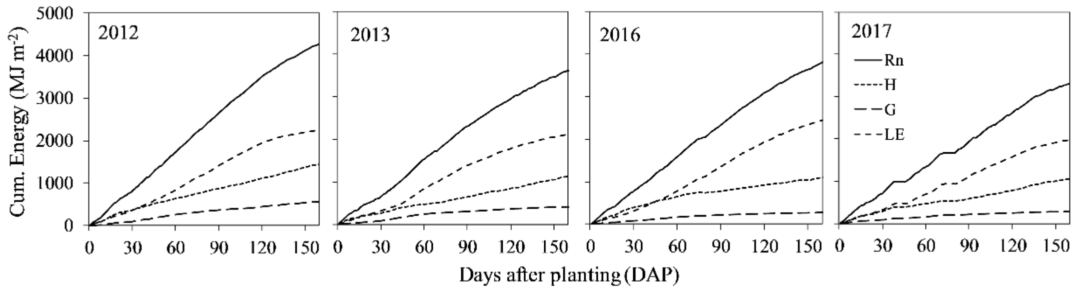

Figure 3.6. Cumulative daily measured energy flux (Rn: net radiation, H: sensible heat flux, G: soil heat flux, LE: latent heat flux) from planting to harvesting date in Clay County, MN.

For all of the study years, regardless of the weather conditions, partitioning of available energy to H was more positive during the early season than the later season. Following crop development, increased demand for water and ground surface coverage by vegetation, the measured H and G values were reduced to minimal rates. However, this reduction in H and G was higher in years with higher SWC and available energy than that in the other years. Therefore, during crop development, tasseling, and reproductive stages, most of the available energy was partitioned into LE, instead of H and G.

Application of SI showed a significant impact on keeping the SWC above the 45% TAW threshold. The time of the SI application showed the most important impact on LE according to the measured fluxes, its diurnal analysis, and its cumulative product of the energy components. The CD practice was effective, especially when the SWC remained near the FC point at the development and tasseling stages. Furthermore, the SI application during the maturity stage is important and can influence crop yields (Stegman, 1986), and increase corn kernel moisture before harvesting.

3.4.5. Evapotranspiration

The daily ET_a values were calculated by summing up the 30-min estimated LE data. Figure 3.7 shows the estimated ET_a, calculated ET_o, and ET_r for the growing season of the study years. As it was expected, in all of the study years, the ET_a rate was increased by increasing canopy cover throughout the season from cold spring to warm summer and then decreased in the fall season after crop maturity. The highest ET_a rates were observed in June and July, when corn was at tasseling and reproductive stages with a complete cover over the soil surface.

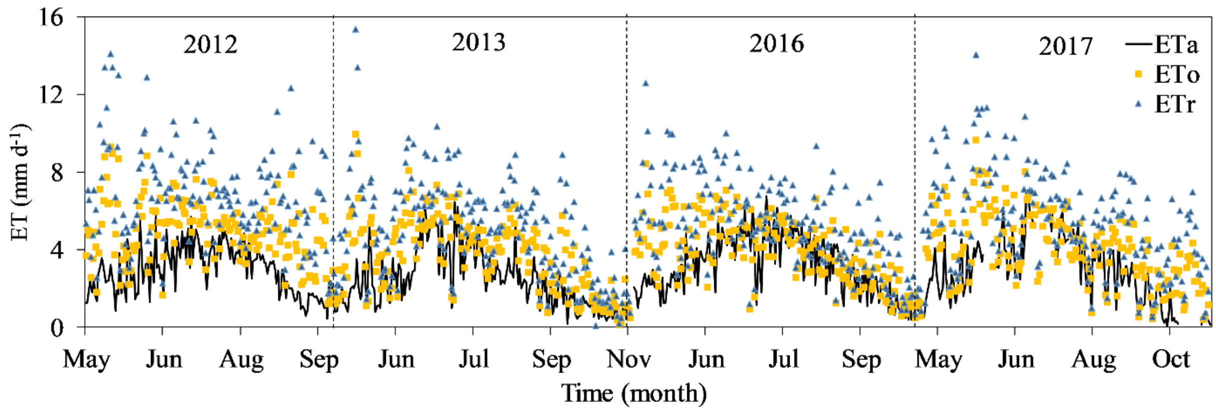

Figure 3.7. Daily estimated evapotranspiration (ET_a) by eddy covariance, and calculated reference grass and alfalfa evapotranspiration (ET_o, ET_r) rates for the growing seasons of the study years.

Table 3.4 summarizes the cumulative ET_a along with the yield and the county average yield for the study region. Although the energy flux components and meteorological analysis in 2013 showed less suitable conditions for crop production than that in 2016, the optimal SWC due to CD resulted in a higher yield (26.7%) than the county average yield. On the other hand, due to several heavy rain events in 2013, most farm lands had ponding and waterlogging problems that caused a lower county yield. At the study site, SD prevented the land from a ponding situation in 2013 and enhanced the crop productivity.

Table 3.4. Measured in-season and reported off-season precipitation (MN DNR, 2019), cumulative estimated evapotranspiration (Cum. ET_a), measured yield, and county average yield for the study years.

Year	Precipitation (mm)		Cum. ET_a (mm)	Yield (Kg/ha)		Yield gain at study site (%)
	In season*	Off-season*		Obtained	County average	
2012	182	198	468	8,850	9,315	-4.9
2013	524	322	476	11,100	8,756	+26.7
2016	427	322	551	12,365	11,405	+8.4
2017	296	334	537	11,110	10,419	+6.6

*In-season: May-October; Off-season: November of previous year-April

In 2012, a perforated irrigation water delivery main was used for the SI system, which led to the inability to supply enough water during the drought conditions. In addition, a late season corn variety was planted (93 day) which resulted in poor germination and could be visually observed (Jia et al., 2014) in the spring of 2012.

In 2013, due to heavy rainfall events in June, the field benefited from the CD practices because additional water was held in the soil profile instead of flowing away. Another study in 2013 in the same region showed that an undrained field was under waterlogged conditions for a long period of time, and a lower crop yield was obtained due to the wet conditions (Jia et al., 2014). Further, Jia et al. (2014) observed that more than 75% of drainage water was kept in the field due to the CD practices compared to the drainage outflow from a conventional drainage field.

Despite 29% less rainfall in 2016 than that in 2013, the highest yield was measured in 2016. Uniform distribution and sufficient rainfall at tasseling and development stages in 2016 enhanced the crop production. Furthermore, the CD practices kept the soil moisture near the FC and increased crop productivity. Not only did our study have the highest yield in 2016, but also the county average had the best yield compared to all other study years. This indicated the growing season in 2016 had the best conditions for crop production in terms of available energy, soil moisture storage, and weather condition. The rainfall amount and weather conditions in 2012 and 2017 were similar; however, because of 12 mm SI application and 334 mm off-season precipitation, the crop growth increased in the 2017 development stage. Application of SI at high water demand periods caused a greater ET_a in 2017 compared to that in the 2012 growing season. More irrigation was applied in September and early October 2017 to increase the soil moisture, but the amount was not significant and did not affect the yield in 2017. Instead, it might benefit the yield in 2018.

3.4.6. Crop coefficients

The highest K_{cr} and K_{co} values for the study years occurred between 80 and 90 DAP, which was between late July and early August. Rapid increases of K_c were observed after the rainfall and SI application. Figure 3.8 shows the calculated K_{co} and K_{cr} for days with SWC>45% TAW for the study years.

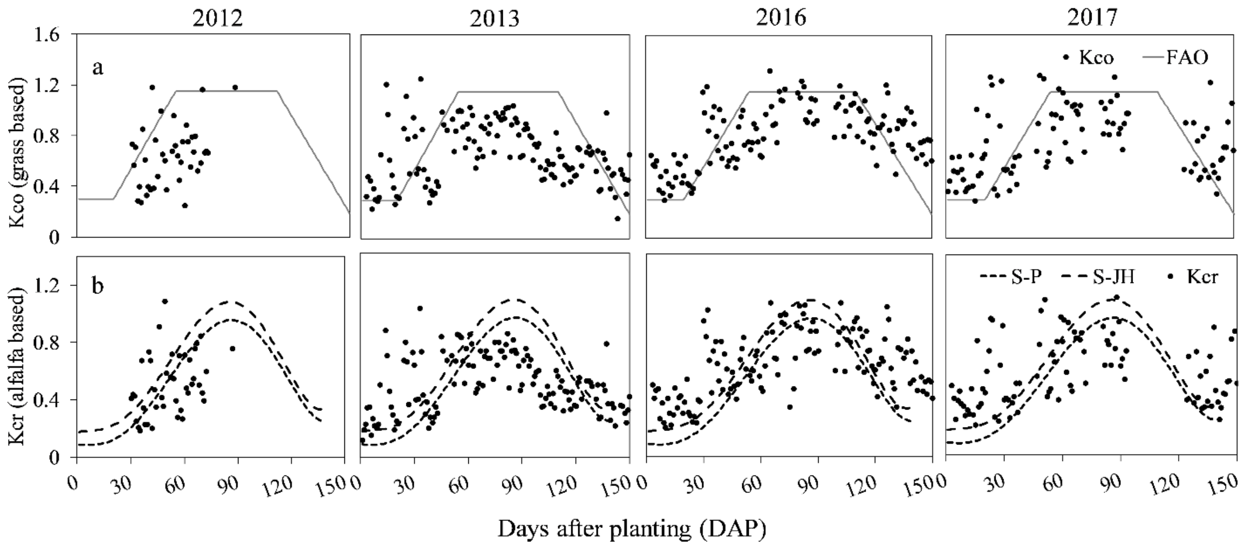

Figure 3.8. Developed crop coefficient based on grass and alfalfa (K_{co} and K_{cr}) reference evapotranspiration for measurements corresponding with soil water content (SWC) greater than 45% of total available water (TAW) in comparison with a) the FAO56 recommended curve for K_{co}, and b) the Kcr developed by Steele et al. (1996) based on the Penman (S-P) and Jensen Haise (S-JH) equations for the study years of corn growing season.

The developed K_{co} reasonably followed the FAO56 recommended K_{co} curve for corn in 2016 and 2017 but not in 2012 and 2013. Although all the years were screened for SWC greater than 45% TAW, the best fit was observed in 2016 that had the highest cumulative LE and near the FC point of SWC during high water demand stages of crop growth. This manner was similar for the calculated K_{cr} in 2016 that matches better with the S-P polynomial curve. Overall, the calculated K_{co} and K_{cr} values for the field with CD+SI in all study years followed similar manner as the recommended FAO56 and previously developed polynomial curves. However, the SWC was not the only factor limiting the crop productivity. The energy flux analysis in the previous section showed that it had the highest R_n values in 2012, but limited SWC condition. Although the SWC was not limited in 2013, the cumulative R_n was less than that in 2016 and 2017. The combined higher cumulative R_n and higher partitioned available energy to LE in 2016 and 2017 resulted in higher crop yield.

The comparison between the calculated K_{cr} and the developed K_{cr} by the S-P method showed a good agreement. Similar to this study, the K_{cr} values developed by Steele et al. (1996) included non-stressed and stressed crop conditions. For example, Prunty and Montgomery, (1991) water balance data for 1985–1988, later used by Steele et al. (1996), included non-stressed conditions of 30–40% depletion of soil water throughout the season as well as 70% depletions early in the season and 60% late in the season. The water stress conditions imposed by Prunty and Montgomery (1991) did not cause yield reductions. For the initial growing stage, a significant difference was observed between the K_{cr} values from Steele et al. (1996) and the calculated K_{cr} values in this study. This could be due to the weaknesses of single K_c or developed polynomial curve approach for initial crop stage, in which the crop did not cover the soil surface, and a significant amount of evaporation was taken into account to the measured ET_a value.

Figure 3.9 shows the median, average, and first, second, and thirds quartiles of calculated K_{co} and K_{cr} for each 10-days. The highest average K_{co} and K_{cr} occurred at 90 DAP (late July and early August). Because of the variable climate conditions during the four study years, the deviation of the calculated K_c was considerable. The median and the average K_{cr} and K_{co} values during the mid-season were nearly the same with a symmetric distribution, which implied that the measured results are not skewed with outliers. For the early and late season, the mean is greater than the median, which indicated the distribution was skewed to the right, and most of the calculated values were slightly lower than the average value.

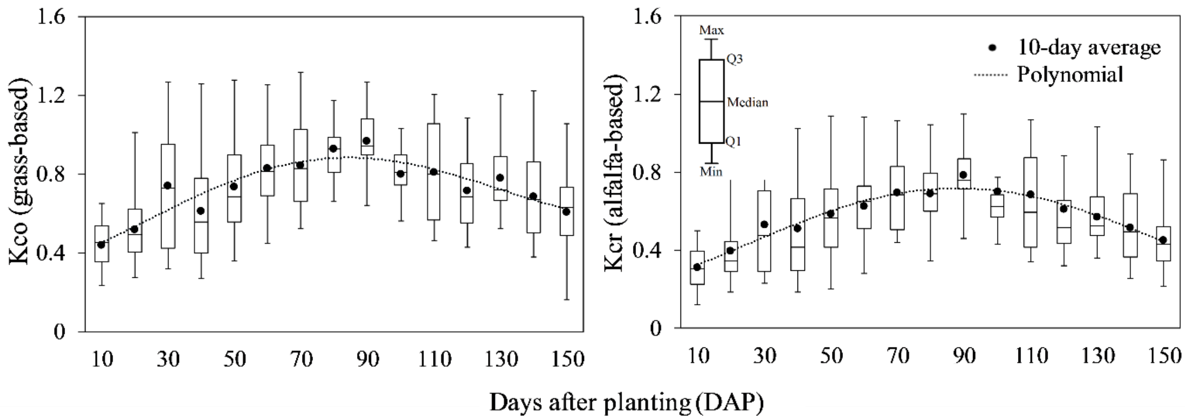

Figure 3.9. Average 10-day boxplot of calculated reference crop coefficient based on grass and alfalfa (Kco, Kcr) controlled drainage and subirrigation (CD+SI) at Clay County, MN.

Table 3.5 shows that the calculated K_{co} and K_{cr} after screening with the SWC for each growing stage agreed well with the reported K_c values from the previous studies in the region. Furthermore, for irrigation scheduling purposes, the polynomial equation developed based on daily obtained K_c values are also provided in table 5.

Table 3.5. Average of the calculated Kco and Kcr (grass and alfalfa-based crop coefficients, respectively) and developed polynomial equations based on days after planting (DAP) by considering soil water content (SWC> 45%TAW) condition in a corn field with controlled drainage (CD) and subirrigation (SI) at Clay County, MN.

DAP	Stage	Grass based			Alfalfa based			
		FAO56*	Rijal*	K_{co}	Rijal	S-JH	S-P	K_{cr}
0-20	Initial	0.3	-	0.49 (0.18)	-	0.19	0.09	0.34 (0.15)
21-60	Development	0.78	0.55	0.73 (0.26)	0.45	0.47	0.37	0.56 (0.23)
61-80	Tasseling	1.15	0.78	0.88 (0.19)	0.63	0.97	0.84	0.69 (0.18)
81-110	Reproductive	1.1	0.83	0.86 (0.20)	0.70	0.99	0.88	0.67 (0.19)
110-150	Maturity	0.45	0.63	0.69 (0.21)	0.51	0.49	0.43	0.53 (0.18)
Developed polynomial equations	K_{co} = 8.664E-09(DAP)^4 - 2.513E-06(DAP)^3 + 1.645E-04(DAP)^2 + 3.904E-03(DAP) + 4.474E-01 Number of points: 150, Standard Error=0.121, R^2= 0.506							
	K_{cr} = 5.921E-09(DAP)^4 - 1.664E-06(DAP)^3 + 8.318E-05(DAP)^2 + 6.212E-03(DAP)+ 2.745E-01 Number of points: 150, Standard Error=0.107, R^2= 0.527							

* FAO56 (Allen et al., 1998) is based on adjusted grass-based reference evapotranspiration; Rijal: Rijal et al. (2012) developed K_c based on ASCE-EWRI grass and alfalfa reference evapotranspiration for corn using eddy covariance; S-P and S-JH: Steele et al. (1996) developed K_{cr} based on Penman and Jensen-Haise reference evapotranspiration. Standard deviations are shown inside the parenthesis for this study.

In comparison with the previously reported K_{co} and K_{cr} values (Steele et al., 1996), the calculated K_c values were higher during the early and late growing seasons. Irmak et al. (2008) also observed significant energy loss during both early and late stages of crop development. Thus, development of the single K_c from energy flux components, which was the method used in current study, might not be the best option to use for the early and late growing season when crop canopy incompletely covers the surface, or crop leaves are dropping during senescence stages.

The result of this study showed that the CD+SI treatment produced higher yield than the county averages in 2013 and 2017. The calculated K_c with the CD + SI practices were lower than the FAO56 recommended values and the K_c values by Steele et al. (1996). Therefore, the CD+SI practices has the capability to provide optimal moisture for the highest crop production.

3.5. Conclusion

Energy balance and evapotranspiration rates were measured in a corn field with controlled drainage and subirrigation practices using an eddy covariance system during the 2012, 2013, 2016, and 2017 growing seasons in the Red River Valley. Soil water content, water table depth, and precipitation were monitored for the growing season and the off-season. The off-season precipitation recharged the soil profile and was beneficial for better crop growth in the spring. The application of controlled drainage and subirrigation kept the soil water content at optimal conditions during the growing season. The measured energy fluxes showed that the application of subirrigation enhanced the measured evapotranspiration rates. The largest benefit of controlled drainage and subirrigation practices was found during a wet year (2013) and dry year (2017). With more available energy for crop production and optimal soil water status, the crop yield in 2016 was the highest among all other years. The corn evapotranspiration rates were

468, 476, 551, and 537 mm for 2012, 2013, 2016, and 2017 growing seasons, respectively. Furthermore, crop coefficient curves were developed using the estimated evapotranspiration rates, screened for days with more than 45% of total available water in the corn root zone, and the standardized reference evapotranspiration equations. The grass reference-based crop coefficients were 0.49, 0.73, 0.88, 0.86, and 0.69 for initial, development, tasseling, reproductive, and maturity stages, respectively. This study showed that good drainage water management with controlled drainage and subirrigation provided good corn production during both wet and dry years.

3.6. Acknowledgments

This project is supported by USDA National Institute of Food and Agriculture project 2015-68007-23193, USDA NCR SARE project LNC11-332, ND Soybean Council, ND Water Resources Research Institute, ND Agricultural Experimental Station, and USDA Hatch project ND01475. The authors would like to express our gratitude to Ms. Debra Baer for her assistance to review the paper, Dr. Daigh, Dr. Lin, Dr. Roy, and many other formal students for their valuable work in field work and data collection.

3.7. References

Allen, R. G., Luis, S. P., RAES, D., & Smith, M. (1998). FAO Irrigation and Drainage Paper No. 56. Crop Evapotranspiration (guidelines for computing crop water requirements). *Irrigation and Drainage*. https://doi.org/10.1016/j.eja.2010.12.001

Anapalli, S. S., Green, T. R., Reddy, K. N., Gowda, P. H., Sui, R., Fisher, D. K., … Marek, G. (2018). Application of an energy balance method for estimating evapotranspiration in cropping systems. *Agricultural Water Management*. https://doi.org/10.1016/j.agwat.2018.04.005

Anderson, R. G., Alfieri, J. G., Tirado-Corbalá, R., Gartung, J., McKee, L. G., Prueger, J. H., … Kustas, W. P. (2017). Assessing FAO-56 dual crop coefficients using eddy covariance flux partitioning. *Agricultural Water Management*, *179*, 92–102. https://doi.org/10.1016/j.agwat.2016.07.027

ASABE Standard, (2004). EP505: Measurement and Reporting Practices for Automatic Agricultural Weather Stations, St. Joseph, MI: ASABE.

ASABE Standards. (2015). S526.4: (2015). *Soil and water terminology*. St. Joseph, MI: ASABE.

ASCE-EWRI. (2005). The ASCE standardized reference evapotranspiration equation: ASCE-EWRI Standardization of Reference Evapotranspiration Task Committe Report. *American Society of Civil Engineers*. https://doi.org/10.3406/arasi.1965.919

Baker, J. M., & Griffis, T. J. (2005). Examining strategies to improve the carbon balance of corn/soybean agriculture using eddy covariance and mass balance techniques. *Agricultural and Forest Meteorology*. https://doi.org/10.1016/j.agrformet.2004.11.005

Beltrão, J., Antunes Da Silva, A., & Asher, J. Ben. (1996). Modeling the effect of capillary water rise in corn yield in Portugal. *Irrigation and Drainage Systems*, *10*(2), 179–189. https://doi.org/10.1007/BF01103700

Chávez, J. L., Howell, T. A., & Copeland, K. S. (2009). Evaluating eddy covariance cotton ET measurements in an advective environment with large weighing lysimeters. *Irrigation Science*. https://doi.org/10.1007/s00271-009-0179-7

Cooper, R.L., Fausey, N.R., Streeter, J.G.,(1991). Yield potential of soybean grown under a subirrigation/drainage water management system. *Agronomy Journal* 83(5), 884. doi:10.2134/agronj1991.00021962008300050021x.

Djaman, K., & Irmak, S. (2013). Actual Crop Evapotranspiration and Alfalfa- and Grass-Reference Crop Coefficients of Maize under Full and Limited Irrigation and Rainfed Conditions. *Journal of Irrigation and Drainage Engineering*. https://doi.org/10.1061/(ASCE)IR.1943-4774.0000559

Facchi, A., Gharsallah, O., Corbari, C., Masseroni, D., Mancini, M., & Gandolfi, C. (2013). Determination of maize crop coefficients in humid climate regime using the eddy covariance technique. *Agricultural Water Management*. https://doi.org/10.1016/j.agwat.2013.08.014

Fidantemiz, Y.F., Jia, X., Daigh, A.L.M., Hatterman-Valenti, H., Steele, D.D., Niaghi, A.R., Simsek, H. (2019). Effect of water table depth on soybean water use, growth, and yield parameters. Water (Switzerland) 11 (5), 931. doi:10.3390/w11050931.

Ghane, E., Fausey, N. R., Shedekar, V. S., Piepho, H. P., Shang, Y., & Brown, L. C. (2012). Crop yield evaluation under controlled drainage in Ohio, United States. *Journal of Soil and Water Conservation*, *67*(6), 465–473. https://doi.org/10.2489/jswc.67.6.465

Irmak, A., Irmak, S., & Martin, D. L. (2008). Reference and Crop Evapotranspiration in South Central Nebraska . I : Comparison and Analysis of Grass and Alfalfa-Reference Evapotranspiration. *Irrigation and Drainage Engineering*, *134*(December), 690–699. https://doi.org/10.1061/(ASCE)0733-9437(2008)134:6(700)

Jensen, M.E., Haise, H.R. (1963). Estimating evapotranspiration from solar radiation. Journal of Irrigation and Drainage, 89 (IR4), 15–41.

Jia, X., Scherer, T. F., Steele, D. D., & DeSutter, T. M. (2017). Subirrigation System Performance and Evaluation in the Red River Valley of the North. *Applied Engineering in Agriculture*, 33(6), 811–818. https://doi.org/10.13031/aea.12286

Jia, X., Scherer, T.F., Steele, D.D., DeSutter, T.M. (2017). Subirrigation System Performance and Evaluation in the Red River Valley of the North. *Applied Engineering in Agriculture*. 33(6), 811–818.

Kandel, H. J., Brodshaug, J. A., Steele, D. D., Ransom, J. K., DeSutter, T. M., & Sands, G. R. (2013). Subsurface drainage effects on soil penetration resistance and water table depth on a clay soil in the Red River of the North Valley, USA. *Agricultural Engineering International: CIGR Journal*.

Kolars, K., Jia, X., Steele, D. D., & Scherer, T. F. (2019). A soil water balance model for subsurface water management. *Applied Engineering in Agriculture*.

Kraus, D. (2014). Consolidated data analysis and presentation using an open-source add-in for the Microsoft Excel ® spreadsheet software . *Medical Writing*. https://doi.org/10.1179/2047480613z.000000000181

Majnooni-Heris, A., Niaghi, A.R., Asadi, E., Haghi, D.Z. (2013). Calibrating net solar radiation of FAO56 Penman-Monteith method to estimate reference evapotranspiration. *Journal of Environmental Biological Science*. 3, 1–7.

Mejia, M. N., Madramootoo, C. A., & Broughton, R. S. (2000). Influence of water table management on corn and soybean yields. *Agricultural Water Management*. https://doi.org/10.1016/S0378-3774(99)00109-2

MN DNR. (2019). Minnesota Department of Natural Resources.

Nagler, P. L., Scott, R. L., Westenburg, C., Cleverly, J. R., Glenn, E. P., & Huete, A. R. (2005). Evapotranspiration on western U.S. rivers estimated using the Enhanced Vegetation Index from MODIS and data from eddy covariance and Bowen ratio flux towers. *Remote Sensing of Environment*. https://doi.org/10.1016/j.rse.2005.05.011

NDAWN. (2018). North Dakota Agricultural Weather Network. Retrieved from North Dakota State University website: https://ndawn.ndsu.nodak.edu/

Ng, H.Y.F., Tan, C.S., Drury, C F, Gaynor, J D. (2002). Controlled drainage and subirrigation influences tile nitrate loss and corn yields in a sandy loam soil in Southwestern Ontario. *Agricultural Ecosystem Environment*. 90,81–88. doi:10.1016/S0167-8809(01)00172-4.

Niaghi, A.R., & Jia, X. (2017). Determination of grass evapotranspiration rates and crop coefficients using eddy covariance method in Eastern North Dakota. *ASCE-EWRI Congress*, 468–483. https://doi.org/10.1061/9780784480601.040

Niaghi, Ali Rashid. (2014). *Spatial and temporal estimation of biomass and evapotranspiration using satellite images (Case Study: Eastern Azerbaijan)*. University of Tabriz.

Niaghi, Ali Rashid, Haji Vand, R., Asadi, E., & Majnooni-Heris, A. (2015). Advances in Environmental Biology Evaluation of Single and Dual Crop Coefficient Methods for Estimation of Wheat and Maize Evapotranspiration. *Advances in Environmental Biology*, *9*(3), 963–971. Retrieved from http://www.aensiweb.com/AEB/

Niaghi, Ali Rashid, & Jia, X. (2017). Determination of Grass Evapotranspiration Rates and Crop Coefficients Using Eddy Covariance Method in Eastern North Dakota. *World Environmental and Water Resources Congress 2017*, 468–483. https://doi.org/10.1061/9780784480601.040

Niaghi, Ali Rashid, Jia, X., Scherer, T., & Steele, D. (2019). Measurement of unirrigated turfgrass evapotranspiration rate in the red river valley. *Vadose Zone Journal*, *18*(1), 1–37. https://doi.org/10.2136/vzj2018.11.0202

O'Brien, P. L., Acharya, U., Alghamdi, R., Niaghi, A. R., Sanyal, D., Wirtz, J., … DeSutter, T. M. (2018). Hydromulch Application to Bare Soil: Soil Temperature Dynamics and Evaporative Fluxes. *Ael*, *3*(1), 0. https://doi.org/10.2134/ael2018.03.0014

Payero, J. O., & Irmak, S. (2013). Daily energy fluxes, evapotranspiration and crop coefficient of soybean. *Agricultural Water Management*. https://doi.org/10.1016/j.agwat.2013.06.018

Prunty, L., Montgomery, B R. (1991). Lysimeter Study of Nitrogen Fertilizer and Irrigation Rates on Quality of Recharge Water and Corn Yield. *Journal of Environmental Quality.* 20, 373–380.

Rana, G., & Katerji, N. (2000). Measurement and estimation of actual evapotranspiration in the field under Mediterranean climate: A review. *European Journal of Agronomy*. https://doi.org/10.1016/S1161-0301(00)00070-8

Ransom, J., Endres, G.J. (2019). Corn growth and management, A1173 cereal crop. NDSU Extension Service. 2, 1–8.

Rienzner, M., Cesari de Maria, S., Facchi, A., Wassar, F., & Gandolfi, C. (2013). Estimating the contribution of rainfall, irrigation and upward soil water flux to crop water requirements of a maize agroecosystem in the Lombardy plain. *Journal of Agricultural Engineering*, *44*(2s). https://doi.org/10.4081/jae.2013.s2.e18

Rijal, I., Jia, X., Zhang, X., Steele, D. D., Scherer, T. F., & Akyuz, A. (2012). Effects of Subsurface Drainage on Evapotranspiration for Corn and Soybean Crops in Southeastern North Dakota. *Journal of Irrigation and Drainage Engineering*, *138*(12), 1060–1067. https://doi.org/10.1061/(ASCE)IR.1943-4774.0000508

Rosa, R., & Tanny, J. (2015). Surface renewal and eddy covariance measurements of sensible and latent heat fluxes of cotton during two growing seasons. *Biosystems Engineering*. https://doi.org/10.1016/j.biosystemseng.2015.05.012

Roy, D., Jia, X., Steele, D. D., & Lin, D. (2018). Development and Comparison of Soil Water Release Curves for Three Soils in the Red River Valley. *Soil Science Society of America Journal*, *0*(0), 0. https://doi.org/10.2136/sssaj2017.09.0324

Russell, E. S., Liu, H., Gao, Z., Finn, D., & Lamb, B. (2015). Impacts of soil heat flux calculation methods on the surface energy balance closure. *Agricultural and Forest Meteorology*. https://doi.org/10.1016/j.agrformet.2015.08.255

Sharma, B. R., & Minhas, P. S. (2005). Strategies for managing saline/alkali waters for sustainable agricultural production in South Asia. *Agricultural Water Management*, *78*(1–2), 136–151. https://doi.org/10.1016/j.agwat.2005.04.019

Shi, T. T., Guan, D. X., Wu, J. B., Wang, A. Z., Jin, C. J., & Han, S. J. (2008). Comparison of methods for estimating evapotranspiration rate of dry forest canopy: Eddy covariance, Bowen ratio energy balance, and Penman-Monteith equation. *Journal of Geophysical Research Atmospheres*, *113*(19), 1–15. https://doi.org/10.1029/2008JD010174

Steele, D. D., Sajid, A. H., & Prunty, L. D. (1996). New Corn Evapotranspiration Crop Curves for Southeastern North Dakota. *Transactions of the ASAE*, *39*(3), 931–936. https://doi.org/10.13031/2013.27578

Stegman, E. C. (1986). Efficient Irrigation Timing Methods for Corn Production. *Transactions of the ASAE*, *29*(1), 0203–0210. https://doi.org/10.13031/2013.30127

Subedi, A., Chávez, J. L., & Andales, A. A. (2017). ASCE-EWRI standardized Penman-Monteith evapotranspiration (ET) equation performance in southeastern Colorado. *Agricultural Water Management*. https://doi.org/10.1016/j.agwat.2016.07.002

Twine, T. E., Kustas, W. P., Norman, J. M., Cook, D. R., Houser, P. R., Meyers, T. P., … Wesely, M. L. (2000). Correcting eddy-covariance flux underestimates over a grassland. *Agricultural and Forest Meteorology*. https://doi.org/10.1016/S0168-1923(00)00123-4

Uddin, J., Hancock, N. H., Smith, R. J., & Foley, J. P. (2013). Measurement of evapotranspiration during sprinkler irrigation using a precision energy budget (Bowen ratio, eddy covariance) methodology. *Agricultural Water Management*. https://doi.org/10.1016/j.agwat.2012.10.008

US Grains Council. (2019). retrieved from https://grains.org/buying-selling/corn/ (accessed 3.20.19)

USDA NASS. (2018). United States Department of Agriculture, National Agricultural Statistics Service.

Wang, X., Hollanders, P. H. J., Wang, S., & Fang, S. (2004). Effect of field groundwater table control on water and salinity balance and crop yield in the Qingtongxia Irrigation District, China. *Irrigation and Drainage*. https://doi.org/10.1002/ird.117

4. NEW APPROACH TO IMPROVE THE SOIL WATER BALANCE METHOD FOR EVAPOTRANSPIRATION ESTIMATION[5]

4.1. Abstract

As an important component of the water budget, quantifying actual crop evapotranspiration (ET) will enable better planning, management, and allocation of the water resources. However, accurate ET measurement has always been a challenging task in agricultural water management. In the upper Midwest, where subsurface drainage is a common practice due to the shallow ground water depth and heavy clayey soil, ET measurement using traditional ground-based methods is more difficult. In this study, ET was measured using the eddy covariance (EC), Bowen ratio-energy balance (BREB), and soil water balance (SWB) methods during the 2018 corn growing season, and the results of the three methods were compared. To close the energy balance for the EC system, the residual method was used. For the SWB method, capillary rise was included in the ET estimation and was calculated using the measured soil water potential. The change of soil water content for ET estimation using the SWB method was calculated in four different ways, including daily average, 24:00–2:00 average, 24:00–4:00 average, and 4:00 measurement. Through the growing season, six observation periods (OPs) with no rainfall or minimal rainfall events were selected for comparisons among the three methods. The estimated latent heat flux (LE) by the EC system using the residual method showed a 29% overestimation compared to LE determined by the BREB system for the entire growing season. After excluding data taken in May and October, LE determined by the EC system was only 10%

[5] The material in this chapter was co-authored by Ali Rashid Niaghi and Xinhua Jia was submitted to the Water Journal as peer review article. Ali Rashid Niaghi had primary responsibility for analyzing the collected data, interpreting the results, developing the conclusion that are advanced here. Dr. Xinhua Jia served as technical and editorial consultant in the development of the manuscript represented by this chapter.
Niaghi, A.R., X. Jia, D. 2019. Measuring crop evapotranspiration by eddy covariance, Bowen ratio, and soil water balance methods. Water, *11*(12), 2478; https://doi.org/10.3390/w11122478

higher, indicating that the main difference between the two systems occurred during the early and late of the growing season. By considering all six OPs, a 6%–22% LE difference between the EC and the BREB systems was observed. Except during the early growing and late harvest seasons, both systems agreed well in LE estimation. The SWB method using the average soil water contents between 24:00 and 2:00 time period to calculate the daily capillary rise produced the best statistical fit when compared to the ET estimated by the BREB, with a root-mean-square error of 1.15 mm/day. Therefore, measuring ET using the capillary rise from a shallow water table between 24:00 and 2:00 could improve the performance of the SWB methodology for ET measurement.

4.2. Introduction

Precise estimates of actual crop evapotranspiration (ET) are crucial for the understanding of land and atmosphere energy exchange, especially for agricultural production. Knowledge about measurement techniques and their related errors is essential for agricultural water management. Over the last decade, development of instrumentation, data acquisition systems, and remote sensing have enhanced the ability of ET measurement over large areas and have significantly intensified the knowledge of ET measurement (Fisher et al., 2017). Numerous methods and techniques are now being used either remotely (Reyes-González et al., 2017) or in-situ (e.g., eddy covariance, Bowen ratio, soil water balance, and lysimeter) (Fidantemiz et al., 2019; Verstraeten et al., 2008; Zhang et al., 2008) for ET estimations. However, most of the ET methods, developed ET models, or proposed ET equations have large discrepancies and exhibit systematic and random errors depending on the measurement device’s location and climate conditions (Dragoni et al., 2007). Despite the development of many methods and equations through past decades, accurate ET estimation is still a challenging task (Amatya et al., 2016), and more efforts is required to increase our knowledge and the benefits of the available methods, while limiting their drawbacks.

In the upper Midwest, where subsurface drainage is a common practice due to the shallow ground water depth and heavy clayey soil, ET measurement is usually conducted using the soil water balance (SWB) method. However, due to the existence of a shallow water table, the accuracy of estimated ET with the SWB method is in doubt. To examine the performance of the SWB method, more precise instrumentation is needed. The eddy covariance (EC) and Bowen ratio-energy balance (BREB) systems are the two dominants in situ measurement methods that can provide ET with finer resolution compared with the SWB method. Furthermore, the results from the EC and the BREB methods may be used to improve the accuracy of the SWB method in the Red River Valley (RRV) region with a shallow water table and heavy clayey soil.

The EC method is one of the most established techniques to determine the exchange of water, energy, and trace gases between the land surface and the atmosphere (Allen et al., 2011). The EC method measures the covariance between vertical wind speed and water vapor density and aims to calculate the vertical moisture flux (and thus, ET) in high frequency (Gebler et al., 2015). With the development of flux measurements, the use of EC is extending rapidly to more heterogenous stands (Gong et al., 2016; Wilson et al., 2002), and this method has been compared with other ET methods (Consoli and Vanella, 2014). Gebler et al. (Gebler et al., 2015) showed a good correlation between ET values measured by lysimeter and EC in the summer. However, the comparison of ET values determined by the EC and other methods is poorly documented for regions with a shallow water table and heavy clay soil.

The BREB method, which is considered a fairly robust and successful tool in ET estimation, depends on the energy balance between the surface energy fluxes and the gaseous properties of water vapor (Allen et al., 2011; Irmak et al., 2014). Bowen ratio, which is the ratio of the sensible heat flux (H) to the latent heat flux (LE), operates on the basis of the concept of sensible and latent heat diffusion. In general, the BREB method can provide a high measurement accuracy if a reasonable set of criteria are adopted (Ohmura, 1982; Perez et al., 1999). The BREB method has been used to estimate ET for various crops, land surfaces, and ecosystems (Brotzge and Crawford, 2003; Watanabe et al., 2004). This method has been compared with other methods, such as weighing lysimeters, EC, and SWB methods, and most of the studies showed close agreement in the absence of sensible heat advection (Gong et al., 2016; Watanabe et al., 2004).

The shallow ground water table can have a great contribution to ET. For example, (Kolars et al., 2019) found the shallow ground water contributed an average of 39 to 51% of ET on clayey soils during the corn growing season in the Red River Valley (RRV). In the presence of a shallow water table, significant quantities of water can move into the root zone or be directly extracted by roots through root water uptake and capillary rise. A number of studies have shown that ET can be between 20% to 40% due to capillary rise at water table depths of 0.7–1.5 m (Ragab and Amer, 1986; Wallender et al., 1979). Prathapar (Prathapar and Meyer, 1993; Pranthapar et al., 1992) reported a 16%–29% contribution of capillary rise to ET in a clay loam soil. Ragab and Amer (Ragab and Amer, 1986) found that a shallow water table and subirrigation application can contribute about 40% of ET over a 75-day period during corn growing season. Thus, it is important to quantify and validate the accuracy of the SWB method by considering capillary rise and compare the estimated values with those obtained from other methods, such as the EC and BREB methods.

Comparisons of the EC, BREB, and SWB methods in ET measurement in the RRV are rare due to experimental limitations. Due to the high required maintenance and expense of the EC and BREB systems, the SWB is more commonly used but often inaccurate, particularly in areas with a shallow water table. Therefore, a comparison of the three methods may fill a knowledge gap and enhance the SWB method accuracy by considering the capillary rise using the soil moisture values at nighttime. This would benefit many researchers who have access only to the SWB method.

In this study, we evaluated the performance of the residual method to close the energy balance of the EC system in comparison with the BREB system. For the SWB method, we calculated the capillary rise using soil water content in different time periods. We then evaluated which method provided the best results by comparing the ET values determined by the three methods. Finally, we compare the ET values obtained with the SWB, BREB, and EC methods in the selected observation periods without climate uncertainties. Specific advantages and limitations of each methods are discussed.

4.3. Materials and methods

4.3.1. Study site, climate, and soil properties

The study site is located in the Buffalo-Red River watershed in Clay County, west central Minnesota (46° 59′ 20” N, 96° 41′ 06” W) at an altitude of 271 m above sea level (Figure 4.1). The climate of the region is sub-humid, with a cold winter and a mild and humid summer. The location receives a mean annual precipitation between 533 and 635 mm, with 428 mm rainfall during the growing season in 2018.

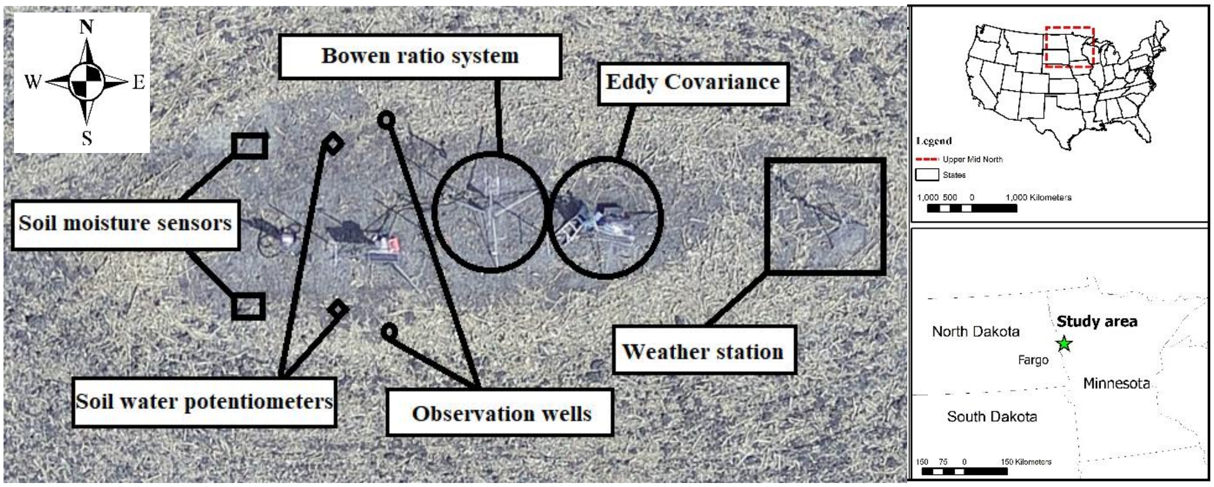

Figure 4.1. Aerial view of the instruments at the study site in Clay County, MN.

The study site is on 54 ha field with less than 1% slope where a subsurface drainage system had been installed in 2011 (Niaghi et al., 2019b), On May 14, 2018 corn was planted in the east west direction with a 76.5 cm row spacing. Corn had fully emerged on 24 May and was harvested on 11 November. From July 23 through July 27 2018, a small amount of water was subirrigated through the drain tile.

Soils in the field are predominantly classified as poorly drained with parts having a Bearden silt loam (50% of the total area), an Overly silty clay loam (27% of the area), and a Colvin silty clay loam (23% of the area), with an impermeable layer at about 3 m depth (Niaghi et al., 2019b).

The soil properties for the different soil layers near the EC and BREB towers were measured by the cylindrical core method (Doran et al., 1996) by the end of the soil release curve measurement at saturation condition. The particle analysis was performed by the pipette method (Gee and Or, 2002). The results are shown in Table 4.1.

Table 4.1. Soil particle size for different soil layers

Layer	Sand	Silt	Clay
cm		percent	
0-30	1.1	61.7	37.2
30-60	0.5	71.8	27.8
60-90	1.0	50.5	48.6
90-120	1.2	65.2	33.7

4.3.2. Evapotranspiration measurement

4.3.2.1. Eddy covariance

Details about the EC system, associated meteorological measurements, soil water and water table depth monitoring, and data processing were previously described by Niaghi et al. (Niaghi et al., 2019b; Niaghi and Jia, 2017). The EC was installed in the middle of the field with fetch over 150 m in all directions. Considering that the field is sufficiently flat and homogenous, the exchange fluxes are one-dimensional and can be calculated using covariance between vertical wind speed and the scalar of interest. H fluxes at the EC site were estimated directly using a CSAT3 sonic anemometer (Campbell Scientific, Inc., Logan, UT, USA). Due to the limitation on the tower height, the instruments were kept approximately 0.6 m above the canopy when the corn reached its maximum height. As a rule of thumb for agricultural weather stations, the EC system should be kept at least 1 m above the crop canopy to avoid any site aridity effects (ASABE Standards, 2004). However, for a humid region with high wind speed conditions (>2 m/s) most of the time, the instrumentation height would have a minimal effect on the flux measurement (Jia et al., 2007). Additionally, the analysis using the 10 Hz flux data revealed that the shapes of the spectral and co-spectral analysis were valid (Niaghi et al., 2019b). The CR3000 datalogger (Campbell Scientific, Inc., Logan, UT, USA) recorded signals from the EC system at a frequency of 10 Hz, which were corrected for wind speed rotation (based on double rotation and detrending by the block method), time lags (using maximum covariance approaches), spike effect (plausibility range within 5 standard deviations), and amplitude resolution (with range variation within 7 standard deviations) (Niaghi et al., 2019b). The corrected data were averaged over 30 min intervals for ET calculations. The soil heat flux (G) was measured with a pair of HFT3-L soil heat plates (REBS Soil Heat Flux Plate, Radiation and Energy Balance Systems, Inc., Bellevue, WA, USA). These sensors were installed at 8 cm depth and at 0.5 m distance between each other to adjust for the spatial variability, and two soil thermocouples were placed at 2 and 6 cm above each of the soil heat flux plates. The measured G was corrected for soil heat storage by considering the soil water content. Finally, the residual method was used to close the energy balance for the EC system by assuming that the H was measured correctly. More details on the EC system and method were described in previous studies (Niaghi et al., 2019b, 2019a).

4.3.2.2. Bowen ratio system

The BREB system was used to directly measure a vertical gradient of temperature and relative humidity. BREB included fan-aspirated housings mounted on a chain-driven automatic exchange mechanism (AEM, Radiation and Energy Balance Systems, Bellevue, WA, USA). The AEM switched the gradient measuring positions between the top and bottom every 15 minutes to reduce the effects of instrument offsets. Each arm of the AEM had a Vaisala T/RH probe inside an air-aspirated shield with 1 m separation between the arms to measure temperature and relative humidity at two heights. Furthermore, each probe included two calibrated thin film platinum resistance temperature sensors (PRTDs) (Vaisala Inc., Model #s HMP 35A and HMP 35D, Finland), one of them measuring the air temperature for a temperature gradient calculation, and the other measuring the air temperature of the humidity sensor cavity of the probe for a saturated vapor pressure calculation. To measure the net radiation (R_n), measurements from two REBS

Q*7.1 net radiometers (Campbell Scientific, Inc., Logan, UT, USA) at 1 m above the crop canopy, with an adjustment by crop growth, were averaged, and the measured values were corrected for a wind speed effect [30]. For the G measurement and correction, 3 sets of soil moisture probes at a 0.5 m distance and 2.5 cm depth (REBS SMP-1), soil heat flow plates at 5 cm depth (REBS-HFT-3), and soil temperature probes integrated at 0 to 5 cm depth (STP-1) were used. G measured by the soil heat flux plates was corrected for heat storage above the plates and the moisture effect. A Met One barometric pressure sensor (Met One Instruments Inc., Grant Pass, OR, USA), (in enclosure), a Met One 020 C wind direction sensor 2 m above the crop canopy, and a Met One 010 C wind speed sensor 2 m above the crop canopy were used. For data collection and storage, a CR1000 data logger (Campbell Scientific, Inc., Logan, UT, USA), with AM16/32 multiplexer was used. To supply the required energy and charging the battery, a 65-watt solar panel model M1910 (Radiation and Energy Balance Systems, Bellevue, WA, USA) was used.

The Bowen ratio (β) was estimated from the vertical gradient of temperature (T_1, T_2) and vapor pressure (e_1, e_2) at two heights using the AEM with 1.2 m separation and a lower arm with a 1 m height above the crop canopy. β can be calculated as follows (Perez et al., 1999):

$$\beta = \frac{P.C_p}{\varepsilon.L_v}\frac{K_h}{K_w}\frac{(T_1-T_2)}{(e_1-e_2)} = \frac{H}{LE} \tag{4.1}$$

where P is atmospheric pressure (kPa), C_p is specific heat of dry air (1 KJ/kg·°C), T_1 and T_2 are measured temperatures at two heights above the crop canopy (°C), ε is the ratio between the molecular weights of water vapor and air (0.622), L_v is the latent heat of vaporization (2,260 KJ/kg), e_1 and e_2 are vapor pressures measured at two heights above the crop canopy (kPa), and K_h and K_w are the eddy diffusivities for heat and water vapor, respectively, assumed to be equal. H is estimated as the residual of the energy balance, and LE is estimated as follows:

$$LE = \frac{R_n - G}{1+\beta} \tag{4.2}$$

When β approaches "−1", the calculated fluxes approach infinity. This situation normally occurs in early mornings and late afternoons, when H changes its sign due to irrigation, precipitation, or low values of vapor pressure difference (close to the resolution limit of the sensor) during times of low available energy (Perez et al., 1999). In practice, when β is close to "−1", LE and H have their minimal values and can be considered negligible. To process and check the quality of the data, the screening criteria described by Perez et al. (Perez et al., 1999) and Ohmura (Ohmura, 1982) were used to exclude the time stamps whenever β approached "−1". Perez et al. (Perez et al., 1999) showed that the range of excluded interval for β around −1 depends on the measured vapor pressure gradient in each period and the resolution of the sensors. Therefore, by considering the resolution of the temperature (0.06 °C) and vapor pressure sensors (0.01 kPa), the excluded range for β (−1±∈) is calculated as follows:

$$\in = \frac{\delta\Delta e - \gamma\delta\Delta T}{\Delta e} \tag{4.3}$$

where δΔe and δΔT are the resolution limits for the vapor pressure and temperature gradient and γ is a psychrometric constant ($\frac{P.C_p}{\varepsilon.L_v}$). During the growing season, only 3.8% of the BREB data was rejected during the early morning and evening time.

ET can then be estimated from the LE values measured by the EC and BREB systems using the following equation:

$$ET = \frac{LE}{L_v} * 1800 \tag{4.4}$$

where ET is in mm 30-min^{-1}, LE is latent heat flux (W/m^2), L_v is latent heat of vaporization (kJ/kg), and 1800 corresponds to 30 min in seconds.

4.3.2.3. Soil water balance

Two observation wells (depth 2 m) were installed near the EC and BREB towers to continuously monitor water table fluctuation using on a half hourly basis. The soil moisture was measured using impedance dielectric sensors (Hydra Prob II, Stevens Water Monitoring System, Inc., Portland, OR, USA) that were placed as a pair on a tile and between tiles at 8 depths (0–5, 5, 15, 30, 45, 60, 75, and 90 cm) near the two towers; the average of each depth was used as a volumetric soil water content (SWC) of the layer. Due to a datalogger malfunction, the recorded soil moisture data were not available during the second half of June.

Due to the shallow water table depth and clayey soil of the study site, frequent capillary rise could increase the soil water content above the water table depth. Guderle and Hildebrandt (Guderle and Hildebrandt, 2015) observed that the uncertainties of the soil water sensors on root water uptake and capillary rise differ considerably among different approaches (e.g., the multi-layer regression method obtained the best estimation for selected 33 days during a dry period under possible measurement uncertainties). Therefore, an independent measurement of soil water potential may help to improve the estimate of the water table contribution to ET. To measure the hydraulic gradient at the lower boundary of the soil profile (1 m), six soil potentiometers (TEROS 21, Meter, Pullman, WA, USA) were installed at a paired location, on a drain tile and between two drain tiles, at 30, 60, and 90 cm depths. The measured water potential was used along with the soil moisture sensors to calculate the contribution of the water table to capillary rise. The average of the measured soil water potential at the two locations was used for 30, 60, and 90 cm soil layers to calculate the hydraulic gradient.

To calculate the capillary rise amount, the averaged soil potential in kPa for each soil layer was converted to a head of water and summed with the difference between the water table and the soil layer depth. The soil surface was considered as a datum, and positions below that were considered as negative depth. Therefore, potential hydraulic gradients were calculated in soil layers between the water table and 90 cm depth, between 90 and 60 cm depth, and between 60 and 30 cm depth. With the information in Table 1 and the soil retention curves developed using the HYPROP and WP4 methods, Van Gunechtan–Maulem parameters were estimated (Roy et al., 2018). Along with the measured soil water content in the 30, 60, and 90 cm-depth layers, the hydraulic conductivity and effective hydraulic conductivity for each soil layer were obtained:

$$k(\theta) = k_s {\theta_s}^{0.5}[1 - (1 - \frac{\theta - \theta_r}{\theta_s - \theta_r})^{1-1/n}]^2 \qquad (4.5)$$

where $k(\theta)$ is hydraulic conductivity (cm/day), k_s is saturated hydraulic conductivity (obtained from web soil survey; 8.64 for 0-30 cm and 0.87 cm/day for 30-90 cm soil layers, respectively), θ, θ_r, and θ_s are soil moisture, residual soil moisture, and saturated soil moisture content of each soil layer (cm^3/cm^3), and n is a constant. Thus, using the 1-D Richards equation between the water table depth and different soil layers for each half-hour time step, the capillary rise can be calculated as follows:

$$q = \frac{\partial \theta}{\partial t} = \frac{\partial}{\partial z}\left[k(h)\left(\frac{\partial h}{\partial z} + 1\right)\right] \qquad (4.6)$$

For Darcy's equation, q is the flux rate (cm/day), h is the soil matric potential in cm, $\partial H / \partial z$ is a gradient of water for each half-hour measurement timesteps and study layer (Δz), in cm of water.

To calculate the ET by SWB method and the change of water storage in the root zone (considered as 90 cm depth), the following equation was used:

$$\theta_i = \theta_{i-1} + \frac{(P_i - RO_i) + I_w - ET_c - DP_i + q_i}{1000\, z_r} \qquad (4.7)$$

where P is precipitation in mm, RO is surface runoff in mm, which was ignored due to the low rainfall, flat topography, and dense planting during the observation periods (Ops), I_w is applied irrigation in mm, DP is deep percolation (mm), which is assumed as zero when θ is less than the field capacity, q is ground water contribution as an upward flow (mm/day), and z_r is root depth in mm, all referred to day i. Thus, the ET by the SWB method was calculated as:

$$ET_i = P_i + q_i - 1000(\theta_i - \theta_{i-1})\, z_r \tag{4.8}$$

To calculate ET using the SWB method, different time periods were considered to obtain the most reliable results (Malek, 1993). ET by the SWB method was calculated using four different time approaches, including daily average of the 30 min soil moisture data, average soil moisture between midnight and 2:00, average soil moisture between midnight and 4:00, and average soil moisture at 4:00.

4.3.3. Available energy analysis

Net radiation is important for LE estimation using the BREB and EC systems, and the net radiation measured by different instruments can vary considerably. To avoid measurement errors, two Q7.1 net radiometer (REBS, Bellevue, WA, USA) used in the BREB and EC systems were compared to a CNR1 net radiometer (Kipp and Zonen, Delf, The Netherland), where showed a good agreement with no significant difference. In this study, the average net radiation from the two Q7.1 net radiometer was used. Similarly, the average G from the two systems was used in the analysis.

4.3.4. Comparison during observation periods

Days with missing data or rainfall events (>10 mm) were excluded in the comparison. From 14 May to 17 October, we recorded 20% and 24% of data by the EC and the BREB systems, respectively, due to system malfunction or lost power, which were excluded from the final analysis.

Imukova et al. (Imukova et al., 2016) observed that the ideal conditions for applying the water balance method are periods with low rainfall and low or absent seepage. Therefore, to minimize the uncertainties in drainage and seepage calculations, dry periods that met the mentioned criteria were selected from the growing season, which led to 6 OPs from May through October. Figure 4.2 shows the climate pattern of the growing season including the selected observation periods.

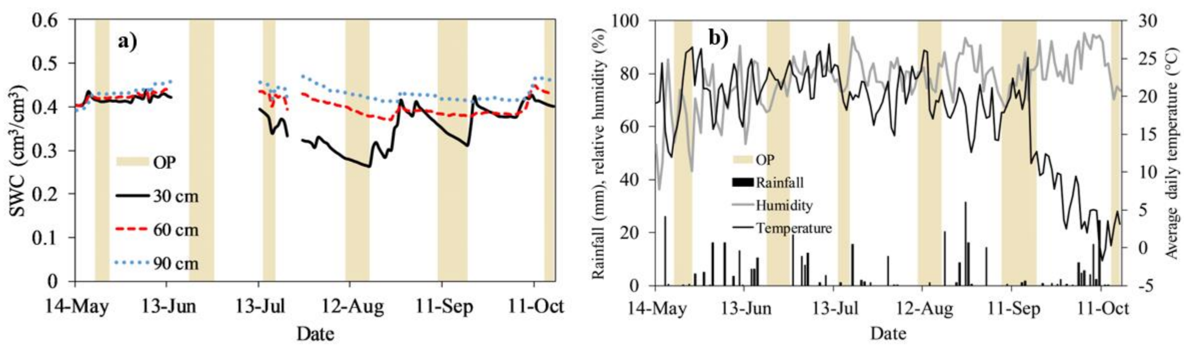

Figure 4.2. (a) Average daily soil water content (SWC), and (b) average daily temperature, relative humidity, and rainfall amount during the 2018 growing season. Tan colored zones show the observation periods (OPs).

After measuring H with the EC and BREB systems, the accuracy of the residual method was compared between the two systems for both the entire growing season and the selected OPs. The error of the BREB system was examined during the study period. The SWB was applied to each OP, and the obtained ET values with and without considering the capillary rise were compared with those measured by the EC and BREB systems.

4.4. Results

4.4.1. Residual method

The validity and accuracy of the residual method for LE estimation using the EC system was evaluated with the BREB method as an independent method. Because the same available energy (R_n-G) was used for both systems, any difference in H could lead to an LE difference. Figure 4.3 illustrates the scatterplot for the measured H during 30 min between the BREB and the EC systems for the entire growing season and the OPs. The H values agreed well between the EC and the BREB systems when excluding the initial and harvesting months in May and October, respectively.

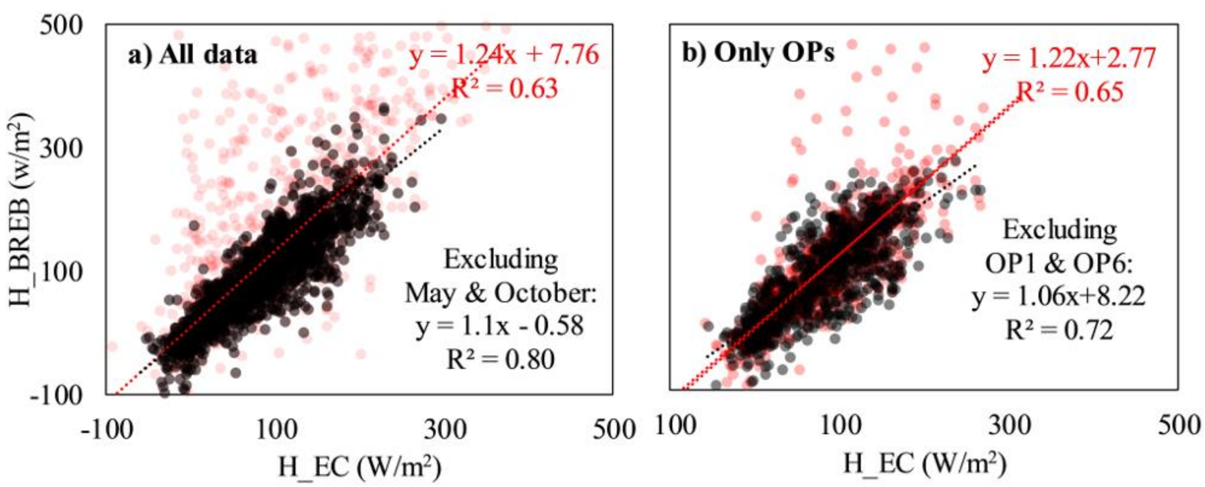

Figure 4.3. Comparison of measured sensible heat flux (H) using eddy covariance (EC) and Bowen ratio (BREB) methods for the entire growing season (a) and the observation periods (OPs) (b). The right corner of the plots listed the fitting equations when excluding data in May and October for all data in a), and OP1 and OP6 for Ops in b).

The statistical analysis of the data for the entire growing season and the OPs showed no significant differences (alpha = 0.01) between LE measured with the BREB system and LE estimated with the EC system. This indicated that the measured H by the EC system agreed well with the H determined by the independent BREB system, and thus, the accuracy of the residual method to estimate H was observed due to rejecting a null hypothesis.

4.4.1. EC and BREB comparison

The diurnal fluctuation of temperature and the vapor pressure deficit (VPD) for the BREB measurements are shown in Figure 4.4. The highest measured error for β during the entire growing season was observed in August and September, when the crop reached its maximum height with a considerable stored energy within the crop canopy. The result agrees well with findings by Ohmura (Ohmura, 1982), indicating that the counter gradient flux during the early morning hours (6:00 am - 8:00 am) and late evening (7:00 pm – 8:00 pm) was a significant component of the energy balance when the H flux was toward the crop canopy. The standard deviation of measurement error fluctuated between 0.03 in July and 0.17 in September with the highest estimated error during 7:00 am - 8:30 am.

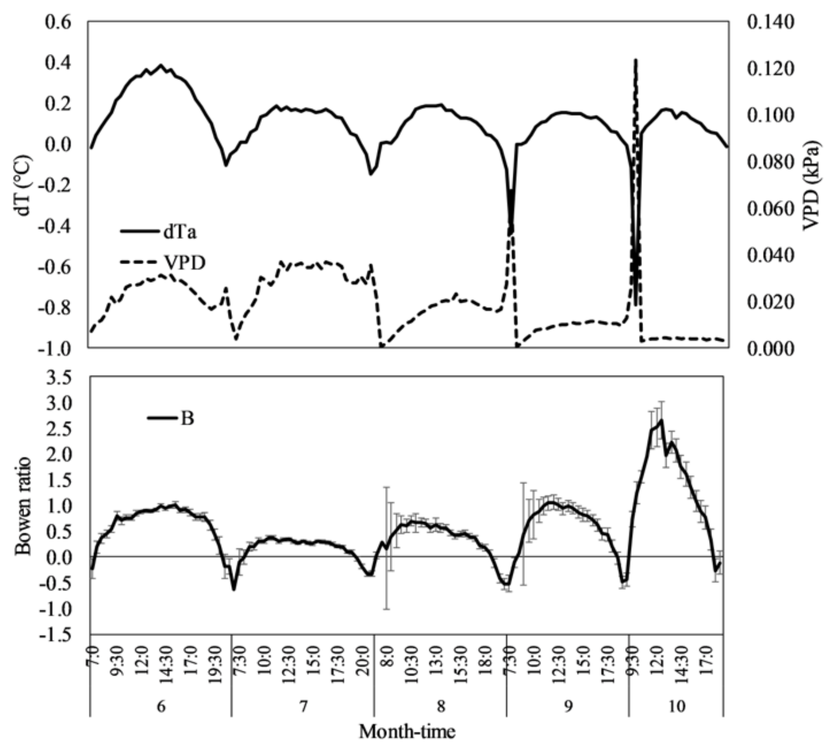

Figure 4.4. (a) Diurnal fluctuation monthly averages of air temperature (dT_a) and vapor pressure deficit (VPD), and (b) measured monthly average Bowen ratio (β) and the calculated error for β on a diurnal basis (error bars represent standard deviations).

Diurnal variation of LE and H from the BREB and EC systems were examined by averaging the half-hour fluxes over each month of the growing season and during the OPs (Figure 4.5). Figure 4.5 indicates that the BREB and EC systems acted differently on partitioning the available energy during the early and late growth stages but agreed well for the mid-growth stage.

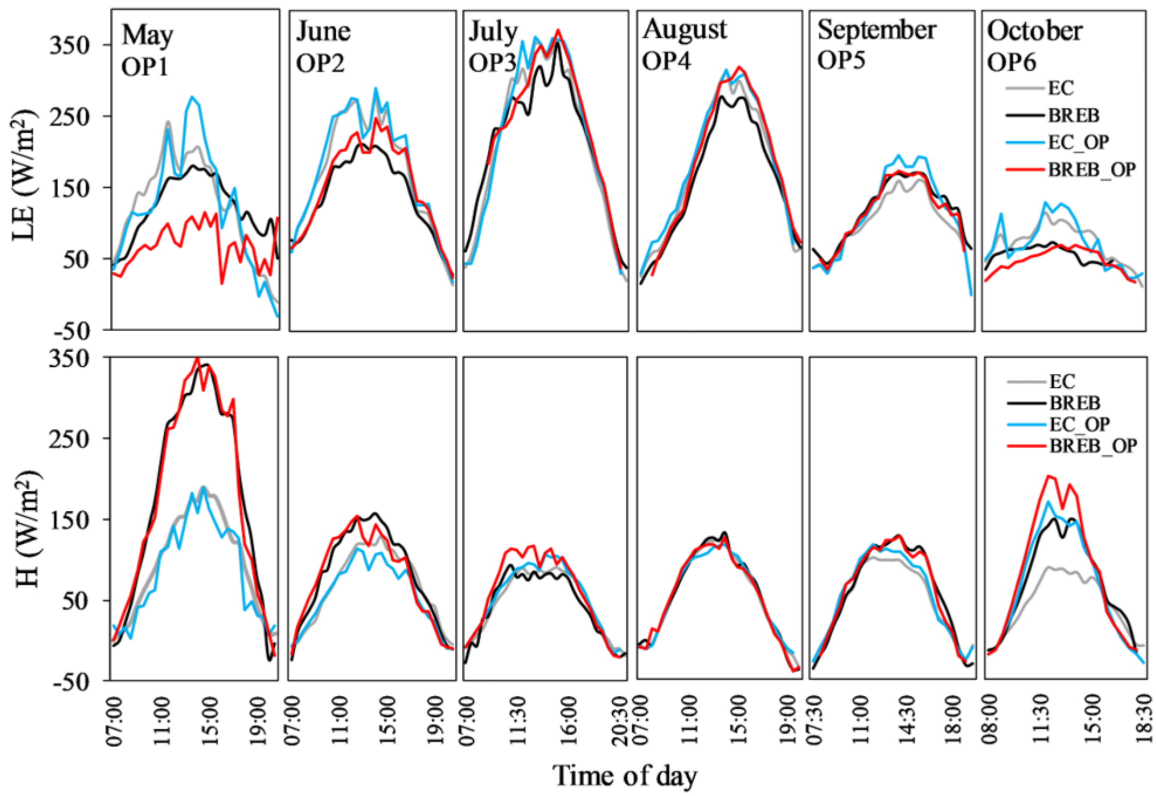

Figure 4.5. Average diurnal latent heat (LE) and sensible heat (H) flux using eddy covariance (EC) and Bowen ratio (BREB) systems for each month of the growing season and the observation periods (OPs).

Table 2 shows the average climate condition and measured energy balance components for the OPs. Higher wind speed (U) and VPD were observed for OP1, in which measurements by the BREB and the EC systems showed the highest difference compared to those for other OPs. With crop growth and more ground coverage, the LE values increased for both systems.

Table 4.2. Summary of daily averages of climate variables and energy balance components for each of the selected observation periods (OP) during the corn growing season in 2018. Air temperature = T, wind speed = U, vapor pressure deficit= VPD, R_n= net radiation, G= soil heat flux, H= sensible heat flux, LE= latent heat flux, and β = Bowen ratio.

Observation Period	OP1 5/20-5/25	OP2 6/20-6/28	OP3 7/14-7/18	OP4 8/10-8/18	OP5 9/7-9/19	OP6 10/14-10/17
Stage	Initial	Development	Reproductive	Tasseling	Maturity	Harvesting
Average climate data						
T, °C	23.0 (6.0)*	25.1 (3.7)	24.3 (4.0)	24.8 (5.6)	21.0 (5.9)	3.4 (3.6)
U, m/s	3.2 (1.9)	1.9 (0.9)	1.2 (0.5)	1.2 (0.6)	2.0 (0.9)	2.4 (0.6)
VPD, kPa	1.7 (1.0)	1.4 (0.7)	1.3 (0.6)	1.3 (0.8)	1.1 (0.8)	0.3 (0.2)
Rainfall, mm	0.8	0	1.3	1	3.3	0.2
Energy, W/m^2						
R_n	246 (79)	313 (28)	390 (70)	322 (48)	233 (79)	148 (75)
G	35 (45)	63 (15)	57 (57)	44 (12)	31 (14)	6 (9)
H_BREB	158 (84)	94 (14)	87 (38)	69 (45)	82 (35)	94 (65)
H_EC	89 (23)	66 (12)	68 (22)	77 (19)	75 (27)	70 (38)
LE_BREB	63 (21)	156 (18)	246 (43)	208 (56)	120 (54)	46 (15)
LE_EC	126 (36)	184 (23)	230 (41)	189 (33)	124 (53)	65 (39)
β _BREB	2.3 (0.3)	0.5 (0.1)	0.3 (0.1)	0.4 (0.4)	0.7 (0.5)	1.8 (1.1)
β _EC	0.8 (0.3)	0.4 (0.1)	0.3 (0.2)	0.4 (0.1)	0.7 (0.3)	1.3 (0.9)

*All values inside the parenthesis indicate standard deviation

4.4.2. Soil water balance and capillary rise

Even though some observed an 80% agreement on the ET measurement by EC and SWB methods (Wilson et al., 2002), uncertainties remained for others because the ET measurements were highly variable during periods with rainfall and rapid water movement within the soil profile. Figure 4.6 shows the average measured soil water potential and the calculated capillary rise along with the water table depth on a daily basis. Figure 4.6a illustrates the soil water potential in the soil profile during the dry periods from July to October. The water potential at the 90 cm depth had the lowest value (more negative), indicating a higher water movement from a deeper layer to the 90 cm layer. The water potential in the 60 cm layer was higher compared to that in the 90 cm depth, but there still was some water movement. The sudden decrease of soil water potential at the 30 cm depth during the mid-season after a rainfall event might have been caused by soil surface cracking and air entry into the sensor. Figure 4.6b shows that the water table depth was almost stable during the growing season, except in July when subirrigation was applied. The water table changed from below 185 cm on 22 July to 142 cm below the soil surface on 28 July. The estimated capillary rise from the soil water potential sensors clearly showed the effect of subirrigation, which increased the water potential in the soil profile and enhanced crop water uptake.

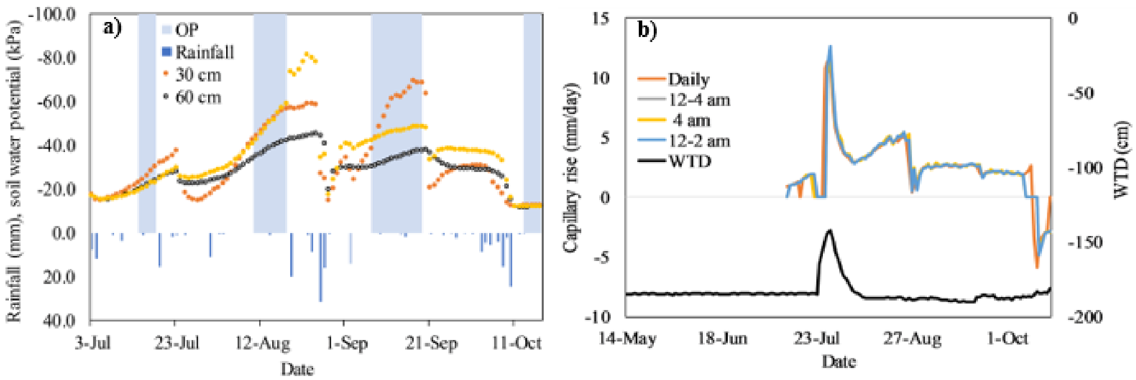

Figure 4.6. a) Daily average soil water potential at three depths during the observation periods (OP), and b) daily average water table depth (WTD) and calculated capillary rise from shallow water table.

4.4.3. Estimated evapotranspiration

Table 3 summarizes the calculated daily capillary rise, the average water table depth below the ground surface, and the average ET using the EC and BREB systems. The calculated average ET with and without considering the capillary rise effect for the different SWB approaches are also shown in Table 3. The ET values by the BREB method were compared with the ET values obtained from the EC and the SWB methods. ET determined by the EC method was, on average, about 10% higher than ET determined by the BREB method. For all OPs, the best agreement between ET values determined using the different SWB approaches and those determined by the BREB method was achieved for the soil water data for the 24:00–2:00 time period.

Table 4.3. Summary of measured and estimated crop evapotranspiration (ET) using eddy covariance (EC), Bowen ratio (BREB), and soil water balance (SWB) methods with different approaches for the capillary rise calculations at different observation periods (OPs).

Observation period		OP1	OP2	OP3	OP4	OP5	OP6
Date		5/20-5/25	6/20-6/28	7/14-7/18	8/10-8/18	9/7-9/19	10/14-10/17
Stage		Initial	Development	Reproductive	Tasseling	Maturity	Harvesting
Rainfall, mm		0.8	0	1	1	3.3	0
Capillary rise, mm		-	-	1.2 ± 0.2	4.1 ± 0.5	2.6 ± 0.1	-
Water table depth, cm		-184.6	-184.5	-184.4	-187.4	-189.4	183.6
Average ET, mm/day							
ET reference		5.2 ± 1.2*	5.2 ± 0.6	5.3 ± 0.8	4.5 ± 1.1	4.1 ± 1.6	1.8 ± 0.5
ET by EC		2.5 ± 0.8	3.7 ± 0.5	4.6 ± 0.8	3.5 ± 0.6	2.1 ± 0.9	0.9 ± 0.6
Total		**15.3 (0.85)** **	**33.2 (0.89)**	**22.9 (0.48)**	**32.7 (0.50)**	**27.4 (0.33)**	**4.3 (0.31)**
ET by BREB		1.9 ± 0.6	3.7 ± 0.6	4.7 ± 0.7	3.5 ± 0.9	2.1 ± 0.9	0.9± 0.3
Total		**11.1**	**28.8**	**22.6**	**33.1**	**26.1**	**3.7**
SWB +non capillary effect	daily	0 ± 2.7	-	1.5 ± 4.7	0.2 ± 2.9	0.2 ± 4.5	0 ± 3.1
	12-4 am	1.3 ± 1.0	-	6.2 ± 2.2	2.6 ± 1.3	3.2 ± 3.4	1.6 ± 0.9
	4 am	1.6 ± 2.0	-	5.5 ± 2.2	2.6 ± 1.3	3.2 ± 3.4	1.1 ± 1.1
	12-2 am	0.6 ± 0.4	-	2.7 ± 1.6	1.2 ± 0.5	1.7 ± 1.0	0.7 ± 0.6
SWB with capillary effect	daily	0 ± 2.7	-	2.1 ± 4.6	4.2 ± 2.8	2.8 ± 4.5	0 ± 3.1
	12-4 am	1.3 ± 1.0	-	5.2 ± 0.8	4.3 ± 0.9	3.2 ± 1.7	1.6 ± 0.9
	4 am	1.6 ± 2.0	-	5.2 ± 0.8	4.3 ± 0.8	3.2 ± 1.7	1.1 ± 1.1
	12-2 am	0.6 ± 0.4	-	4.5 ± 1.3	4.1 ± 0.5	3.4 ± 1.0	0.7 ± 0.6

* Standard deviation; ** value inside the parenthesis indicates root means square error

4.5. Discussion

The discrepancy between H values measured with the EC and BREB methods was probably due to a rapid corn growth during the early stage and the different in the instruments' heights. As indicated by Niaghi et al.(Niaghi et al., 2019b), the EC system was initially set up at 2.5 m in height and was later increased to about 3.2 m, whereas the BREB system was installed at 2 m in height (lower arm) and was increased up to 3.5 m in height (lower arm) in August. In addition, when the corn canopy did not cover the ground, advection and heat transfer from the surrounding area may have introduced an error in both systems. Schmid (Schmid, 1997) reported that the footprint of the EC system is not fixed and varies in space due to wind direction and sensor height. The various wind speeds and directions in the study region during the early season may have led to a lack of accuracy for the early growing stages when the ground was not fully covered by crop (Grare et al., 2016). When the corn grew and covered the ground, both the EC and the BREB systems had a similar footprint. Moreover, when compared to the H estimation by the BREB system, the underestimation of H by the EC system can be explained by the sonic anemometer frequency response, given atmospheric stability, canopy height, and wind speed. Dugas et al. (Dugas et al., 1991) indicated that a correction of H due to the sonic anemometer frequency response would make H approximately 5% more negative. Another reason for H underestimation could be the short averaging period of the reference temperature time constant for sonic temperature correction (Moore, 1986). On the other hand, for a stable condition when the ratio of heat and vapor diffusivity (β) was less than 1 (indication of BREB system failure) due to local advection, the measured β with the BREB system would be increased, and the H value would be more similar to the H value measured by EC.

Most research has shown that the sum of H and LE from EC instrumentation was always less than the available energy (Imukova et al., 2016; Leuning et al., 2012; Niaghi et al., 2019a). Thus, using the residual method, which accounts for the residual energy on LE, can lead to overestimation of LE (or ET) by the EC method with respect to the BREB method. However, LE overestimation by the EC method with respect to LE determined by the BREB method was 2.8%, −3.4%, and 4.9% for the development, tasseling, and reproductive stages, respectively. Therefore, in the current study, LE determined by the BREB method was compared with LE determined by the EC method, and the results revealed that the EC method is as accurate as the BREB method when crop is fully developed (fully covered ground) and when the residual method is applied to close the energy balance for the EC method. From OP2 to OP5, the available energy partitioning obtained by the EC and BREB systems showed a non-significant statistical difference. The lowest β value was observed for OP3, indicating a higher ratio of LE to H due to the higher crop water demand and more extensive ground coverage at the reproductive stage. The error and the standard deviation of the estimated β increased from OP5 to OP6 compared to the previous OPs. This error could be the result of stored heat within the crop canopy and exchange of that heat during early morning and late evening.

The BREB method has the advantage of obtaining ET independently without requiring information about the aerodynamic characteristics of the land surface (Shi et al., 2008). However, due to the low available energy and large temporal R_n change around sunrise, the BREB method does not work properly, and the β value approaches "−1" at this time of the day. Thus, the equality assumption of the BREB method of turbulent exchange coefficient for heat and water vapor is not always met (Barr et al., 1994), and the recorded LE during this period needs to be either excluded or replaced using an interpolated value. Todd et al. (Todd et al., 2000) observed that 91% of half-hour daytime LE observations by the BREB system are valid. The comparison between ET values determined by a lysimeter and the BREB method showed that the greatest difference during the early growing season for alfalfa, while the ET values determined by the two systems were in agreement for the rest of the growing season (Todd et al., 2000).

Several approaches were attempted to quantify the water table contribution to ET. However, insufficient literature is available to address the effect of upward flux on the final SWB methodology and improve the accuracy of the SWB method. Using different approaches to calculate the soil water exchange on a day-to-day basis, we showed that the average nighttime soil moisture works better than the entire day average for ET calculation, due to the unstable conditions and uncertainties during daytime. In addition to the nighttime averaging method, considering the upward flux effect on the final ET calculation using the SWB method in areas with shallow water table can improve ET estimation, when compared to the in-situ measurements of ET by the BREB and EC methods.

Figure 4.7 shows the boxplot comparison of ET determined at the different times with the SWB method with ET determined by the BREB and the EC method in OP3, OP4, and OP5. As shown in Figure 4.7, using the daily average soil moisture data to calculate the soil water exchange gave the worst ET result. Among the different approaches, using the average 24:00–2:00 soil water content for the daily ET calculation provided the best result in comparison with the ET values determined by the BREB and the EC methods and, statistically, showed no significant differences at a 95% confidence level.

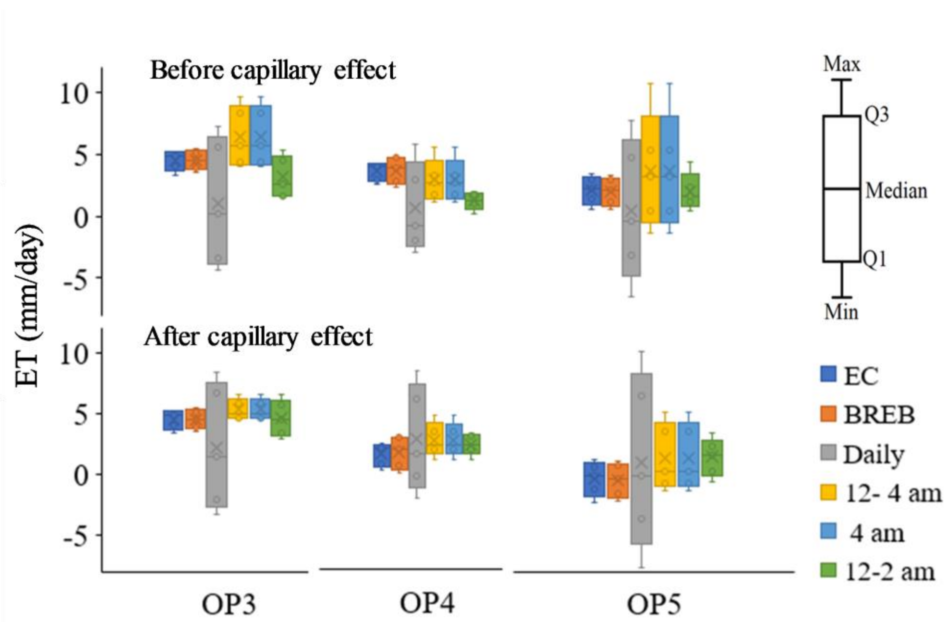

Figure 4.7. Boxplot of estimated crop evapotranspiration (ET) using soil water balance (SWB) method with different approaches (daily average soil moisture: daily, 12-4 am average soil moisture: 12-4 am, 4 am soil moisture: 4 am, and 12-2 am average soil moisture: 12-2 am), Bowen ratio (BREB), and eddy covariance (EC) methods without (before) capillary effect and with (after) capillary effect for July, August, and September observation periods (OP3, OP4, and OP5).

Using the soil water exchange during the specific study period provides valuable information to calculate ET. This becomes more important during dry periods with high atmospheric demand (Guderle and Hildebrandt, 2015; Hupet and Vanclooster, 2002). The distinction between soil water exchange through the soil profile and water extraction by evaporation or transpiration is the major challenge of SWB application (Guderle and Hildebrandt, 2015), since these fluxes occur concurrently during daytime (Feddes and Raats, 2004). Using the nighttime approach, this problem may be avoided. Li et al. (Li et al., 2002) used a similar approach to derive the root water uptake pattern from soil moisture exchange using different time approaches. When using soil water content at nighttime, it can be inherently assumed that both nighttime evapotranspiration and hydraulic redistribution are negligible.

4.6. Conclusion

ET obtained from the EC system using the residual method to close the energy balance was evaluated with the BREB system for the entire growing season and for the selected OPs. The estimated LE by the EC system using the residual method showed a 29% overestimation compared to LE determined by the BREB system for the entire growing season. After excluding data in May and October, LE by the EC system was only 10% higher, indicating that the main difference between the two systems occurred during the early and later parts of the growing season. The overestimation of H by the EC method compared to the BREB method was about 24% for the total growing season and 22% for the OPs. These values decreased to 10% and 6% for the entire growing season and OPs, respectively, after excluding data in May and October. Overall, the comparison of H values measured by the EC and the BREB systems showed the best agreement when corn was fully developed (fully covered ground) and illustrated the advantages of using the residual method to close the energy balance in the EC method. The average diurnal

LE and H showed good agreement between the EC and BREB methods during corn development, tasseling, and reproductive stages. In general, ET measured with the EC method was slightly higher than that determined by the BREB system. The current study shows that the residual method can be a reliable post-closure method with a higher accuracy when corn has covered the ground.

To compare and improve corn ET using the SWB method, four different time approaches (daily average, 24:00–2:00 average, 24:00–4:00 average, and 4:00 measure) were studied with and without considering the effect of capillary rise. Among the different time approaches, ET by the SWB method using the average soil water contents between 24:00 to 2:00 time period showed the best agreement with the ET measured by the BREB system. When considering the daily calculated hydraulic conductivity and upward flux in the soil water balance equation, ET accuracy was improved for all SWB approaches. For the 24:00–2:00 approach, the root-mean-square error (RMSE) and standard error values were calculated as 1.15 and 0.28 mm/day, respectively. Non-significant differences (alpha = 0.05) were observed between the daily ET obtained with the 24:00–2:00 SWB approach and that obtained with the BREB system for OPs, indicating equal variance of the two methods. The shallow water table can significantly contribute to ET and therefore, improve the ET measurement by the SWB method when the soil water condition is a limiting factor. The application of the capillary rise to ET estimation using the SWB method during the mid to late crop stages can be as accurate as other expensive and complex ET methods, such as the EC and BREB methods.

4.7. Acknowledgements

This project is supported by USDA National Institute of Food and Agriculture project 2015-68007-23193, NASA ROSES Project NNX15AC47G, ND Water Resources Research

Institute, ND Agricultural Experimental Station, and USDA Hatch project ND01475. The authors would like to express our gratitude to Ms. Debra Baer for her assistance to review the paper, Dr. Aaron Daigh, Dr. Don Lin, and many other formal students for their valuable work in field work and data collection.

4.8. References

Allen, R. G., Pereira, L. S., Howell, T. A., & Jensen, M. E. (2011). Evapotranspiration information reporting: I. Factors governing measurement accuracy. *Agricultural Water Management*, *98*(6), 899–920. https://doi.org/10.1016/j.agwat.2010.12.015

Amatya, D. M., Irmak, S., Gowda, P., Sun, G., Nettles, J. E., & Douglas-Mankin, K. R. (2016). Ecosystem evapotranspiration: Challenges in measurements, estimates, and modeling. *Transactions of the ASABE*, *59*(2), 555–560. https://doi.org/10.13031/trans.59.11808

ASABE Standards. (2015). S526.4: (2015). *Soil and water terminology.* St. Joseph, MI: ASABE.

Barr, A. G., King, K. M., Gillespie, T. J., Den Hartog, G., & Neumann, H. H. (1994). A comparison of bowen ratio and eddy correlation sensible and latent heat flux measurements above deciduous forest. *Boundary-Layer Meteorology*. https://doi.org/10.1007/BF00709218

Brotzge, J. A., & Crawford, K. C. (2003). Examination of the Surface Energy Budget: A Comparison of Eddy Correlation and Bowen Ratio Measurement Systems. *Journal of Hydrometeorology*, *4*(2), 160–178. https://doi.org/10.1175/1525-7541(2003)4<160:EOTSEB>2.0.CO;2

Campbell Scientific Inc. (1996). Q-7.1 Net Radiometer. In *Revision* (Vol. 5). Retrieved from http://scholar.google.com/scholar?hl=en&btnG=Search&q=intitle:Q-7.1+Net+Radiometer#0

Consoli, S., & Vanella, D. (2014). Mapping crop evapotranspiration by integrating vegetation indices into a soil water balance model. *Agricultural Water Management*, *143*, 71–81. https://doi.org/10.1016/j.agwat.2014.06.012

Doran, J. W., Jones, A. J., Arshad, M. A. (Charlie), Lowery, B., & Grossman, B. (1996). *Physical Tests for Monitoring Soil Quality*. https://doi.org/10.2136/sssaspecpub49.c7

Dragoni, D., Schmid, H. P., Grimmond, C. S. B., & Loescher, H. W. (2007). Uncertainty of annual net ecosystem productivity estimated using eddy covariance flux measurements. *Journal of Geophysical Research Atmospheres*, *112*(17), 1–9. https://doi.org/10.1029/2006JD008149

Dugas, W. A., Fritschen, L. J., Gay, L. W., Held, A. A., Matthias, A. D., Reicosky, D. C., … Steiner, J. L. (1991). Bowen ratio, eddy correlation, and portable chamber measurements of sensible and latent heat flux over irrigated spring wheat. *Agricultural and Forest Meteorology*. https://doi.org/10.1016/0168-1923(91)90101-U

Feddes, R. A., & Raats, P. A. C. (2004). Parameterizing the soil - water - plant root system. *Wageningen Frontis Series*.

Fidantemiz, Y. F., Jia, X., Daigh, A. L. M., Hatterman-Valenti, H., Steele, D. D., Niaghi, A. R., & Simsek, H. (2019). Effect of water table depth on soybean water use, growth, and yield parameters. *Water (Switzerland)*. https://doi.org/10.3390/w11050931

Fisher, J. B., Melton, F., Middleton, E., Hain, C., Anderson, M., Allen, R., … Wood, E. F. (2017). The future of evapotranspiration: Global requirements for ecosystem functioning, carbon and climate feedbacks, agricultural management, and water resources. *Water Resources Research*, *53*(4), 2618–2626. https://doi.org/10.1002/2016WR020175

Gebler, S., Hendricks Franssen, H.-J., Pütz, T., Post, H., Schmidt, M., & Vereecken, H. (2015). Actual evapotranspiration and precipitation measured by lysimeters: a comparison with eddy covariance and tipping bucket. *Hydrol. Earth Syst. Sci*, *19*, 2145–2161. https://doi.org/10.5194/hess-19-2145-2015

Gee, G. ., & Or, D. (2002). Methods of Soil Analysis. In *Soils Science Society of Amercia*. https://doi.org/10.1007/s10310-016-0542-5

Gong, J., Shurpali, N. J., Kellomäki, S., Wang, K., Zhang, C., Salam, M. M. A., … Ward, K. (2016). Comparing different methods for determining forest evapotranspiration and its components at multiple temporal scales. *Agricultural and Forest Meteorology*, *13*(1), 595–605. https://doi.org/10.1007/BF00190238

Grare, L., Lenain, L., & Melville, W. K. (2016). The influence of wind direction on Campbell scientific CSAT3 and Gill R3-50 sonic anemometer measurements. *Journal of Atmospheric and Oceanic Technology*, *33*(11), 2477–2497. https://doi.org/10.1175/jtech-d-16-0055.1

Guderle, M., & Hildebrandt, A. (2015). Using measured soil water contents to estimate evapotranspiration and root water uptake profiles-a comparative study. *Hydrology and Earth System Sciences*, *19*(1), 409–425. https://doi.org/10.5194/hess-19-409-2015

Hupet, F., & Vanclooster, M. (2002). Intraseasonal dynamics of soil moisture variability within a small agricultural maize cropped field. *Journal of Hydrology*. https://doi.org/10.1016/S0022-1694(02)00016-1

Imukova, K., Ingwersen, J., Hevart, M., & Streck, T. (2016). Energy balance closure on a winter wheat stand: Comparing the eddy covariance technique with the soil water balance method. *Biogeosciences*, *13*(1), 63–75. https://doi.org/10.5194/bg-13-63-2016

Irmak, S., Kilic, A., & Chatterjee, S. (2014). On the Equality Assumption of Latent and Sensible Heat Energy Transfer Coefficients of the Bowen Ratio Theory for Evapotranspiration Estimations: Another Look at the Potential Causes of Inequalities. *Climate*, *2*(4), 181–205. https://doi.org/10.3390/cli2030181

Jia, X., Dukes, M. D., Jacobs, J. M., & Haley, M. (2007). Impact of weather station fetch distance on reference evapotranspiration calculation. *Restoring Our Natural Habitat - Proceedings of the 2007 World Environmental and Water Resources Congress*.

Kolars, K., Jia, X., Steele, D. D., & Scherer, T. F. (2019). A soil water balance model for subsurface water management. *Applied Engineering in Agriculture*.

Leuning, R., van Gorsel, E., Massman, W. J., & Isaac, P. R. (2012). Reflections on the surface energy imbalance problem. *Agricultural and Forest Meteorology*, *156*, 65–74. https://doi.org/10.1016/j.agrformet.2011.12.002

Li, Y., Fuchs, M., Cohen, S., Cohen, Y., & Wallach, R. (2002). Water uptake profile response of corn to soil moisture depletion. *Plant, Cell and Environment*. https://doi.org/10.1046/j.1365-3040.2002.00825.x

Malek, E. (1993). Comparison of the Bowen ratio-energy balance and stability-corrected aerodynamic methods for measurement of evapotranspiration. *Theoretical and Applied Climatology*, *48*(2–3), 167–178. https://doi.org/10.1007/BF00864923

Moore, C. J. (1986). Frequency response corrections for eddy correlation systems. *Boundary-Layer Meteorology*. https://doi.org/10.1007/BF00122754

Niaghi, A. R., & Jia, X. (2017). Determination of Grass Evapotranspiration Rates and Crop Coefficients Using Eddy Covariance Method in Eastern North Dakota. *World*

Environmental and Water Resources Congress, 468–483. https://doi.org/10.1061/9780784480601.040

Niaghi, A. R., Jia, X., Scherer, T., & Steele, D. (2019). Measurement of unirrigated turfgrass evapotranspiration rate in the red river valley. *Vadose Zone Journal*, *18*(1), 1–37. https://doi.org/10.2136/vzj2018.11.0202

Niaghi, A. R., Jia, X., Steele, D. D., & Scherer, T. F. (2019). Drainage water management effects on energy flux partitioning, evapotranspiration, and crop coefficients of corn. *Agricultural Water Management*, *225*, 105760. https://doi.org/10.1016/j.agwat.2019.105760

Ohmura, A. (1982). Objective criteria for rejecting data for Bowen ratio flux calculations. *Journal of Applied Meteorology*. https://doi.org/10.1175/1520-0450(1982)021<0595:OCFRDF>2.0.CO;2

Ohmura, Atsumu. (2002). Objective Criteria for Rejecting Data for Bowen Ratio Flux Calculations. *Journal of Applied Meteorology*. https://doi.org/10.1175/1520-0450(1982)021<0595:ocfrdf>2.0.co;2

Perez, P. J., Castellvi, F., Ibañez, M., & Rosell, J. I. (1999). Assessment of reliability of Bowen ratio method for partitioning fluxes. *Agricultural and Forest Meteorology*, *97*(3), 141–150. https://doi.org/10.1016/S0168-1923(99)00080-5

Prathapar, S. A., & Meyer, W. S. (1993). Measurement and estimation of capillary upflow from watertables under maize on irrigated soils. *Australian Journal of Soil Research*. https://doi.org/10.1071/SR9930119

Prathapar, S. A., Robbins, C. W., Meyer, W. S., & Jayawardane, N. S. (1992). Models for estimating capillary rise in a heavy clay soil with a saline shallow water table. *Irrigation Science*, *13*(1), 1–7. https://doi.org/10.1007/BF00190238

Ragab, R. A., & Amer, F. (1986). Estimating water table contribution to the water supply of maize. *Agricultural Water Management*, *11*(3–4), 221–230. https://doi.org/10.1016/0378-3774(86)90040-5

Reyes-González, A., Kjaersgaard, J., Trooien, T., Hay, C., & Ahiablame, L. (2017). Comparative Analysis of METRIC Model and Atmometer Methods for Estimating Actual Evapotranspiration. *International Journal of Agronomy*, *2017*. https://doi.org/10.1155/2017/3632501

Roy, D., Jia, X., Steele, D. D., & Lin, D. (2018). Development and Comparison of Soil Water Release Curves for Three Soils in the Red River Valley. *Soil Science Society of America Journal*, *0*(0), 0. https://doi.org/10.2136/sssaj2017.09.0324

Schmid, H. P. (1997). Experimental design for flux measurements: Matching scales of observations and fluxes. *Agricultural and Forest Meteorology*. https://doi.org/10.1016/S0168-1923(97)00011-7

Shi, T. T., Guan, D. X., Wu, J. B., Wang, A. Z., Jin, C. J., & Han, S. J. (2008). Comparison of methods for estimating evapotranspiration rate of dry forest canopy: Eddy covariance, Bowen ratio energy balance, and Penman-Monteith equation. *Journal of Geophysical Research Atmospheres*, *113*(19), 1–15. https://doi.org/10.1029/2008JD010174

Todd, R. W., Evett, S. R., & Howell, T. A. (2000). The Bowen ratio-energy balance method for estimating latent heat flux of irrigated alfalfa evaluated in a semi-arid, advective environment. *Agricultural and Forest Meteorology*. https://doi.org/10.1016/S0168-1923(00)00139-8

Verstraeten, W. W., Veroustraete, F., & Feyen, J. (2008). Assessment of evapotranspiration and soil moisture content across different scales of observation. *Sensors*, *8*(1), 70–117. https://doi.org/10.3390/s8010070

Wallender, W. W., Grimes, D. W., Henderson, D. W., & Stromberg, L. K. (1979). Estimating the Contribution of a Perched Water Table to the Seasonal Evapotranspiration of Cotton. *Agronomy Journal*, *71*, 1056–1060. https://doi.org/10.2134/agronj1979.00021962007100060038x

Watanabe, K., Yamamoto, T., Yamada, T., Sakuratani, T., Nawata, E., Noichana, C., … Higuchi, H. (2004). Changes in seasonal evapotranspiration, soil water content, and crop coefficients in sugarcane, cassava, and maize fields in Northeast Thailand. *Agricultural Water Management*, *67*(2), 133–143. https://doi.org/10.1016/j.agwat.2004.02.004

Wilson, K., Goldstein, A., Falge, E., Aubinet, M., Baldocchi, D., Berbigier, P., … Verma, S. (2002). Energy balance closure at FLUXNET sites. *Agricultural and Forest Meteorology*. https://doi.org/10.1016/S0168-1923(02)00109-0

Zhang, B., Kang, S., Li, F., & Zhang, L. (2008). Comparison of three evapotranspiration models to Bowen ratio-energy balance method for a vineyard in an arid desert region of northwest China. *Agricultural and Forest Meteorology*, *148*(10), 1629–1640. https://doi.org/10.1016/J.AGRFORMET.2008.05.016

5. GENERAL CONCLUSION

An eddy covariance (EC) system and two sets of soil moisture sensors were used to measure the actual evapotranspiration rates on a mixed turfgrass field in eastern North Dakota. Meteorological data from the Fargo NDAWN site was used to calculate the grass-based reference evapotranspiration (ET_o) rates using the standardized ASCE-EWRI method. Due to high variability in the precipitation amounts, the turfgrass ET measurements were also different. The mean ratio of actual turfgrass ET to ET_o (ET/ET_o) was estimated to be 0.96 using screened daily data from all three years when the soil had greater than 50% of the available water (50% AWC) in the root zone, with rainfall less than or equal to 10 mm, and a 6-day recovery period after drought. For non-irrigated and natural condition, the soil moisture sensors can be useful for turfgrass stress detection, and a useful tool to select well-watered and ideal turfgrass growing conditions for reference evapotranspiration measurements.

The ASCE-EWRI ET_o can be used to estimate turfgrass ET even in cold and sub-humid climate conditions and can be used for water management of turfgrass in northern climates. Since this is the first reported study on turfgrass ET measurement in this area, the results can provide a baseline on turfgrass water management under various weather conditions. The results indicated that a monthly refinement of ET/ET_o values may be required to maintain the landscape turfgrasses more precisely in terms of water consumption. This research also verified that the standardized ET_o equation can be applied in eastern North Dakota to guide crop water management.

Energy balance and ET rates were measured in a corn field with controlled drainage and subirrigation practices using an EC system during several corn growing seasons in the Red River Valley. Soil water content, water table depth, and precipitation were monitored for the growing season and the off-season. The off-season precipitation recharged the soil profile and was beneficial for better crop growth in the spring. The application of controlled drainage and subirrigation kept the soil water content at optimal conditions during the growing season. The measured energy fluxes showed that the application of subirrigation enhanced the measured ET rates. The largest benefit of controlled drainage and subirrigation practices was found during a wet and dry year. Furthermore, crop coefficient curves were developed using the estimated ET rates, screened for days with more than 45% of total available water in the corn root zone, and the standardized reference ET equations. This study showed that good drainage water management with controlled drainage and subirrigation provided good corn production during both wet and dry years.

ET obtained from the EC system using the residual method to close the energy balance was evaluated with the BREB system for the entire growing season and for the selected OPs. Overall, the comparison of H values measured by the EC and the BREB systems showed the best agreement when corn was fully developed (fully covered ground) and illustrated the advantages of using the residual method to close the energy balance in the EC method. In general, ET measured with the EC method was slightly higher than that determined by the BREB system. The current study shows that the residual method can be a reliable post-closure method with a higher accuracy when corn has covered the ground.

To compare and improve corn ET using the SWB method, four different time approaches (daily average, 24:00–2:00 average, 24:00–4:00 average, and 4:00 measure) were studied with and without considering the effect of capillary rise. Among the different time approaches, ET by the SWB method using the average soil water contents between 24:00 to 2:00 time period showed the best agreement with the ET measured by the BREB system. Non-significant differences (alpha = 0.05) were observed between the daily ET obtained with the 24:00–2:00 SWB approach and that obtained with the BREB system for OPs, indicating equal variance of the two methods. The shallow water table can significantly contribute to ET and therefore, improve the ET measurement by the SWB method when the soil water condition is a limiting factor. The application of the capillary rise to ET estimation using the SWB method during the mid to late crop stages can be as accurate as other expensive and complex ET methods, such as the EC and BREB methods.

APPENDIX A. COESPECRUM ANLAYSIS

The variance or energy spectrum quantifies the amount of variance (or energy) associated with a particular frequency or wavelength scale. The energy spectrum of a scalar or a wind velocity component is derived through a Fourier transformation of a temporal (spatial) series of a given variable. The Fourier transform (Fourier, 1822) converts the time (or space) series into a frequency domain by representing it as an infinite sum of sine and cosine terms. Integration of spectral energy densities (S_{ww}) across the whole range of significant frequencies yields the total variance of the velocity (w'w') or scalar quantity under scrutiny.

$$\overline{w'w'} = \int_0^\infty S_{ww}(\omega)d\omega \tag{A.1}$$

In a similar way, the real component of the cross-spectrum, co-spectrum (S_{wc}) quantifies the amount of "flux" that is associated with a particular scale.

$$\overline{w'c'} = \int_0^\infty S_{wc}(\omega)d\omega \tag{A.2}$$

In a natural environment, a distinct property of turbulence is a wide spectrum of motion scales (eddies) associated with the fluid flow. The largest scales of turbulence are produced by forces driving the mean fluid flow. The large eddies break down into progressively smaller scales and this breaking down continuous until the eddies are so small that energy is consumed by working against viscous forces that convert kinetic energy into heat. Therefore, in application, the method must acquire both short and long scale contributions to the turbulent flux. However, this dependency, imposes several constrains on instrument design, measurement principles, and sensors sampling. Reviews of EC method have been produced by numerous investigators and further detail can be found here (Baldocchi, 2010; Baldocchi, 2003; Massman & Lee, 2002). Overall, with regards to instrumental placement, design and implementation, the accuracy of any flux measurement will be influenced by:

- 1)Sensor size
- 2) separation of instruments
- 3) placement height and position
- 4) mechanical filtering or distortion of turbulence
- 5) rotation of coordination, and 6) flow interference by towers and booms

As fluxes are calculated over a 30-min averaging period, longer-term turbulent contributions are under sampled, and resulting in flux losses. Therefore, the high-pass filtering correction is applied in EddyPro based on Moncrieff et al. (2004). In addition, fluxes are attenuated due to the actual damping of the small-scale turbulent fluctuations, as well as instrument and setup limitations that do not allow measuring the full spatiotemporal turbulent fluctuations. The correction for these flux losses is called low-pass filtering correction and the correction method from Moncrieff et al. (1997) is used.

In the current study, the CSAT3 sonic anemometer and KH20 gas analyzer were installed on the tower with maximum height of 2.5 m. Due to the tower height limitation, the instruments were kept approximately 0.6 m above the canopy when corn reached its maximum height. As a rule of thumb for agricultural weather stations, the EC system should be kept at least 1 m above the crop canopy to avoid any site aridity effects. However, for a humid region with high wind speed conditions during most of the time, the instrumentation height would have minimal effect to the flux measurement (Jia et al., 2007). Additional 10 Hz flux data analysis also revealed that the shapes of the spectral and co-spectral analysis were validated.

To show the quality of the measured fluxes using eddy covariance, worst case scenario has been selected based on Monin-Obukhov length equation and height of measurement.

Basically, we looked at typical case and worst case and based on that argued that the CSAT3 could capture either low or high frequency fluxes.

What is most undesirable is that the lost flux is correlated with crop growth, because the crop grows closer to the sensor, and so it is confounding to the analysis itself. Therefore, we looked at the cospectrum of the collected data by CSAT3 during 2016 and 2017 growing season. as example here, we looked at time of day in 2016 and 2017 when the canopy height was about 1.5 m and reach to the maximum height in August. We believe that these are exactly the evidence to prove the quality of collected data by neglecting the height of eddy covariance.

In most of the literatures, minimum recommended height to measure the flux above the crop canopy is to provide an ability to capture both large and small eddies. Figure A.1 shows that how the cospectrum goes to zero at higher frequencies which mean that all eddies are captured from large to small. It would be expected that as we get closer to the canopy, the cospectrum would shift to the right, and we would lose some flux in the highest frequencies. This may be true in some cases, however, in our study, we showed that all eddies are captured and the fluxes carrying the scalars we care about.

By looking to the "worst case" situations, as $|z/L| \Rightarrow 0$, "Given the proximity of the sensor to the canopy, cospectra were inspected to verify that they assumed to be zero, particularly at the highest frequencies, particularly under worst case scenarios when z/L approached zero (Wolf and Laca 2007)". Therefore, cospectral analysis for 2016 and 2017 in august when the crop had the highest height showed that the eddy covariance was capable to capture all eddies that we were looking for.

In summary, based on the communication with Dr. Adam Wolf (arable labs Inc.) who has several publications on eddy covariance analysis, he was in agree with the result of cospectral analysis that we provided. Figure A.1 shows that the required eddies are captured, and the atmospheric turbulence is properly sampled. Therefore, we can use the recorded data to calculate sensible heat flux with an acceptable accuracy. Thus, the ET can be calculated by using the calculated LE from residual method. The raw collected 10 Hz data was processed and statistical tests for raw data screening were applied as follow:

- Wind speed rotated based on double rotation method and detrend using block method. Time lags also detected with maximum covariance approaches.
- Spike count/removal based on Vickers and Mahrt (1997) considering accepted spikes as 1%, replacing spikes with linear interpolation, maximum number of consecutive outliers as 3, and plausibility range of 5 std. for wind speed in 3 directions.
- amplitude resolution correction with range of variation as 7 std, number of bins as 100, and accepted empty bins of 70%.
- drop-outs correction with 10 bins and accepted central and extreme drop-outs as 10 and 6%, respectively.
- Absolute limits correction of (-30, 30) for U, (-5, 5) for W, (-40,50) for T sonic.
- skewness and kurtosis correction and time lags correction.
- To derive the cospectra, frequency bins for cospectra reduction selected as 50. Minimum friction velocity for unstable condition was 0.2 m/s, 0.05 m/s for stable condition and maximum of 5 m/s. minimum number of cospectra for valid averages was 10. The spectra and cospectra were filtered according to Vicker and Mahrt (1997) test result and low data quality was flagged according to micrometeorological quality test result by Mauder and Foken (2004). To correct the spectral, Moncrieff et al.

(2004) methodology was used for high-pass and low-pass filtering effect (fully analytic method).

d in the figure is the displacement height (or zero plane displacement height) of a vegetated surface which is the height at which the wind speed would go to zero if the logarithmic wind profile was maintained from the outer flow all the way down to the surface (that is, in the absence of the vegetation).

Table A1. List of figures to represent the analyzed days for coespetrum analysis

Figure No.	Date and time	Wind Speed (m/s)	Measuring height (m)	Z/L	U^*
a	2016/08/06-12:30	0.16	1 m	0.4	0.19408
b	2016/08/08-1630 pm	2.36	1.4	0.000056213 (Neutral condition)	0.76
c	2017/06/30-13:00 PM	3.59	1.7	-0.022	0.5
d	2017/07/07-10:00 am	3.60	1.5	-0.010967	0.71
e	2017/07/07-10:00 am	3.60	1.5	-0.010967	0.71
f	2017/08/16-13:30 pm	0.4	1.258	-0.11437	0.13
g	2017/08/16-13:30 pm	0.4	1.258	-0.11437	0.13

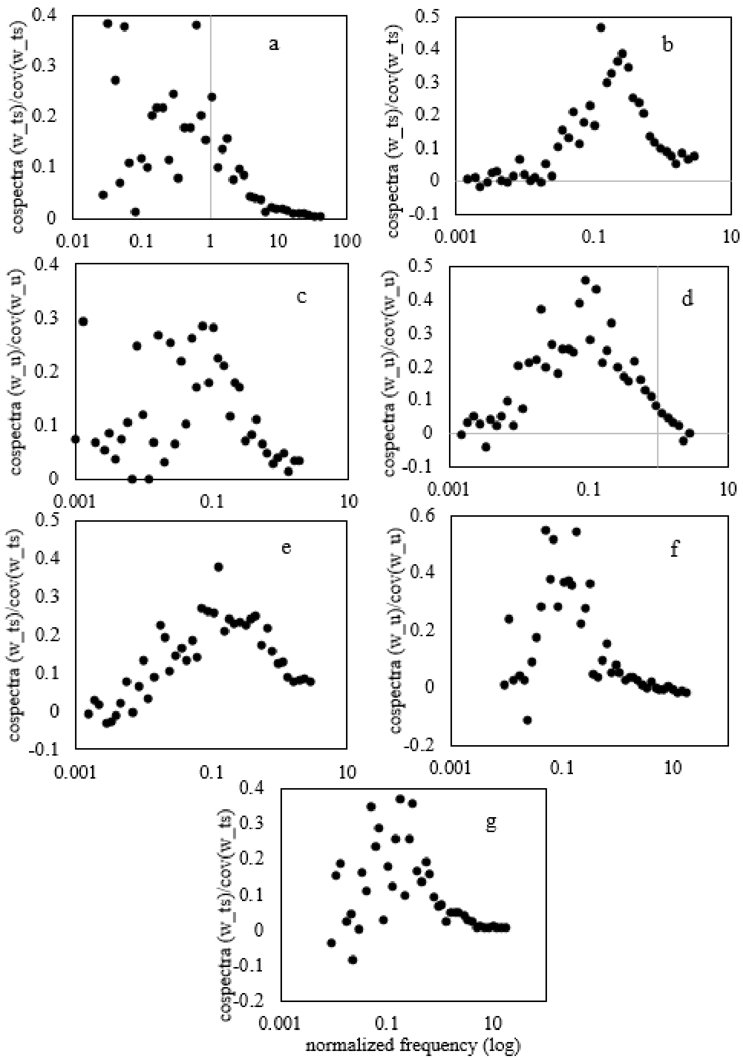

Figure A1. Cospectral analysis of eddy covariance for the selected days during the corn growing season in 2016 and 2017.

A.1. References

Baldocchi, D. (2010). Evaluating the Flux Covariance. Time, 1–29.

Baldocchi, D. (2003). Assessing the eddy covariance technique for evaluating carbon dioxide exchange rates of ecosystems: past, present and future. Global Change Biology, (October 2002), 479–492. https://doi.org/10.1016/0376-6357(93)90090-E

Fourier, J. B. J. (1822). Théorie Analytique de la Chaleur. In Théorie Analytique de la Chaleur. https://doi.org/10.1017/cbo9780511693229

Jia, X., Dukes, M. D., Jacobs, J. M., & Haley, M. (2007). Impact of weather station fetch distance on reference evapotranspiration calculation. Restoring Our Natural Habitat - Proceedings of the 2007 World Environmental and Water Resources Congress.

Massman, W. J., & Lee, X. (2002). Eddy covariance flux corrections and uncertainties in long-term studies of carbon and energy exchanges. Agricultural and Forest Meteorology, 113(1–4), 121–144. https://doi.org/10.1016/S0168-1923(02)00105-3

Mauder, M., & Foken, T. (2006). Impact of post-field data processing on eddy covariance flux estimates and energy balance closure. Meteorologische Zeitschrift. https://doi.org/10.1127/0941-2948/2006/0167

Moncrieff, J. B., Massheder, J. M., De Bruin, H., Elbers, J., Friborg, T., Heusinkveld, B., … Verhoef, A. (1997). A system to measure surface fluxes of momentum, sensible heat, water vapour and carbon dioxide. Journal of Hydrology. https://doi.org/10.1016/S0022-1694(96)03194-0

Moncrieff, J., Clement, R., Finnigan, J., & Meyers, T. (2004). Averaging, Detrending, and Filtering of Eddy Covariance Time Series. In Handbook of Micrometeorology. https://doi.org/10.1007/1-4020-2265-4_2

Vickers, D., & Mahrt, L. (1997). Quality control and flux sampling problems for tower and aircraft data. Journal of Atmospheric and Oceanic Technology. https://doi.org/10.1175/1520-0426

Wolf, A., & Laca, E. A. (2007). Cospectral analysis of high frequency signal loss in eddy covariance measurements. Atmospheric Chemistry and Physics Discussions. https://doi.org/10.5194/acpd-7-13151-2007

APPENDIX B. FOOTPRINT ANALYSIS

For footprint analysis, Kljun et al. (2004) method was used and for some figures, the 90% footprint coverage included.

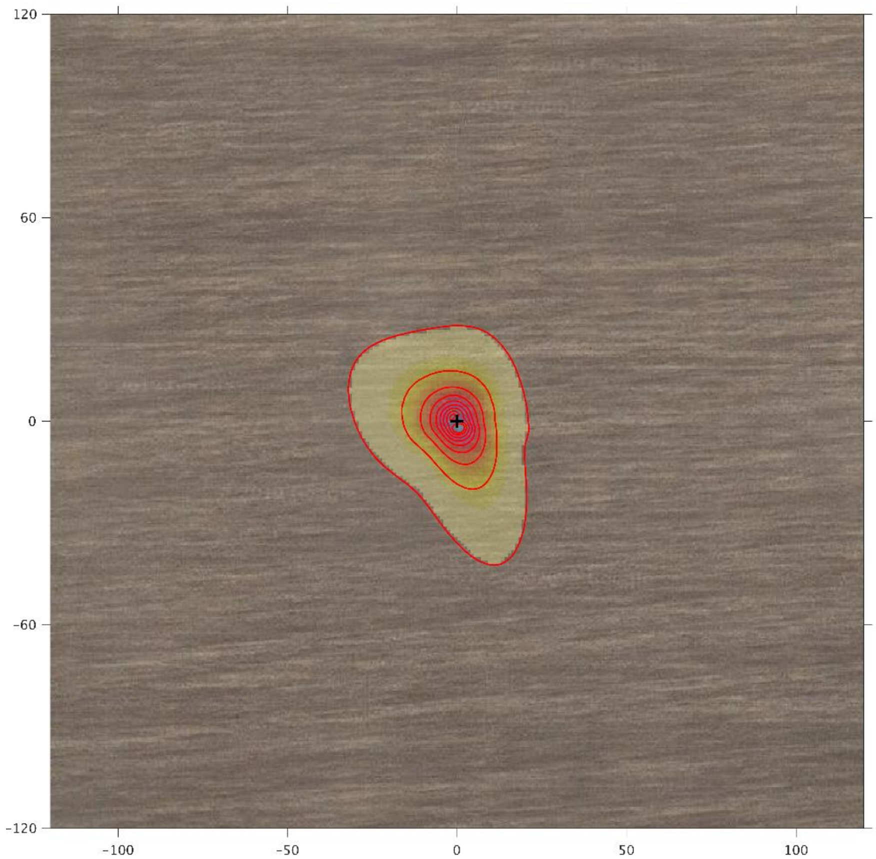

Figure B1. Footprint analysis using Kljun et al. (2004) methodology by considering the maximum crop height at 2.6 m and sonic anemometer at 3 m above the ground.

B.1. References

Kljun, N., Calanca, P., Rotach, M. W., & Schmid, H. P. (2004). A simple parameterisation for flux footprint predictions. *Boundary-Layer Meteorology*. https://doi.org/10.1023/B:BOUN.0000030653.71031.96